

**EFFECTS OF AGING AND CORTICOFUGAL MODULATION ON
STARTLE BEHAVIOR AND AUDITORY PHYSIOLOGY**

by
Marisa Dowling

A Thesis

Submitted to the Faculty of Purdue University

In Partial Fulfillment of the Requirements for the degree of

Master of Science



Weldon School of Biomedical Engineering

West Lafayette, Indiana

May 2019

**THE PURDUE UNIVERSITY GRADUATE SCHOOL
STATEMENT OF COMMITTEE APPROVAL**

Dr. Edward Bartlett, Chair

Department of Biological Sciences

Department of Biomedical Engineering

Dr. Ananthanarayan Krishnan

Department of Speech, Language, and Hearing Sciences

Dr. Mark Sayles

Department of Biomedical Engineering

Department of Speech, Language, and Hearing Sciences

Dr. Thomas Talavage

Department of Biomedical Engineering

Department of Electrical and Computer Engineering

Approved by:

Dr. George R. Wodicka

Head of the Graduate Program

To my parents, brother, and close friends for their support in my academic endeavors, career pursuit, and traveling adventures

ACKNOWLEDGMENTS

I would like to thank Dr. Edward Bartlett for his mentorship, guidance and advice throughout my undergraduate and graduate research career. While working in the Central Auditory Processing Lab, I was able to develop a multitude of research skills and discover my passion for research and neuroscience.

To past and present members of the Central Auditory Processing Lab, particularly Brandon Coventry, Nanami Miyazaki, Alex Sommer, Caitlin Swanberg, Urbi Saha, Maria Fischer, Maria Puerto-Fals, Zhengyang Wang, and Emily Han. They provided support prior to and throughout my master's career, whether it was training me on a new research skill or training me on how to make sushi. Working in the lab has been a highlight of my time at Purdue University and is one of the reasons I am so grateful that I chose to come to Purdue.

To all my friends and family that have supported me throughout this master's program, thank you for keeping me sane. A special thanks to Rachael Swenson, Ethan Biggs, Shanna High, Evan Surma, Austin Dowling, and my parents for all of your support, advice, friendship, and laughs throughout my time at Purdue.

TABLE OF CONTENTS

LIST OF TABLES	ix
LIST OF FIGURES	x
ABBREVIATIONS	xvii
ABSTRACT.....	xix
1. INTRODUCTION	1
1.1 Overview of the Auditory System.....	1
1.2 Cortical Projections	3
1.3 Non-semantic Pitch Sweeps	5
1.3.1 Iterative Rippled Noise.....	6
1.3.2 Amplitude Modulated Frequency Modulation	7
1.4 Electrophysiological Measure	8
1.4.1 Auditory Brainstem Response.....	8
1.4.2 Envelope Following Response	10
1.5 Behavioral Measure.....	10
1.6 Techniques for Neuromodulation.....	12
1.6.1 Pharmacogenetics.....	12
1.7 Research Questions	16
2. METHODS	17
2.1 Standard Behavioral and Electrophysiological Techniques to Show Pitch Sweep Discrimination.....	17
2.1.1 Acoustic Stimuli.....	17
2.1.2 Electroencephalogram Recordings.....	17
2.1.2.1 Auditory Brainstem Response.....	18
2.1.2.1.1 Data Acquisition and Recording.....	18
2.1.2.1.2 Data Analysis and Classification	18
2.1.2.2 Envelope Following Response	20
2.1.2.2.1 Data Acquisition and Recording.....	20
2.1.2.2.2 Data Analysis and Classification	20
2.1.3 Acoustic Startle Training	22

2.1.3.1	Data Acquisition and Recording	22
2.1.3.2	Data Analysis and Classification.....	23
2.2	Aging Effects on IRN Pitch Sweep Discrimination	25
2.2.1	Subjects	25
2.2.2	Acoustic Stimuli	25
2.2.3	Electroencephalogram Recordings.....	26
2.2.4	Acoustic Startle Training	27
2.3	Aging and Habituation Prepulse Effects on Pitch Sweep Discrimination and Differentiation.....	28
2.3.1	Subjects	28
2.3.2	Acoustic Stimuli	28
2.3.3	Electroencephalogram Recordings.....	29
2.3.4	Acoustic Startle Training	30
2.4	Corticofugal Modulation Effects on Pitch Sweep Discrimination and Differentiation .	31
2.4.1	Subjects	31
2.4.2	Acoustic Stimuli	32
2.4.3	Stereotaxic Viral Injections Surgery	32
2.4.3.1	Viral Vectors	32
2.4.3.2	Surgical Procedure	32
2.4.3.3	Dye Injection Test Surgeries	36
2.4.4	Electroencephalogram Recordings.....	36
2.4.5	Acoustic Startle Training	37
2.4.6	Histology	39
2.4.6.1	Perfusion.....	39
2.4.6.2	Tissue Blocking and Sectioning.....	39
2.4.6.3	Primary Auditory Cortex Histology	39
2.4.6.3.1	Staining and Mounting.....	39
2.4.6.3.2	Confocal Imaging.....	40
2.4.6.4	Dye Injection Surgery Slices.....	40
2.4.6.4.1	Mounting.....	40
2.4.6.4.2	Confocal Imaging.....	40

2.4.6.5	Histological Image Quantification	41
3.	RESULTS	42
3.1	Aging Effects on IRN Pitch Sweep Discrimination	42
3.1.1	Electroencephalogram Recordings.....	42
3.1.1.1	Auditory Brainstem Response.....	42
3.1.1.2	Envelope Following Response	43
3.1.1.2.1	Startle Stimuli	43
3.1.1.2.2	Related IRN Stimuli.....	45
3.1.2	Acoustic Startle Response	49
3.2	Aging and Habituation Prepulse Effects Pitch Sweep Discrimination and Differentiation	50
3.2.1.1	Electroencephalogram Recordings.....	50
3.2.1.2	Auditory Brainstem Response.....	50
3.2.1.3	Envelope Following Response	51
3.2.1.3.1	Startle Stimuli	52
3.2.1.3.2	Related Stimuli.....	55
3.2.2	Acoustic Startle Response	59
3.3	Corticofugal Modulation Effects on Pitch Sweep Discrimination and Differentiation .	63
3.3.1	Dye Injection Surgery	63
3.3.2	Electroencephalogram Recordings.....	64
3.3.2.1	Auditory Brainstem Response.....	64
3.3.2.2	Envelope Following Response	66
3.3.2.2.1	Startle Stimuli	66
3.3.2.2.2	Related Stimuli.....	70
3.3.3	Acoustic Startle Response	74
3.3.4	Histology	78
4.	DISCUSSION.....	81
4.1	Aging Effects on IRN Pitch Sweep Discrimination	81
4.2	Aging and Habituation Prepulse Effects on Pitch Sweep Discrimination and Differentiation.....	81

4.2.1	Aging and Habituation Prepulse Effects on Combination of Acoustic Startle Response and Envelope Following Response	81
4.2.2	Aging and Habituation Prepulse Effects on Acoustic Startle Response	82
4.2.3	Aging and Habituation Prepulse Effects on Envelope Following Response	83
4.3	Corticofugal Modulation Effects on Pitch Sweep Discrimination and Differentiation .	84
4.3.1	Corticofugal Modulation Effects on Combination of Acoustic Startle Response and Envelope Following Response	84
4.3.2	Corticofugal Modulation Effects on Acoustic Startle Response.....	86
4.3.3	Corticofugal Modulation Effects on Envelope Following Response.....	88
5.	CONCLUSION.....	90
5.1	Aging Effects on Behavioral and Electrophysiological IRN Pitch Sweep Learning	90
5.2	Aging and Habituation Prepulses Effects on Behavioral and Electrophysiological Pitch Sweep Learning and Differentiation.....	90
5.3	Corticofugal Modulation Effects on Behavioral and Electrophysiological Pitch Sweep Learning and Differentiation.....	90
	APPENDIX A. INCOMPLETE DATA	92
	APPENDIX B. EEG DATA TABLES	95
	APPENDIX C. HISTOLOGY IMAGES	109
	APPENDIX D. DETAILED INSTRUCTIONS	115
	REFERENCES	124

LIST OF TABLES

Table 2.1 Subject Groups.....	28
Table 3.1 Aging Effects Model Pre and Post Training Acoustic Hearing Threshold (dB SPL) from Channel 1	42
Table 3.2 Aging and Habituation Prepulse Effects Model Pre and Post Training Acoustic Hearing Threshold (dB SPL) from Channel 1	51
Table 3.3 Acoustic Hearing Thresholds (dB SPL) throughout Experiment from Channel 1	65
Table 3.4 DREADDs Activation Hemisphere	79
Table 3.5 DREADDs Quantification of Activation by Hemisphere.....	80
Table 4.1 Learning Results Legend	81
Table 4.2 Summary of Aging Effects on Learning Results for IRN Pitch Sweep. Legend: Table 4.1.....	81
Table 4.3 Summary of Aging and Habituation Prepulse Effects on Learning and Pitch Sweep Differentiation. Legend: Table 4.1.....	82
Table 4.4 Aging and Habituation Prepulse Effects on Acoustic Startle Response. Legend: Table 4.1.....	83
Table 4.5 Aging and Habituation Prepulse Effects on Envelope Following Response. Legend: Table 4.1	84
Table 4.6 Corticofugal Modulation Effects on Learning and Pitch Sweep Differentiation. Legend: Table 4.1	85
Table 4.7 Corticofugal Modulation Effects on Acoustic Startle Response. Legend: Table 4.1 ...	87
Table 4.8 Corticofugal Modulation Effects on Envelope Following Response. Legend: Table 4.1	89

LIST OF FIGURES

- Figure 1.1 Auditory Pathway. A) Ascending auditory pathway. B) Descending auditory pathway. Areas of interest are inferior colliculus (IC) and Auditory Cortex. Adapted Figure [18]. 2
- Figure 1.2 The schematic diagram showing the lemniscal and non-lemniscal portions of IC, MGB, and AC and the ascending and descending pathways. The A1/IC corticofugal pathway begins mostly in layer 5 of A1 and ends mostly in DCIC/ECIC. The A1/MGB corticofugal pathway mostly goes from layer 6 to MGD/MGM. Adapted Figure. [26] 4
- Figure 1.3 Simplified schematic of IC, MGB, and AC pathway with corticofugal modulation of IC..... 5
- Figure 1.4 Complex sound wave with the temporal envelope highlighted in red and the temporal fine structure highlighted in blue. Adapted Figure [35] 6
- Figure 1.5 Spectrogram of types of iterative ripple noise. T1 is a flat tone, T2 is a curvilinear tone, and T2L is a linear tone. The white dots show the perceived pitch sweeps across time and frequency. The left y-axis is the final frequency and the right y-axis is the initial frequency. Adapted figure [38]...... 7
- Figure 1.6 Spectrogram of FM/AM signal with a centered tone around 2800 Hz and a decreasing pitch sweep added to the centered tone to model /ai/ vowel sound. Adapted figure [40] 8
- Figure 1.7 Animal ABR Waveform with corresponding associated brain regions. Peak 1 is associated with the auditory nerve (AN). Peak 2 is associated with the cochlear nucleus (CN). Peak 3 is associated with superior olivary complex (SOC), specifically the medial superior olive (MSO) and lateral superior olive (LSO). Peak 4 is associated with lateral lemniscus (LL) and inferior colliculus (IC). Peak 5 is also associated with IC. Based on another figure [48]...... 9
- Figure 1.8 Stimulus and Response plots of stimuli. The EFR locks to the envelope of the stimulus in the time domain. Adapted Figure [53]...... 10
- Figure 1.9 Schematic drawing of acoustic startle reflex in rat brainstem. First, a startle-eliciting stimulus activates the cochlea and the auditory nerve carries the signal to the cochlear root neurons (CRN). The signal is then carried to the trapezoid body (TB), where it is sent almost exclusively to the giant pontine reticular formation (PnC). The signal is then carried to the motor neurons and visible the acoustic startle response (ASR) occurs [60]...... 11
- Figure 1.10 Cre-dependent DREADDs activation method. Presence of Cre-recombinase triggers the inversion of inverted DREADDs between loxP sites [78]...... 13
- Figure 1.11 Summary of DREADDs activation pathway. The two types of designer drugs (CNO and SALB) are shown activating their labelled designer receptors to either increase or decrease neuronal firing. Adapted Figure [76]...... 14
- Figure 1.12 Types of transgenic expression of viral vectors for pharmacogenetics. A) The use of stereotaxic viral vector injections for a cell type specific promoter leading to cell-type specific impact but with limited pathway specificity. B) Dual injections of Cre-dependent DREADDs and

Cre-recombinase viral vectors for cell type and projection specific targeting leading to pathway specific effects. C) Cell type specific viral vectors in combination with local infusion of designer drug for pathway specific effects. D) Combination of different viral vectors for multiplexed cell manipulation. Adapted figure [45].	15
Figure 2.1 ABR Waveform of 4 channels at 95 dB SPL.	19
Figure 2.2 EFR Waveform of 4 Channels at 70 dB SPL. Response waveform is in blue and the stimulus end at 250 ms is shown in red.	21
Figure 2.3 Photo of Startle Setup in Larger Anechoic Chamber.	22
Figure 2.4 Example boxplot of normalized startle response of one animal across training days. The normalized response is the prepulse startle response normalized to the average of the SES control.	24
Figure 2.5 Acoustic startle training IRN pitch sweep stimuli (100-500 Hz and 1000-500 Hz) Spectrograms.	26
Figure 2.6 EEG 4 Channel Recording Differential Electrode Positioning	26
Figure 2.7 Acoustic Startle Training Test Day. A) The different components of a test day with the 5 minutes acclimation, habituation to create PPI, and test session to determine the PPI that was created. B) The test session has 9 blocks of 9 trials with 6 PPI trials and 3 controls. Based on figure [45].	27
Figure 2.8 FM/AM stimuli (8kHz + 100-500 Hz and 8kHz - 100-500 Hz) spectrogram	29
Figure 2.9 Acoustic Startle Training Test Day. A) The different components of a test day with the 5 minutes acclimation, habituation to create PPI, and test session of 7 block with 11 or 12 trials to determine the PPI that was created. B) The two types of test sessions. Type 1 with 7 PPI trials and 3 different controls (maximum startle, baseline, and decreased baseline). Type 2 with 8 PPI and 3 controls (2 maximum startle and 1 baseline)	31
Figure 2.10 DREADDs Injection Pathway	32
Figure 2.11 ECIC/DCIC Injection Location. A) Sketch of rat skull with the injection site location. B) Sketch of rat brain with the angled injection into ECIC/DCIC	34
Figure 2.12 Primary Auditory Cortex Injection Location. A) Sketch of rat skull with skull ridge location B) Sketch of rat brain with angled injection into primary auditory cortex (A1)	35
Figure 2.13 DREADDs EEG Recording A) EEG recording schedule B) EEG 6 Channel Recording Differential Electrode Positioning	37
Figure 2.14 Acoustic Startle Training A) Acoustic Startle Training Schedule and breakdown of test day procedures. B) Types of test sessions. Type 1 with 7 PPI trials and 3 different controls (maximum startle, baseline, and decreased baseline). Type 2 with 8 PPI trials and 3 baseline controls. Type 3 with 8 PPI and 3 controls (2 maximum startle and 1 baseline)	38
Figure 3.1 Example plot of peak 1 amplitudes from ABR of an animal across varying sound pressure levels before and after training	43

Figure 3.2 Aging Effects on training-related changes to correlation of response to envelope and temporal fine structure of IRN 100-500 stimulus. A) Shows the envelope emphasized pre-training response correlation and change between pre and post training response correlation to IRN 100-500 Hz for young (N=3) and aged (N=4) animals B) Shows the temporal fine structure emphasized pre-training response correlation and change between pre and post training response correlation to IRN 100-500 Hz for young (N=3) and aged (N=4) animals..... 44

Figure 3.3 Aging Effects on training-related changes to correlation of response to envelope and temporal fine structure of IRN 1000-500 stimulus A) Shows the envelope emphasized pre-training response correlation and change between pre and post training response correlation to IRN 1000-500 Hz for young (N=3) and aged (N=4) animals B) Shows the temporal fine structure emphasized pre-training response correlation and change between pre and post training response correlation to IRN 1000-500 Hz for young (N=3) and aged (N=4) animals..... 45

Figure 3.4 Aging Effects on training-related changes to correlation of response to envelope and temporal fine structure of IRN 500-1000 stimulus. A) Shows the envelope emphasized pre-training response correlation and change between pre and post training response correlation to IRN 500-1000 Hz for young (N=3) and aged (N=4) animals B) Shows the temporal fine structure emphasized pre-training response correlation and change between pre and post training response correlation to IRN 500-1000 Hz for young (N=3) and aged (N=4) animals 46

Figure 3.5 Aging Effects on training-related changes to correlation of response to envelope and temporal fine structure of IRN 500-100 stimulus. A) Shows the envelope emphasized pre-training response correlation and change between pre and post training response correlation to IRN 500-100 Hz for young (N=3) and aged (N=4) animals B) Shows the temporal fine structure emphasized pre-training response correlation and change between pre and post training response correlation to IRN 500-100 Hz for young (N=3) and aged (N=4) animals..... 47

Figure 3.6 Aging Effects on training-related changes to correlation of response to envelope and temporal fine structure of IRN 1000 flat tone stimulus. A) Shows the envelope emphasized pre-training response correlation and change between pre and post training response correlation to IRN 1000 Hz flat tone for young (N=3) and aged (N=4) animals B) Shows the temporal fine structure emphasized pre-training response correlation and change between pre and post training response correlation to IRN 1000 Hz flat tone for young (N=3) and aged (N=4) animals 48

Figure 3.7 Aging Effects on training-related changes to correlation of response to envelope and temporal fine structure of IRN 500 Hz flat tone. A) Shows the envelope emphasized pre-training response correlation and change between pre and post training response correlation to IRN 500 Hz flat tone for young (N=3) and aged (N=4) animals B) Shows the temporal fine structure emphasized pre-training response correlation and change between pre and post training response correlation to IRN 500 Hz flat tone for young (N=3) and aged (N=4) animals 49

Figure 3.8 Peak Deviation of Startle Response from the first test day of startle in both the median as well as the spread of the response. The bold and italic labels mean that the results were statistically significantly different from the first day from a one-way ANOVA test ($p < 0.05$) .. 50

Figure 3.9 Example plot of peak 1 amplitudes from ABR of an animal across varying sound pressure levels before and after training 51

Figure 3.10 Aging and habituation effects on training-related changes to correlation of response to envelope and temporal fine structure of IRN 100-500 stimulus. A) Shows the envelope emphasized pre-training response correlation and change between pre and post training response correlation to IRN 100-500 Hz for young (N=4;1 prepulse N:2; 2 prepulse N:2) and aged (N=2; 1 prepulse N:1; 2 prepulse N:1) animals B) Shows the temporal fine structure emphasized pre-training response correlation and change between pre and post training response correlation to IRN 100-500 Hz for young(N=4;1 prepulse N:2; 2 prepulse N:2) and aged (N=2; 1 prepulse N:1; 2 prepulse N:1) animals. 52

Figure 3.11 Aging and habituation effects on training-related changes to correlation of response to envelope and temporal fine structure of FM 8 kHz + 100-500. A) Shows the envelope emphasized pre-training response correlation and change between pre and post training response correlation to FM 8 kHz + 100-500 Hz for young (N=4;1 prepulse N:2; 2 prepulse N:2) and aged (N=2; 1 prepulse N:1; 2 prepulse N:1) animals B) Shows the temporal fine structure emphasized pre-training response correlation and change between pre and post training response correlation to FM 8 kHz + 100-500 Hz for young(N=4;1 prepulse N:2; 2 prepulse N:2) and aged (N=2; 1 prepulse N:1; 2 prepulse N:1) animals. 53

Figure 3.12 Aging and habituation effects on training-related changes to correlation of response to envelope and temporal fine structure of FM 8 kHz - 100-500. A) Shows the envelope emphasized pre-training response correlation and change between pre and post training response correlation to FM 8 kHz - 100-500 Hz for young (N=4;1 prepulse N:2; 2 prepulse N:2) and aged (N=2; 1 prepulse N:1; 2 prepulse N:1) animals B) Shows the temporal fine structure emphasized pre-training response correlation and change between pre and post training response correlation to FM 8 kHz - 100-500 Hz for young(N=4;1 prepulse N:2; 2 prepulse N:2) and aged (N=2; 1 prepulse N:1; 2 prepulse N:1) animals. 54

Figure 3.13 Aging and habituation effects on training-related changes to correlation of response to envelope and temporal fine structure of IRN 1000-500 stimulus. A) Shows the envelope emphasized pre-training response correlation and change between pre and post training response correlation to IRN 1000-500 Hz for young (N=4;1 prepulse N:2; 2 prepulse N:2) and aged (N=2; 1 prepulse N:1; 2 prepulse N:1) animals B) Shows the temporal fine structure emphasized pre-training response correlation and change between pre and post training response correlation to IRN 1000-500 Hz for young(N=4;1 prepulse N:2; 2 prepulse N:2) and aged (N=2; 1 prepulse N:1; 2 prepulse N:1) animals. 55

Figure 3.14 Aging and habituation effects on training-related changes to correlation of response to envelope and temporal fine structure of IRN 500-100 stimulus. A) Shows the envelope emphasized pre-training response correlation and change between pre and post training response correlation to IRN 500-100 Hz for young (N=4;1 prepulse N:2; 2 prepulse N:2) and aged (N=2; 1 prepulse N:1; 2 prepulse N:1) animals B) Shows the temporal fine structure emphasized pre-training response correlation and change between pre and post training response correlation to IRN 500-100 Hz for young(N=4;1 prepulse N:2; 2 prepulse N:2) and aged (N=2; 1 prepulse N:1; 2 prepulse N:1) animals. 56

Figure 3.15 Aging and habituation effects on training-related changes to correlation of response to envelope and temporal fine structure of IRN 500-1000 stimulus. A) Shows the envelope emphasized pre-training response correlation and change between pre and post training response correlation to IRN 500-1000 Hz for young (N=4;1 prepulse N:2; 2 prepulse N:2) and aged (N=2;

1 prepulse N:1; 2 prepulse N:1) animals B) Shows the temporal fine structure emphasized pre-training response correlation and change between pre and post training response correlation to IRN 500-1000 Hz for young(N=4;1 prepulse N:2; 2 prepulse N:2) and aged (N=2; 1 prepulse N:1; 2 prepulse N:1) animals. 57

Figure 3.16 Aging and habituation effects on training-related changes to correlation of response to envelope and temporal fine structure of IRN 1000 Hz flat tone stimulus. A) Shows the envelope emphasized pre-training response correlation and change between pre and post training response correlation to IRN 1000 Hz flat tone for young (N=4;1 prepulse N:2; 2 prepulse N:2) and aged (N=2; 1 prepulse N:1; 2 prepulse N:1) animals B) Shows the temporal fine structure emphasized pre-training response correlation and change between pre and post training response correlation to IRN 1000 Hz flat tone for young(N=4;1 prepulse N:2; 2 prepulse N:2) and aged (N=2; 1 prepulse N:1; 2 prepulse N:1) animals. 58

Figure 3.17 Aging and habituation effects on training-related changes to correlation of response to envelope and temporal fine structure of IRN 125 Hz flat tone stimulus. A) Shows the envelope emphasized pre-training response correlation and change between pre and post training response correlation to IRN 125 Hz flat tone for young (N=4;1 prepulse N:2; 2 prepulse N:2) and aged (N=2; 1 prepulse N:1; 2 prepulse N:1) animals B) Shows the temporal fine structure emphasized pre-training response correlation and change between pre and post training response correlation to IRN 125 Hz flat tone for young(N=4;1 prepulse N:2; 2 prepulse N:2) and aged (N=2; 1 prepulse N:1; 2 prepulse N:1) animals. 59

Figure 3.18 Peak Deviation of Startle Response to IRN 100-500 Hz pitch sweep prepulse and IRN 1000-500 Hz pitch sweep background stimulus from the first test day of startle in both the median as well as the spread of the response. The bold and italic labels mean that the results were statistically significantly different from the first day from a one-way ANOVA test ($p < 0.05$) .. 60

Figure 3.19 Peak Deviation of Startle Response to FM 8 kHz pitch sweeps prepulses and IRN 1000-500 Hz pitch sweep background stimulus from the first test day of startle in both the median as well as the spread of the response. The bold and italic labels mean that the results were statistically significantly different from the first day from a one-way ANOVA test ($p < 0.05$) A) Peak deviation of startle response from FM 8 kHz – 100-500 Hz prepulse. B) Peak deviation of startle response from FM 8 kHz + 100-500 Hz prepulse..... 61

Figure 3.20 Peak Deviation of Startle Response to white gaussian noise from the first test day of startle in both the median as well as the spread of the response. The bold and italic labels mean that the results were statistically significantly different from the first day from a one-way ANOVA test ($p < 0.05$) A) Peak deviation of startle response from white gaussian noise 40 dB above threshold or at 80 dB with a background stimulus of IRN 1000-500 Hz. B) Peak deviation of startle response from white gaussian noise 30 dB prepulse without a background stimulus. C) Peak deviation of startle response from white gaussian noise 50 dB prepulse without a background stimulus. D) Peak deviation of startle response from white gaussian noise 70 dB prepulse without a background stimulus. 63

Figure 3.21 IC Injection Site with Cresyl Violet dye injection (orange) and background fluorescence to show structure of slice (green)..... 64

Figure 3.22 A1 Injection Site Ranged Image of GFP fluorescence (gray)..... 64

Figure 3.23 Example plot of peak 1 amplitudes from ABR of an animal across varying sound pressure levels throughout experiment 66

Figure 3.24 Corticofugal Inhibition effects on training-related changes to correlation of response to envelope and temporal fine structure of IRN 100-500 Hz stimulus. A) Shows the envelope emphasized change between pre and post training response correlation and change between pre and post CNO response correlation to IRN 100-500 Hz stimulus for young (N=11) animals B) Shows the temporal fine structure emphasized change between pre and post training response correlation and change between pre and post CNO response correlation to IRN 100-500 Hz stimulus tone for young (N=11) animals. 67

Figure 3.25 Corticofugal Inhibition effects on training-related changes to correlation of response to envelope and temporal fine structure of FM 8 kHz + 100-500 Hz stimulus. A) Shows the envelope emphasized change between pre and post training response correlation and change between pre and post CNO response correlation to FM 8 kHz + 100-500 Hz stimulus for young (N=11) animals B) Shows the temporal fine structure emphasized change between pre and post training response correlation and change between pre and post CNO response correlation to FM 8 kHz + 100-500 Hz stimulus tone for young (N=11) animals. 68

Figure 3.26 Corticofugal Inhibition effects on training-related changes to correlation of response to envelope and temporal fine structure of FM 8 kHz - 100-500 Hz stimulus. A) Shows the envelope emphasized change between pre and post training response correlation and change between pre and post CNO response correlation to FM 8 kHz - 100-500 Hz stimulus for young (N=11) animals B) Shows the temporal fine structure emphasized change between pre and post training response correlation and change between pre and post CNO response correlation to FM 8 kHz - 100-500 Hz stimulus tone for young (N=11) animals. 69

Figure 3.27 Corticofugal Inhibition effects on training-related changes to correlation of response to envelope and temporal fine structure of IRN 1000-500 Hz stimulus. A) Shows the envelope emphasized change between pre and post training response correlation and change between pre and post CNO response correlation to IRN 1000-500 Hz stimulus for young (N=11) animals B) Shows the temporal fine structure emphasized change between pre and post training response correlation and change between pre and post CNO response correlation to IRN 1000-500 Hz stimulus tone for young (N=11) animals. 70

Figure 3.28 Corticofugal Inhibition effects on training-related changes to correlation of response to envelope and temporal fine structure of IRN 500-100 Hz stimulus. A) Shows the envelope emphasized change between pre and post training response correlation and change between pre and post CNO response correlation to IRN 500-100 Hz stimulus for young (N=11) animals B) Shows the temporal fine structure emphasized change between pre and post training response correlation and change between pre and post CNO response correlation to IRN 500-100 Hz stimulus tone for young (N=11) animals. 71

Figure 3.29 Corticofugal Inhibition effects on training-related changes to correlation of response to envelope and temporal fine structure of IRN 500-1000 Hz stimulus. A) Shows the envelope emphasized change between pre and post training response correlation and change between pre and post CNO response correlation to IRN 500-1000 Hz stimulus for young (N=11) animals B) Shows the temporal fine structure emphasized change between pre and post training response

correlation and change between pre and post CNO response correlation to IRN 500-1000 Hz stimulus tone for young (N=11) animals 72

Figure 3.30 Corticofugal Inhibition effects on training-related changes to correlation of response to envelope and temporal fine structure of IRN 1000 Hz flat tone stimulus. A) Shows the envelope emphasized change between pre and post training response correlation and change between pre and post CNO response correlation to IRN 1000 Hz flat tone stimulus for young (N=11) animals B) Shows the temporal fine structure emphasized change between pre and post training response correlation and change between pre and post CNO response correlation to IRN 1000 Hz flat tone stimulus tone for young (N=11) animals 73

Figure 3.31 Corticofugal Inhibition effects on training-related changes to correlation of response to envelope and temporal fine structure of IRN 125 Hz flat tone stimulus. A) Shows the envelope emphasized change between pre and post training response correlation and change between pre and post CNO response correlation to IRN 125 Hz flat tone stimulus for young (N=11) animals B) Shows the temporal fine structure emphasized change between pre and post training response correlation and change between pre and post CNO response correlation to IRN 125 Hz flat tone stimulus tone for young (N=11) animals 74

Figure 3.32 Peak Deviation of Startle Response to IRN 100-500 Hz pitch sweep prepulse and IRN 1000-500 Hz pitch sweep background stimulus from the first test day of startle in both the median as well as the spread of the response. The bold and italic labels mean that the results were statistically significantly different from the first day from a one-way ANOVA test ($p < 0.05$) .. 75

Figure 3.33 Peak Deviation of DREADDs animal Startle Response to FM 8 kHz pitch sweeps prepulses and IRN 1000-500 Hz pitch sweep background stimulus from the first test day of startle in both the median as well as the spread of the response. The bold and italic labels mean that the results were statistically significantly different from the first day from a one-way ANOVA test ($p < 0.05$) A) Peak deviation of startle response from FM 8 kHz – 100-500 Hz prepulse. B) Peak deviation of startle response from FM 8 kHz + 100-500 Hz prepulse. 76

Figure 3.34 Peak deviation of DREADDs animal startle response to white gaussian noise from the first test day of startle in both the median and spread of the response. A) Peak deviation of startle response from white gaussian noise 40 dB above threshold or at 80 dB with a background stimulus of IRN 1000-500 Hz. B) Peak deviation of startle response from whit gaussian noise 30 dB prepulse without a background stimulus. C) Peak deviation of startle response from white gaussian noise 50 dB prepulse without a background stimulus. D) Peak deviation of startle response from whit gaussian noise 70 dB prepulse without a background stimulus..... 77

Figure 3.35 Example of DREADDs mCherry fluorescence showing activation in auditory cortex 78

Figure 3.36 Example of DREADDs mCherry fluorescence showing activation in auditory cortex and stained slice with VGlut2 highlighting layers 3 and 6 of auditory cortex. 79

ABBREVIATIONS

A1	Primary auditory cortex
AAV	Adeno-associated virus
ABR	Auditory brainstem response
AC	Auditory cortex
AEP	Auditory evoked potential
AM	Amplitude modulation
AN	Auditory nerve
A/P	Anterior/Posterior
ARHL	Age-related hearing loss
ASR	Acoustic startle response
BPN	Bandpass noise
BSA	Bovine serum albumin
CIC	Central inferior colliculus
CN	Cochlear nucleus
CNO	Clozapine N-oxide
CRN	Cochlear root neurons
DCIC	Dorsal cortex inferior colliculus
DREADD	Designer receptors exclusively activated by designer drugs
D/V	Dorsal/Ventral
EBFP	Blue fluorescent protein
ECIC	External cortex inferior colliculus
EEG	Electroencephalogram
EFR	Envelope following response
EP	Evoked potential
FM	Frequency modulation
GFP	Green fluorescent protein
IC	Inferior colliculus
IM	Intramuscular
IP	Intraperitoneal

IQR	Interquartile range
IRN	Iterated rippled noise
LL	Lateral lemniscus
LSO	Lateral superior olive
MGB	Medial geniculate body
M/L	Medial/Lateral
MNTB	Medial nucleus of the trapezoid body
MSO	Medial superior olive
OCT	Optical cutting temperature
PBS	Phosphate buffered solution
PBST	Phosphate buffered solution-Triton
PnC	Pontine reticular formation
PPI	Prepulse inhibition
ROD	Relative optical density
SES	Startle eliciting stimulus
SOC	Superior olivary complex
SPL	Sound pressure level
Sub-Q	Subcutaneous
WBN	Wide band noise
WGN	White gaussian noise

ABSTRACT

Author: Dowling, Marisa, A. MS

Institution: Purdue University

Degree Received: May 2019

Title: Effects of Aging and Corticofugal Modulation on Startle Behavior and Auditory Physiology

Committee Chair: Edward Bartlett

Frequency-modulated (FM) sweeps play a key role in species specific communication. Evidence from previous studies have shown that central auditory processing has been shown to vary based on the language spoken, which leads to the idea of experience-driven pitch encoding. Other studies have also shown that there is a decrease in this pitch encoding with aging. Using both iterated rippled noise (IRN) and frequency modulated amplitude modulation (FM/AM) methods to create complex pitch sweeps mimicking speech, allows for the processing of pitch to be determined. Neuromodulation using pharmacogenetics allows for the targeted inhibition of a specific neural pathway. Based on previous studies, the primary auditory cortex to inferior colliculus (A1/IC) pathway is hypothesized to be important in pitch encoding. However, there is a lack of evidence on specifically how the pitch information is encoded in the auditory system and how aging impacts the processing. To solve these issues, age-related changes in pitch encoding and maintaining pitch encoding through neuromodulation were characterized in the using behavioral and electrophysiology methods. Behavioral discrimination abilities, measured by modulation of the acoustic startle response, between pitch sweep direction and pitch sweep creation methods highlighted a reduced discrimination in aging and A1/IC inhibited rats. Electrophysiology changes was assessed using envelope-following responses (EFRs) and suggested a decreased initial frequency locking in aging and decrease in frequency locking overall with A1/IC pathway inhibition. Comparison of behavioral and electrophysiology to IRN and FM/AM stimuli show that the decrease in age-related processing as well as A1/IC pathway processing is larger in the behavioral pitch sweep discrimination than in the reduction in EFRs.

1. INTRODUCTION

Frequency modulated (FM) sweeps have been shown to play an important role in species-specific communication, including human speech [1–7]. Central auditory encoding of FM sweeps has been shown to vary between English and Chinese speakers [8–10]. This leads to the idea of experience-driven pitch encoding of the sweeps in the auditory processing system [8]. Furthermore, central auditory encoding of FM sweeps has been shown to be impacted by age-related hearing loss (ARHL) [11–16]. This leads to the idea of a decrease in pitch encoding of the sweeps in the aged auditory system [16].

1.1 Overview of the Auditory System

Understanding the auditory processing system is the first step in determining the pathways involved in experience-driven pitch encoding. The auditory system must both be able to rapidly process temporal fluctuations in sound and extract behaviorally meaningful signals from background noise; it handles the complexity of processing through parallel systems in both the ascending and descending auditory pathways (Figure 1.1). The ascending pathway is used to encode the auditory information, such as frequency and origin location of sound, and the descending pathway is used to control auditory attention and focus on the behaviorally meaningful signals [17].

The ascending pathway begins after a sound pressure wave enters the ear when the mechanical wave is converted to an electrical signal in the cochlea and converted to action potentials at the inner hair cell-auditory nerve synapse [18]. Then it travels through the auditory nerve into the cochlear nucleus (CN), where temporal fluctuations and extraction of stimuli are separated into parallel processing, temporal and intensity processing. The action potentials are then sent to both the contralateral and ipsilateral superior olivary complex (SOC) [18]. The SOC is made up of the medial superior olive (MSO), the lateral superior olive (LSO), and the medial nucleus of the trapezoid body (MNTB) [18]. The MSO processes the temporal differential between ears, while the LSO processes the difference in interaural intensity [19]. The medial nucleus of the trapezoid body (MNTB) determines the location of the sound as well as temporal features of complex sounds

between the ears [20]. Brainstem auditory afferents targeting the IC separate into the lemniscal or non-lemniscal pathway. The lemniscal pathway send the action potentials from the CN and LSO and travels to both the contralateral and ipsilateral inferior colliculus (IC), specifically central IC (CIC), through the lateral lemniscus (LL). The non-lemniscal pathway propogates the action potentials directly to both the contralateral and ipsilateral IC, specifically dorsal and external cortex IC (DCIC and ECIC) [21]. The lemniscal and non-lemniscal components of IC integrate the sound localization, sound identification, and response to temporally complex stimuli. They take the acoustic characteristics and begins combining them into recognizable auditory objects [18]. CIC is tonotopic and integrates the different components of sound. DCIC/ECIC detect novel auditory signals and focuses auditory attention [22]. The parallel pathway of the signals are then passed from IC to the medial geniculate body (MGB). In MGB, the spatial, spectral, and temporal features are integrated to better define auditory objects that are passed onto auditory cortex (AC), specifically primary auditory cortex (A1). A1 is significant in processing frequency discrimination and specifically significant in recognition of short stimuli. Another key role of A1 is in processing complex auditory tasks such as understanding speech [18].

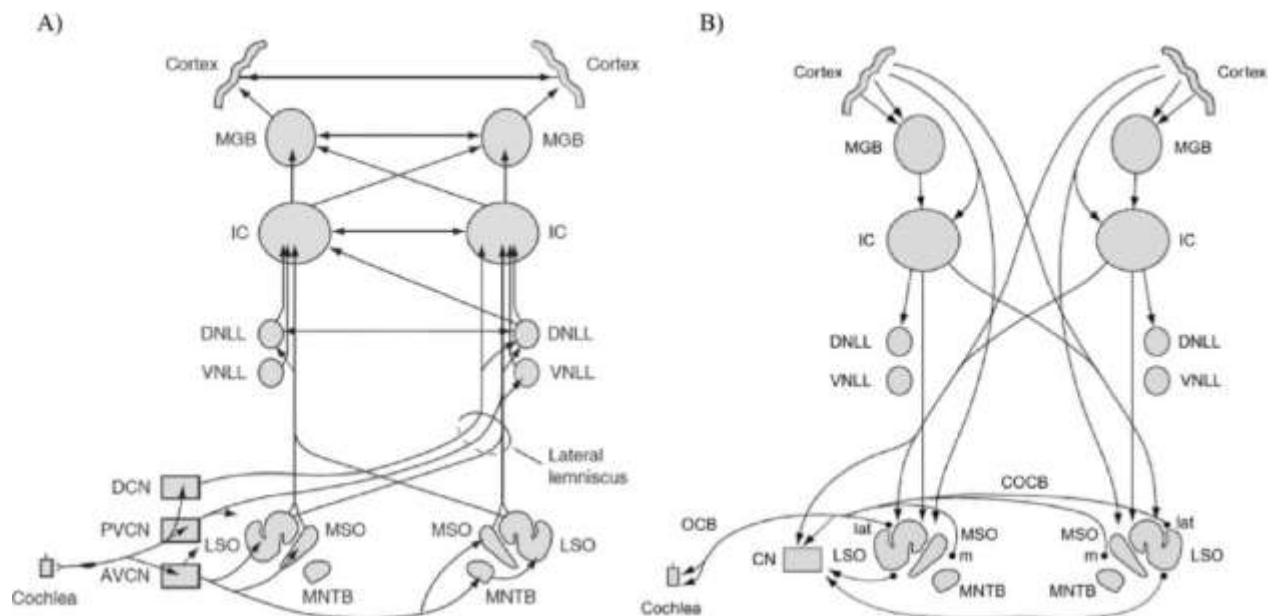


Figure 1.1 Auditory Pathway. A) Ascending auditory pathway. B) Descending auditory pathway. Areas of interest are inferior colliculus (IC) and Auditory Cortex. Adapted Figure [18].

The descending auditory pathway begins in the AC and travels throughout the auditory system, where it highlights the importance of the frequency modulated sweeps and auditory objects identified in the ascending pathway. This process in turn decreases responses in auditory cortex through the ascending pathway [18]. The strongest parallel descending pathways go from AC to IC or AC to MGB [23]. From IC, the descending pathway passes information all the way back to the auditory nerve, where it neurally inhibits the response, and the cochlea, where it reduces the degree of active mechanical activation [18].

1.2 Cortical Projections

A main hypothesized function of the auditory cortex, specifically A1, is pitch sweep perception [24]. This was shown in an fMRI study where there was an increase in activation of auditory cortex to the pitch sweeps in comparison to steady-state sound [3]. The corticofugal pathways involved in the variation of response between sweeps and steady-state sound are the pathways to IC and MGB. As the projections to IC and MGB modulate the ascending pathways response to repeated stimuli, they decrease response to repeated noise and emphasize behaviorally relevant signals. The pathways almost exclusively end in the non-lemniscal part of IC (DCIC/ECIC) and MGB [25].

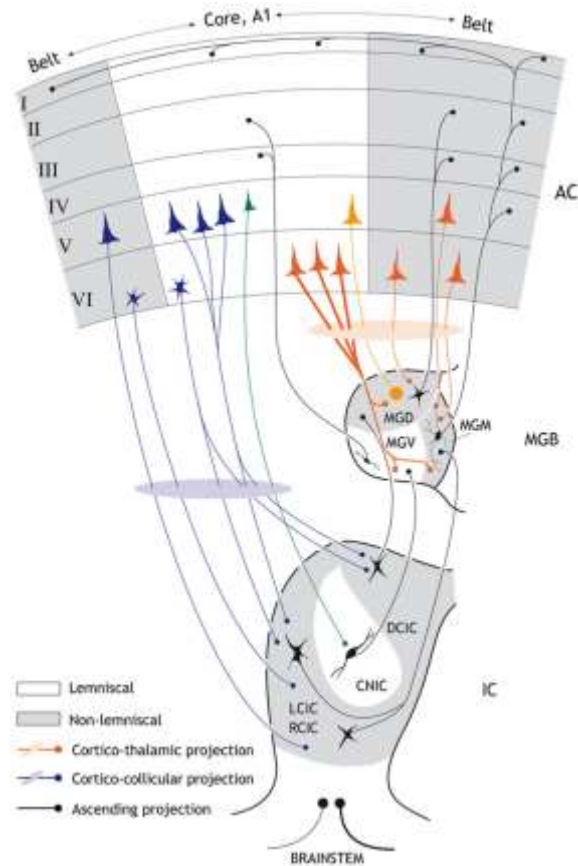


Figure 1.2 The schematic diagram showing the lemniscal and non-lemniscal portions of IC, MGB, and AC and the ascending and descending pathways. The A1/IC corticofugal pathway begins mostly in layer 5 of A1 and ends mostly in DCIC/ECIC. The A1/MGB corticofugal pathway mostly goes from layer 6 to MGD/MGM. Adapted Figure. [26]

Previous studies have shown changes in response properties in IC after auditory conditioning [27–29]. Therefore, corticofugal pathway from layer 5 of A1 to DCIC/ECIC has been particularly theorized to drive experience-dependent pitch encoding (Figure 1.2 and Figure 1.3) [8]. The general question of this study is whether the corticofugal A1/IC pathway is relevant to experience-driven pitch processing using both behavioral and electrophysiological measures.

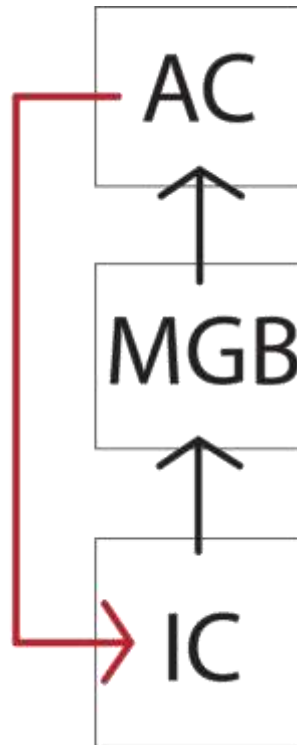


Figure 1.3 Simplified schematic of IC, MGB, and AC pathway with corticofugal modulation of IC.

In order to determine the role of the A1/IC pathway for experience-driven pitch encoding, causal modulation of an animal model would need to be employed. There are numerous studies on rats pitch processing, making a rat model an effective option to display experience-driven pitch encoding of non-semantic pitch sweeps [2, 30–32].

1.3 Non-semantic Pitch Sweeps

In order to ensure linguistically relevant processing without the lexical information, two main types of stimuli are used: iterative rippled noise (IRN) and amplitude modulated frequency modulation (FM/AM). Both stimuli mimic the same auditory features and characteristics present in speech for the brain to process without the encoded semantic information provided in speech [33]. In processing speech, sound can be broken into two auditory characteristics: the envelope and temporal fine structure (TFS) (*Figure 1.4*). The temporal envelope is the amplitude modulations of the sound wave in time. The temporal fine structure is the rapid oscillations close to the center frequency of the band [34].

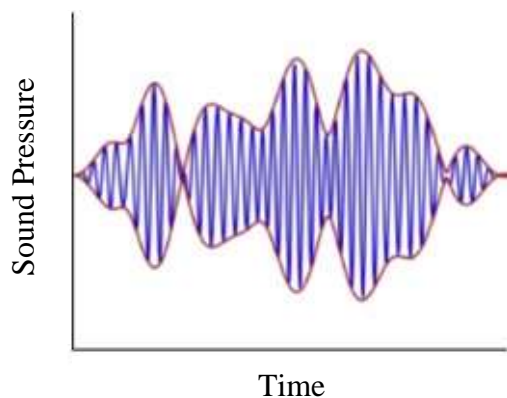


Figure 1.4 Complex sound wave with the temporal envelope highlighted in red and the temporal fine structure highlighted in blue. Adapted Figure [35]

The envelope of both stimuli types is the pitch sweep of interest. The temporal fine structure of IRN is wideband noise and FM/AM is the 8 kHz tone.

1.3.1 Iterative Rippled Noise

Current methods for encoding auditory features with minimal interactions of language involve using IRN to create Chinese-like tones [3, 8, 36, 37]. IRN is broadband noise with temporal regularities created by iterative delay and add operations at regular intervals to create perceivable pitch without the confounding semantic information [36]. This perceived pitch sweep can be a linear, flat, or curvilinear FM as shown in the narrowband spectrograms in Figure 1.5. T1 and T2 are modeled after lexical Mandarin tones. T2L is a simplified linear version of the standard T2 tone that can be used to show learning. These tones have been used on human both native tonal language speakers and non-tonal language speakers to determine differences in overall neural response to pitch changes alone using auditory evoked potentials (AEP) extracted from electroencephalogram (EEG) recordings [38].

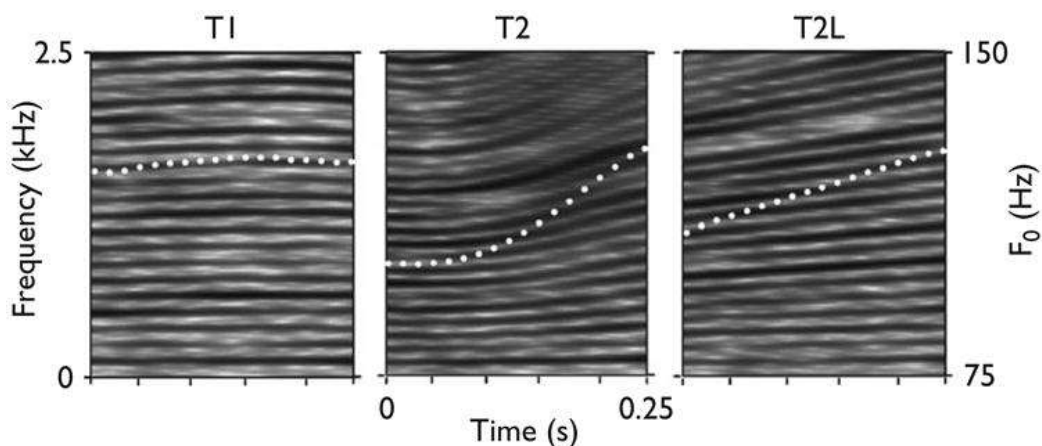


Figure 1.5 Spectrogram of types of iterative ripple noise. T1 is a flat tone, T2 is a curvilinear tone, and T2L is a linear tone. The white dots show the perceived pitch sweeps across time and frequency. The left y-axis is the final frequency and the right y-axis is the initial frequency. Adapted figure [38].

The T2L stimulus is a linear pitch sweep from 105 to 150 Hz. Given that the normal hearing range for rats is for frequencies between 250 Hz and 80 kHz with increased sensitivity at 8 kHz, T2L is outside the normal processing [39]. Previous preliminary experiments suggested a lack of response in rats to the smaller pitch contours. By creating a larger sweep from 100 to 500 Hz, it maintains the frequencies in the original pitch sweep but expands them to create a larger pitch contour for the rats to recognize.

1.3.2 Amplitude Modulated Frequency Modulation

Another current method for encoding auditory features without the other interactions of language involve using amplitude modulated frequency modulation (FM/AM) [40, 41]. The FM/AM stimuli are made using a tone to center the pitch and then adding or subtracting the pitch sweep of interest, similar to how vowel sounds are made (Figure 1.6) [40].

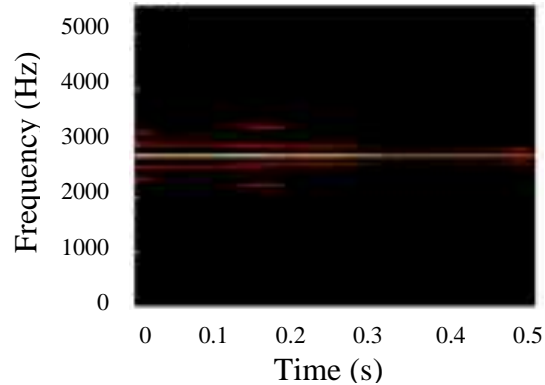


Figure 1.6 Spectrogram of FM/AM signal with a centered tone around 2800 Hz and a decreasing pitch sweep added to the centered tone to model /ai/ vowel sound. Adapted figure [40]

Since rats have increased sensitivity at 8 kHz, centering the FM/AM stimuli at 8 kHz would model a vowel sound clearly in the rats hearing [39]. Keeping the same pitch sweep of interest from 100 to 500 Hz and using the reversal to create these sweeps would model vowel processing.

1.4 Electrophysiological Measure

A standard non-invasive *in vivo* electrophysiological recording method for monitoring and measuring changes in neural activity is EEG recording. EEG recordings monitor scalp electrical activity of the entire brain. EEGs use surface or subdermal electrodes to record the voltage changes in the brain from neural activity [42]. Event related potentials (ERP) are temporally locked patterns of neural activity in response to external events or tasks [43]. Evoked potentials (EP) are responses to sensory stimulation, generally either visual or auditory. The EPs that are driven by auditory stimuli are known as auditory evoked potentials (AEP) [44]. AEPs are made up of repeatable peaks and latencies at amplitudes that provide information about changes to the central and periphery auditory processing [45]. Two common AEPs are auditory brainstem response (ABR) and envelope or frequency following response (EFR or FFR) [11]. Since the first 0-12 ms of all AEPs have ABRs present, the first 0-12 ms of the EFR will contain an ABR also [44].

1.4.1 Auditory Brainstem Response

Auditory brainstem responses (ABRs) are AEPs that are neural activity that is synchronized to onset of a brief stimulus, such as a click stimulus. A triggered average of the response creates a

consistent waveform given the recording location (Figure 1.7). Recording ABRs at varying sound levels is commonly used as an effective way to check hearing threshold [46]. The waveform is made up of 5 reproducible peaks (I-V). Peaks I, III, IV have all been shown to have clinical significance in ensuring the functionality of the auditory system. Peak I is predicted to show the functionality of the AN [44]. Peak II is believed to show the functionality of cochlear nucleus [44]. Peak III is associated with superior olivary complex (SOC), specifically with MSO and LSO, and peak IV is dependent on the functionality of LL and IC [44]. Peak 5 has also been shown to be related to IC [47].

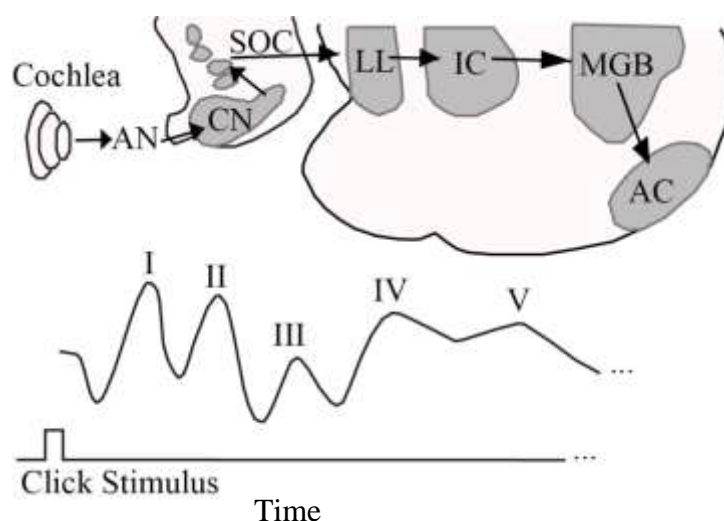


Figure 1.7 Animal ABR Waveform with corresponding associated brain regions. Peak 1 is associated with the auditory nerve (AN). Peak 2 is associated with the cochlear nucleus (CN). Peak 3 is associated with superior olivary complex (SOC), specifically the medial superior olive (MSO) and lateral superior olive (LSO). Peak 4 is associated with lateral lemniscus (LL) and inferior colliculus (IC). Peak 5 is also associated with IC. Based on another figure [48].

As the waveform is consistent, playing the click stimulus at varying decibels of sound pressure levels allows the waveforms to be compared to determine the auditory detection threshold. The auditory detection threshold has been shown to increase with age as part of ARHL. Another key feature is the ABR peak amplitude, as it shows how well the auditory system is functioning across the different decibel levels [11]. There can still be auditory damage caused by loud noises that is not shown only in the threshold measurement. Exposure to noises above the level of 100 dB SPL for long durations of time can lead to death of low-spontaneous response neurons in the auditory nerve [49]. In a previous study, the threshold returned to normal but the amplitude of peak I

drastically decreases after the sound exposure because of the death of low-spontaneous rate neurons in the auditory nerve [50]. In the current study, both the auditory detection threshold and peak 1 amplitude must remain unchanged to ensure changes in recordings were not due to hearing damage.

1.4.2 Envelope Following Response

Envelope following responses (EFR) are AEPs with sustained stimulus-locked neural activity [51]. As shown in Figure 1.8, EFRs show the modulation of the envelope and latency of the auditory brainstem and midbrain by using an envelope frequency varying stimulus, such as the FM/AM stimulus [52].

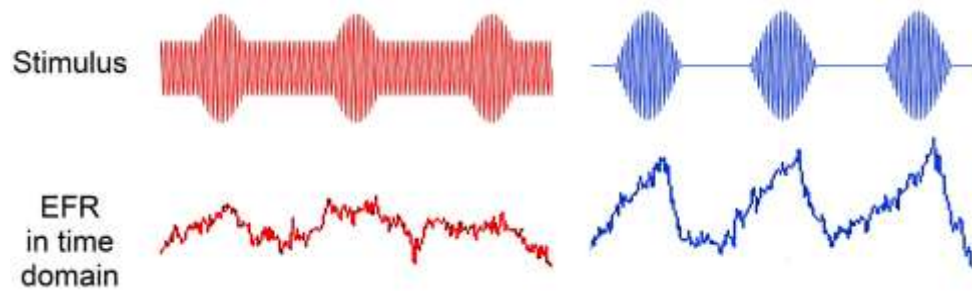


Figure 1.8 Stimulus and Response plots of stimuli. The EFR locks to the envelope of the stimulus in the time domain. Adapted Figure [53].

The EFR temporally locks with the varying frequency and preserves the pitch-relevant information. There is a strong correlation between EFR and perceived pitch sweeps [54]. Previous studies have shown a decrease in EFR response in aged animals [47, 55]. In this study, the IRN and FM/AM stimuli were used to determine how well the response locked in time with the pitch sweep of interest.

1.5 Behavioral Measure

In order to evaluate the effect of differences in neural processing on behavior, startle behavior is a broadly applied paradigm for behavioral sensory studies as it involves a reflexive rapid defense mechanism known as acoustic startle response (ASR) [56–65]. ASR is a transient contraction of skeletal muscles in response to startle-eliciting stimulus (SES) [57]. The SES is a sudden, short,

intense noise generally about 80 dB above auditory detection threshold [58]. As the ASR is a simple brainstem-spinal cord reflex, it has an extremely short latency and shouldn't be distorted by any corticofugal modulation [59]. The ASR is modulated by the pontine reticular formation, that activates the motor neurons in the spine (Figure 1.9) [60].

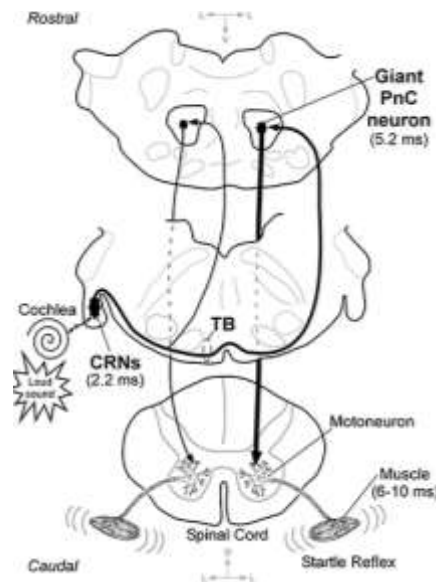


Figure 1.9 Schematic drawing of acoustic startle reflex in rat brainstem. First, a startle-eliciting stimulus activates the cochlea and the auditory nerve carries the signal to the cochlear root neurons (CRN). The signal is then carried to the trapezoid body (TB), where it is sent almost exclusively to the giant pontine reticular formation (PnC). The signal is then carried to the motor neurons and visible the acoustic startle response (ASR) occurs [60].

The ASR can be significantly modulated by using a different auditory stimulus, known as a prepulse, to predict SES. The prepulse is a non-startling stimulus that is played prior to the SES. The amount of inhibition of ASR when the prepulse is played is prepulse inhibition (PPI). The animal's prepulse detection ability is proportional to the PPI [61]. Since the hypothesized neural pathway for prepulse detection travels from the cochlea to IC and then through superior colliculus to the caudal nucleus of the pontine reticular formation, there needs to be 20-500 ms between the prepulse and the SES to ensure there is enough time for the signal to inhibit ASR [62]. As PPI is a measure of sensorimotor gating, it regulates the sensory input to the brain and allows early stage information processing without disruption [59]. Prepulses with diverse temporal characteristics can still induce PPI. The standard prepulse tends to be white gaussian noise for a maximum of 100 ms [63]. The speech sounds tend to be between 100 to 300 ms. In a previous study, the startle

behavior paradigm was used to show young Sprague-Dawley rats could discriminate between speech sounds, such as [pae] and [bae] [64]. Another previous study showed a decrease in discrimination of aged F-344 rats compared to the young F-344 rats [65]. This study involves the discrimination behavior of the animals of both young and aged F-344 rats to pitch sweep prepulse stimuli, such as IRN.

1.6 Techniques for Neuromodulation

When modulating neural activity, common methods involve pharmacological blockades, electrical stimulation, pharmacogenetics modulation, and optogenetics modulation [66–70]. Pharmacological blockades and electrical stimulation can provide useful information in the understanding overall central auditory processing regions, such as auditory cortex, but can't selectively target any specific cell types or layers of auditory cortex. A pharmacological blockade, such as musimol, can effectively inhibit and modulate the auditory cortex but inhibits everything that is near it and not confined to a specific layer [67]. Electrical stimulation of auditory cortex can effectively reduce tinnitus, but this was achieved through nonspecific stimulation of auditory cortex [68]. Pharmacogenetics and optogenetics modulation have the potential for a much more focused and specific pathway modulation. Pharmacogenetics is a lock-and-key approach using designer receptors to selectively modulate neural processing using pharmaceuticals. Optogenetics uses light-sensitive proteins to modulate neuronal processing. Both of these methods involve using viral vectors to specifically target the pathway of interest [69]. Pharmacogenetics, unlike optogenetics, can be immediately implemented into freely moving behavior experiments to determine the role of specific neural pathways [70]. As mentioned previously, the neural pathway of interest for this study is A1/IC in the descending auditory circuit.

1.6.1 Pharmacogenetics

The main method of pharmacogenetics used is Designer Receptors Exclusively Activated by Designer Drugs (DREADDs), as they allow for highly specific intermittent modulation of neural circuits [45, 71–76]. Stereotaxic injections of the DREADDs viral vectors creates a localization of designer receptors only in the injected area [76]. With this in mind, there is a wide selection of types of DREADDs based on the goal of the neuromodulation. The DREADDs construct is made up of the plasmid type, promoter, receptor, and fluorescent tag. Firstly, the plasmid type depends

on two components: the viral construct and Cre-dependence. The standard viral construct options are herpes simplex virus (HSV), adeno-associated virus (AAV), lentivirus (LV), and canine adenovirus (CAV2) [72]. While all of these options are available the most commonly used virus is AAV as they always target the soma of the cell type of interest making the replication process easier by having the necessary replication supplies being localized [71]. The AAV has different serotypes that function best based on the cell population of interest. Serotypes 1, 2, 4, 5, 8, and 9 work best for central nervous system (CNS) targets. The serotype with the highest expression is also dependent on the brain region of interest, such as for auditory cortex, in order from highest to lowest, 9, 8, 6, 5, 1, and 2 [77]. The final portion of the virus serotype selection is the direction of virus movement. The virus naturally moves from the soma to the axons; retrograde viruses can be used in cases for the virus needs to move from axons to soma. Once a viral construct is selected, the second part of the plasmid type focuses on pathway specificity. This is done using Cre-recombinase and Cre-dependent DREADDs: the DREADDs only activate in cells expressing Cre. Cre-recombinase is an enzyme derived from P1 bacteriophage that recognizes loxP sites and their locations and orientations. When loxP sites are on the same strand of DNA and in opposite orientation, the genes between the loxP sites are inverted. For Cre-dependent DREADDs, the receptor and fluorescent tag are inverted between two loxP sites and the presence of Cre cause the DREADDs to be uninverted and activate only on the pathway where the Cre and DREADDs injection sites meet (Figure 1.10) [72].

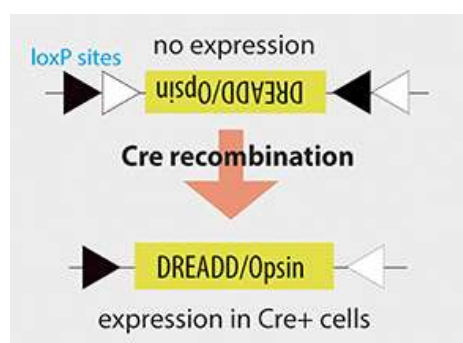


Figure 1.10 Cre-dependent DREADDs activation method. Presence of Cre-recombinase triggers the inversion of inverted DREADDs between loxP sites [78]

The promoter for DREADDs is dependent on the cell type of interest. When the target cells are neurons generally, the promoter options are synapsin1 and CaMKIIa [71]. The receptor for the

DREADDs can be either excitatory or inhibitory (Figure 1.11). This determines whether the activation of the DREADDs inhibits or excites the target location. The common excitatory receptor is hM3Dq and the two common inhibitory receptors are hM4Di and KORD. The receptors hM3Dq and hM4Di are activated by the designer drug clozapine N-oxide (CNO). The KORD receptor is activated by SALB [76].

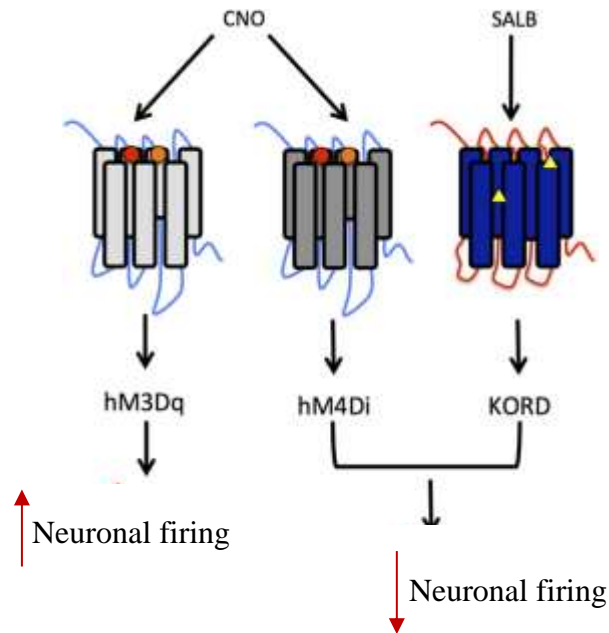


Figure 1.11 Summary of DREADDs activation pathway. The two types of designer drugs (CNO and SALB) are shown activating their labelled designer receptors to either increase or decrease neuronal firing. Adapted Figure [76].

The fluorescent tag varies dependent on the viral construct but a fairly common tag is mCherry. All of these components together make up a DREADDs vector that can be used to modulate activity, some potential variations in activity modulation is shown in Figure 1.12.

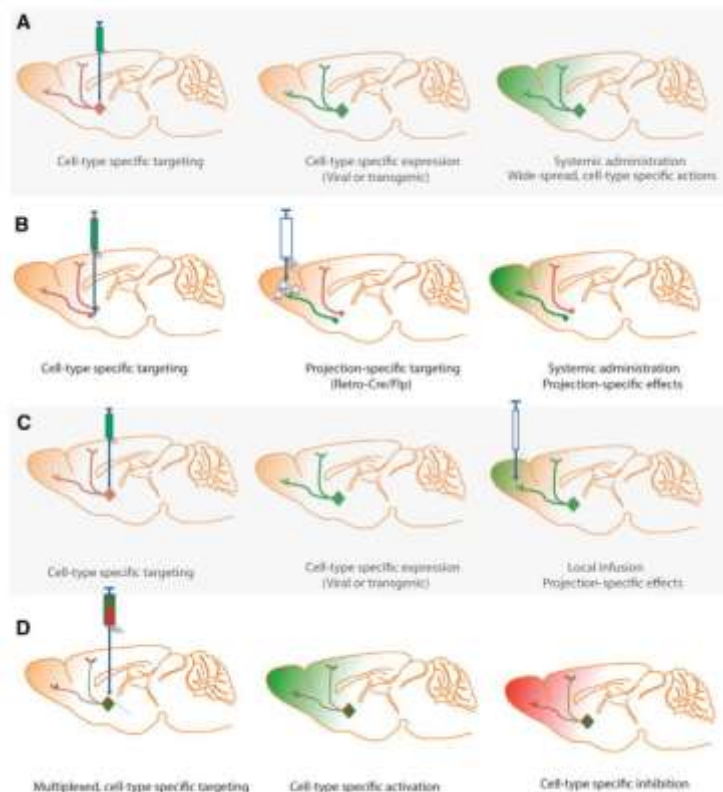


Figure 1.12 Types of transgenic expression of viral vectors for pharmacogenetics. A) The use of stereotaxic viral vector injections for a cell type specific promoter leading to cell-type specific impact but with limited pathway specificity. B) Dual injections of Cre-dependent DREADDs and Cre-recombinase viral vectors for cell type and projection specific targeting leading to pathway specific effects. C) Cell type specific viral vectors in combination with local infusion of designer drug for pathway specific effects. D) Combination of different viral vectors for multiplexed cell manipulation. Adapted figure [45].

After the DREADDs selection and injection into the location or locations of interest, the viral vectors need time to map, move along the neuronal pathway, to the location of interest, generally between 3 and 4 weeks [45]. Once they are mapped the designer drug can be administered either systemically or locally to activate the DREADDs. Upon completion of the behavioral model the brains should be imaged to determine location of the fluorescence of the DREADDs and the Cre viral vectors [76].

1.7 Research Questions

In this study, it is hypothesized that the animals can behaviorally discriminate between the IRN and FM/AM pitch sweeps based on changes to their ASR behavior. Also, it is hypothesized that there will be changes in the EFR recording to the prepulse stimuli before and after the ASR behavioral training. It is hypothesized that aged animals due to aged-related changes in auditory processing would have poorer discrimination and decreased changes in the EFR recordings than their young counterparts. Furthermore, it is hypothesized that behavioral discrimination to IRN and FM/AM pitch sweeps is comparable to the standard white gaussian noise ASR behavioral discrimination. It is further hypothesized that exposure to multiple stimuli during the habituation training of ASR behavior would increase the discrimination behavior in the recorded testing ASR behavior. Finally, that the A1/IC pathway is important in the discrimination of the pitch sweeps and inhibiting the pathway would cause a decrease in behavioral discrimination and changes in EFR recordings before and after training.

2. METHODS

2.1 Standard Behavioral and Electrophysiological Techniques to Show Pitch Sweep Discrimination

2.1.1 Acoustic Stimuli

In order to estimate the audiometric detection thresholds for the animals and to evoke an ABR response waveform, 2000 repetitions of the 0.1 ms rectangular click stimulus was played from 95 to 15 dB sound pressure level (SPL) at varying 10 dB SPL steps from 95 dB to 60 dB and from 25 to 15 dB and 5 dB SPL steps from 60 to 25 dB. The frequency domain response was a sinc function centered around 10 kHz with a bandwidth from 0 to 40 kHz [32]. To understand how the brain processes perceived pitch sweeps, various IRN and FM/AM stimuli were used. The IRN stimuli were all created from wideband noise from 0 to 30 kHz and used time delay and attenuation to create the perceived sweeps. The stimuli were generated prior to the experiment using SigGenRP (TDT) at 100 kHz sampling rate.

2.1.2 Electroencephalogram Recordings

The EEG recordings were performed using subdermal needle electrodes (Ambu) in a 9' by 9' anechoic chamber (Industrial Acoustic Corporation) with the stimuli presented free-field to the right ear at a distance of 115 cm from the speaker (Bower and Wilkins DM601) before and after the acoustic behavioral training. Initial anesthetization used 4% isoflurane induction in air upon checking inhibition of the righting reflex, a lower concentration of 2% in air delivered through a nose cone was used with the animal on a continuous heating pad at 38 °C and given eye ointment. This allowed the placement of either 4 or 6 subdermal needle electrodes. The ground electrode is placed on the base of the neck and the negative electrode is placed along the right jawline. The channel 1 electrode is placed along the midline of the skull between the ears and eyes. The channel 2 electrode is placed near lambda between the ears. The channel 3 electrode was placed parallel to the channel 1 electrode near the left ear. The channel 4 electrode was placed parallel to the channel 1 electrode near the right ear. The electrodes were connected to low-impedance 4-channel headstage (TDT RA4LI) and a Medusa Preamp for preprocessing, including taking the differential measurement between the channel electrodes and the negative electrode. The placed electrodes were checked to ensure they were properly placed and had a resistance of less than 3 k Ω using the

low-impedance headstage. After the placement of the electrodes, an intramuscular (IM) injection of either 0.15 or 0.2 mg/kg of dexmedetomidine (Dexdormitor) was given into the hind leg and isoflurane induction was stopped. The duration of isoflurane induction was around 10 minutes to complete the setup process. A 15 minute wait period was used after the removal of isoflurane to ensure neural activity returned to normal after isoflurane suppression, as a previous study of similar setup found normal neural activity after 9 minutes [47]. Then BioSig software (TDT) was employed for stimulus presentation and response acquisition. The waveforms were converted into sound using a multichannel processor (TDT RX6). Two AEPs were recorded from these stimuli: ABR and EFR. The responses to the stimuli were recorded and digitized using a multichannel recording and stimulation system (TDT RZ5). After the AEPs, the electrodes were removed and cleaned with 70% Ethanol. An IM injection of atipamezole hydrochloride (Antisedan), a dexmedetomidine reversal agent, of 0.5 mg/kg was given into the other hind leg.

2.1.2.1 Auditory Brainstem Response

2.1.2.1.1 Data Acquisition and Recording

The click stimulus was played 2000 times to determine the average from each positive channel (1-4) differentially to the negative channel at varying dB between 25 and 95 dB SPL with a varying step size of 5 or 10 dB SPL. Each recording was empirically viewed to ensure a consistent noise floor. The averaged responses are then digitally filtered using a bandpass filter between 80 and 3000 Hz [45]. The 2 channel configuration preserved most of the standard waveforms for ABRs. Channel 1 preserved peak I and III, while channel 2 preserved peak I, IV, V [47]. By comparing the responses from the different dB SPLs, the threshold was determined to be the smallest SPL that the peak 1 could be seen (Figure 2.1). The magnitude of peak 1 supra-threshold at 75 dB SPL was also determined to compare the magnitudes before and after the behavior and surgical model.

2.1.2.1.2 Data Analysis and Classification

The unfiltered recorded responses were then separated into their individual channels and exported from BioSig into text files. The data sets were loaded into MATLAB and bandpass filtered with a Chebyshev type 2 filter between 80 and 3000 Hz, an example after the filtering at 95 dB SPL is shown in Figure 2.1. The signals were then normalized to the noise of the signal by dividing the signal by the standard deviation of the noise from time 2 to 3 ms. Peak 1 was identified for all of

the channels and sound levels above the auditory detection threshold. The auditory detection threshold was the lowest dB SPL that the normalized response was 4 or more times the standard deviation of the noise [79]. The peaks were then normalized to the amplitude at 85 dB SPL for that recording so that they could be easily compared between recordings. A one-way repeated measure ANOVA test was run, where each group was the different timing of the recording, ex. pre and post training, and each point in the group was an animals threshold or peak 1 amplitude at 75 dB SPL. If there was a significant difference between groups for either threshold or peak 1 amplitude, the differences in EFR recordings were considered to be potentially caused by damage to the auditory system.

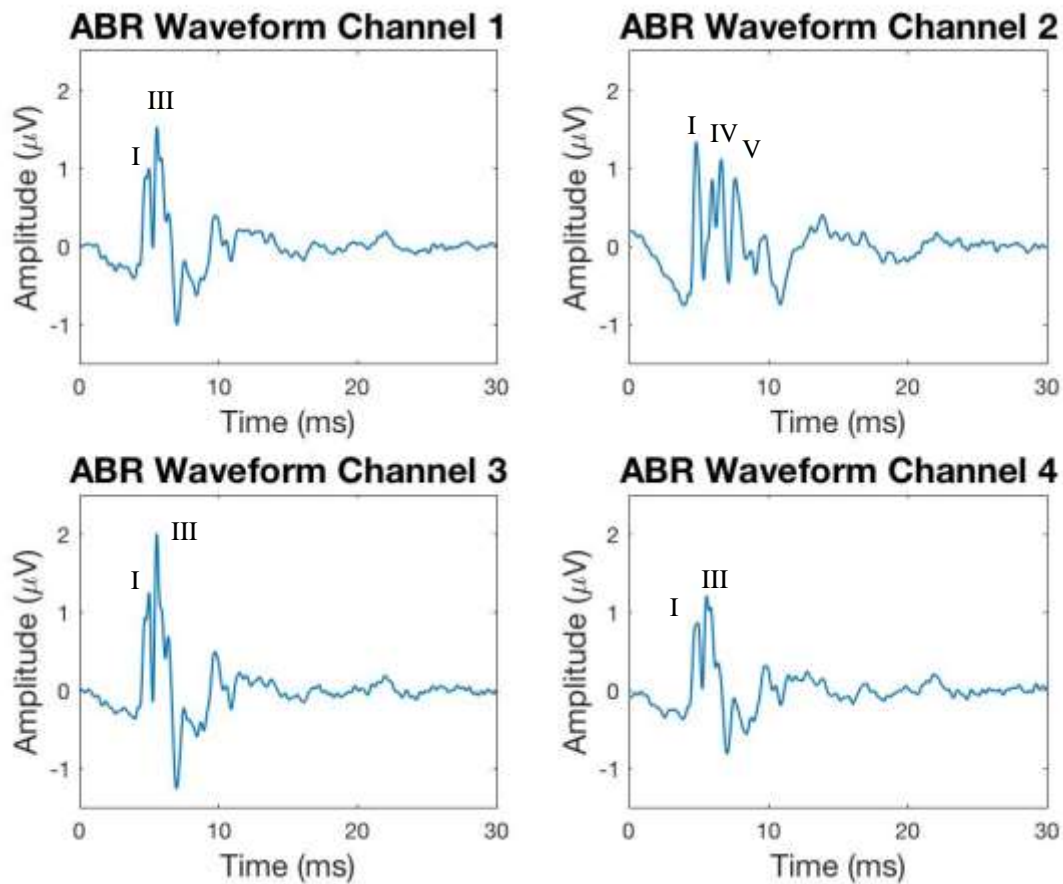


Figure 2.1 ABR Waveform of 4 channels at 95 dB SPL.

2.1.2.2 Envelope Following Response

2.1.2.2.1 Data Acquisition and Recording

The pitch sweep stimuli were played 200 times to determine the average from each positive channel (1-4) differentially to the negative channel at either 40 dB SPL above the threshold or at a maximum of 80 dB SPL to ensure suprathreshold recording responses [80]. The time-varying stimuli allow the EFR to represent the synchronized activity of the overall population of neurons [53].

2.1.2.2.2 Data Analysis and Classification

The recorded responses were then separated into their individual channels and exported from BioSig into text files. The files were then loaded into MATLAB and sorted into the different conditions based on when in the model the measurement was recorded (Figure 2.2). The first 10 ms of the response was removed as there is a large onset artifact around 100 Hz at the beginning of the records. The remaining recording was bandpass filtered between 90 and 2000 Hz using a Chebyshev type 2 filter. As the pitch sweep stimuli and the inverted pitch sweep stimuli were both played, the responses to these stimuli were added to emphasize the envelope of the response and subtracted to emphasize the temporal fine structure of the response.

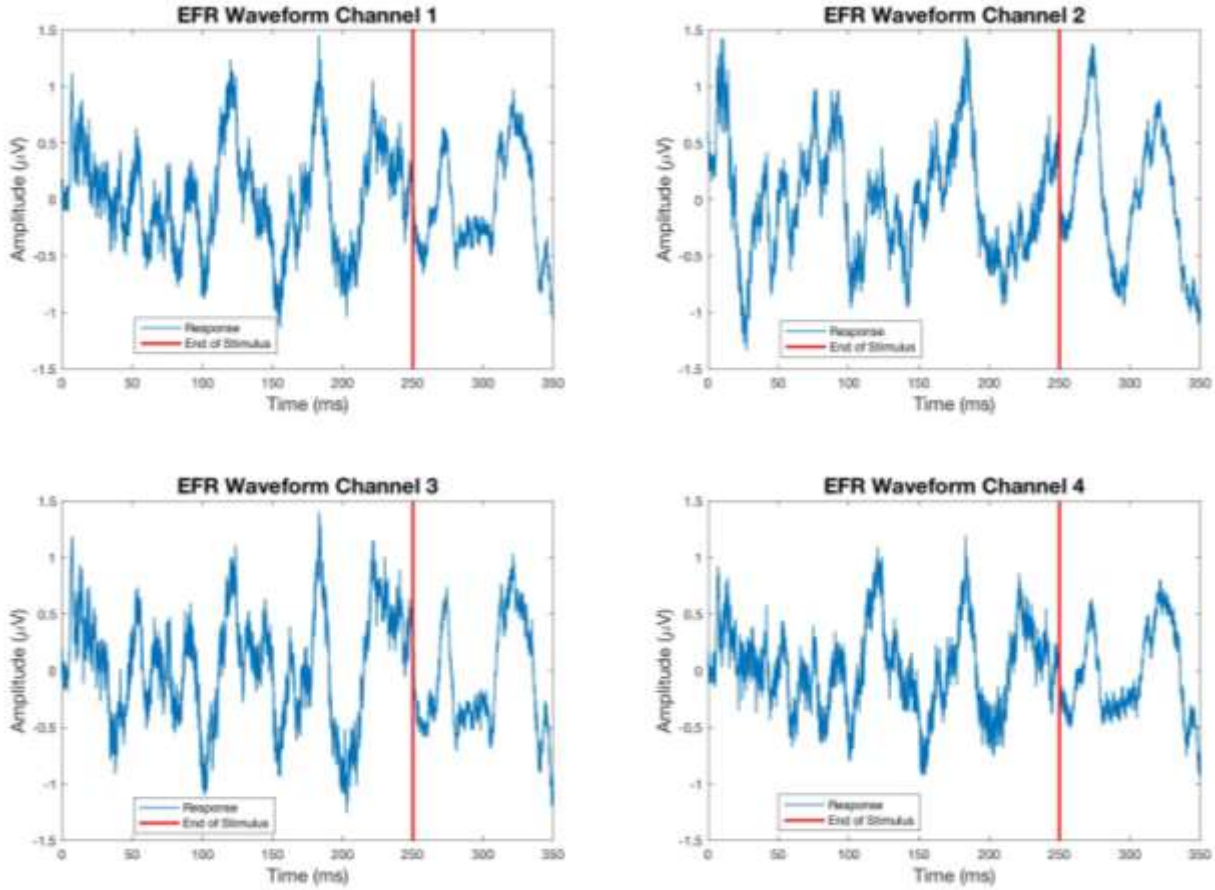


Figure 2.2 EFR Waveform of 4 Channels at 70 dB SPL. Response waveform is in blue and the stimulus end at 250 ms is shown in red.

The responses were then cross correlated with the perceived pitch sweep to find the correlation coefficient (Equation 2.1 *Normalized correlation coefficient equation*), which was normalized to the autocorrelation of the response and the pitch sweep stimulus. The threshold to unrelated noise was created by randomizing the actual response for each signal 100 times and averaging the maximum cross correlation coefficient value.

Equation 2.1 *Normalized correlation coefficient equation*

$$R_{xy,coeff}(m) = \frac{1}{\sqrt{\hat{R}_{xx}(0)\hat{R}_{yy}(0)}}\hat{R}_{xy}(m)$$

The correlation between the filtered data was compared to ensure it was above the calculated noise threshold and therefore significant correlation. The correlations were then compared pre and post training to determine if there were any consistent training related correlations. The

training related changes in correlation were compared with a paired t-test between the correlation coefficients before and after training. A one-way repeat measure ANOVA was used to determine the significant differences in correlation of responses to the various stimuli between animals.

2.1.3 Acoustic Startle Training

2.1.3.1 Data Acquisition and Recording

The acoustic startle training occurred in a sound attenuating cubicle (Med Associates) in a larger anechoic chamber, where the animals were in a grid rod animal holder that was attached to a motion sensitive platform (Figure 2.3). The movements of the animal were detected and converted to a voltage signal by a transducer, amplified, and sent to the TDT RZ6 and a computer so that the vertical startle response could be analyzed.

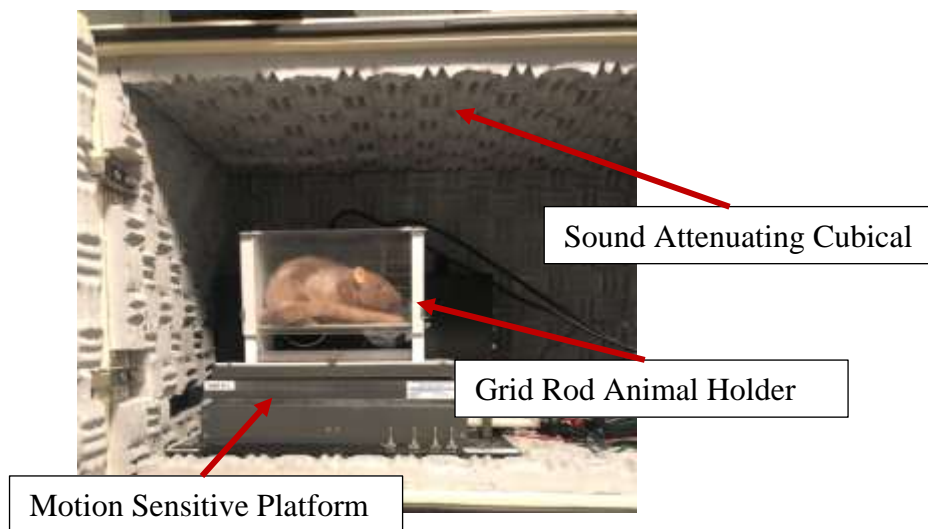


Figure 2.3 Photo of Startle Setup in Larger Anechoic Chamber.

As mentioned previously (Section 1.5), the acoustic startle training involves using a prepulse to predict a startle eliciting stimulus (SES) and therefore minimize the animal's acoustic startle response (ASR) to the SES. The prepulse for this model used the previously mentioned pitch sweeps. To ensure they are learning the pitch sweep itself and not simply the presence of sound, a IRN pitch sweep from 1000 to 500 Hz is played in the background until the prepulse is played. This training was accomplished by initially acclimating the animal to the chamber itself for 3 days at increase intervals of time (5 min, 7 min, 10 min) in which time the background tone is played.

After acclimation, there were several test days with a spacing of 48 hours between each test day. Each test day had the 3 parts to it, acclimation, habituation, and testing. The acclimation was similar to the acclimation days for 5 minutes. The habituation was a series of 20 trials in which the prepulse is always played before the SES to create the association between prepulse and the SES and create prepulse inhibition (PPI). The testing part was broken into either 7 or 9 blocks with a total of around 80 trials. Each block had 3 control trials and the rest were PPI trials. The controls were prepulse without SES, SES without prepulse, and neither prepulse nor SES. The maximum startle response should occur from the SES without prepulse control. The baseline response should be the neither prepulse nor SES trial and the decreased baseline response should be the prepulse without SES control.

2.1.3.2 Data Analysis and Classification

After the test day, their responses and the stimulation parameters were recorded and saved into a matrix file. The responses to startle were first analyzed to determine the controls and the prepulse startle response. The responses were all first normalized to the baseline movement per trial so only the change in movement caused by the startle was analyzed. The startle response was determined to be the largest movement in the time the startle occurred that was not caused by a baseline shift. The prepulse startle response was then normalized to the averaged response that day to the controls and the data was broken up into quartiles in a box plot shown below (Figure 2.4).

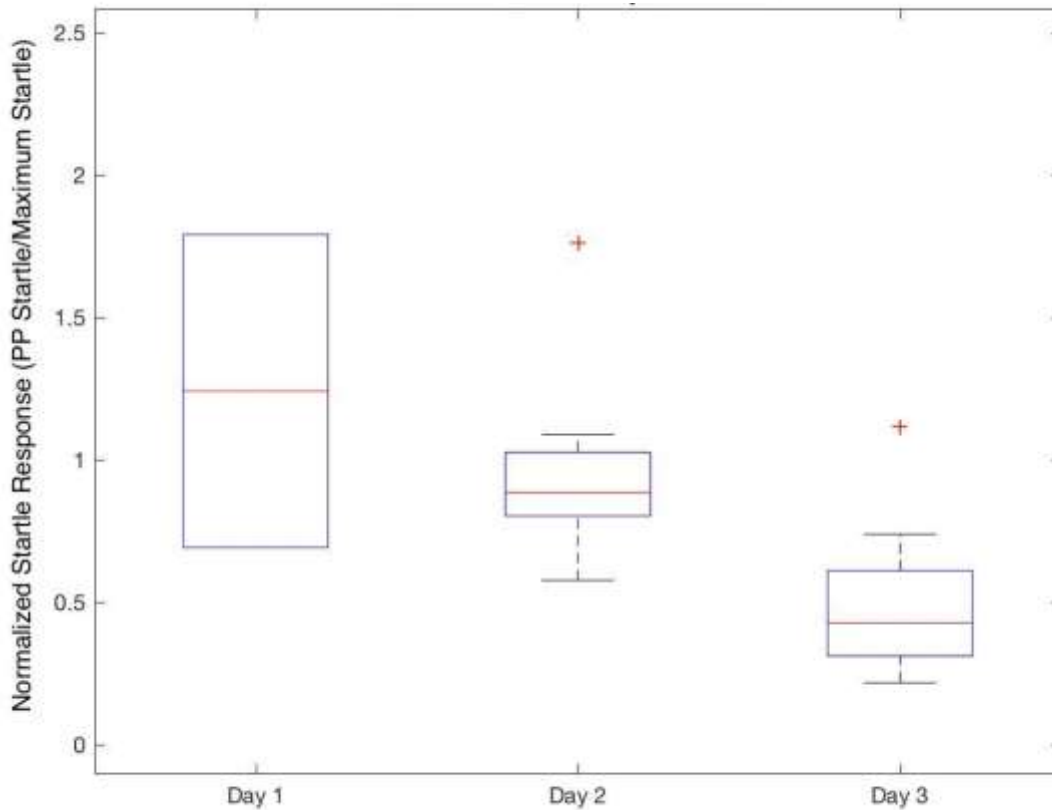


Figure 2.4 Example boxplot of normalized startle response of one animal across training days. The normalized response is the prepulse startle response normalized to the average of the SES control.

The interquartile range (IQR) and median from each of the days was there compared to the first day to show increased discrimination by a decrease in both median and spread of the response. The below equations were used to determine the peak deviation between day. The peak deviation of the median was calculated between the current day and day 1 (Equation 2.2). The peak deviation of the spread of the data between the current day and day was calculated (Equation 2.3).

Equation 2.2 Peak deviation of the median between the current day and day 1

$$median_{peakdev} = \frac{median_{day} - median_{day1}}{median_{day} + median_{day1}}$$

Equation 2.3 Peak deviation of the spread between the current day and day 1

$$spread_{peakdev} = \frac{\frac{median_{day}}{IQR_{day}} - \frac{median_{day1}}{IQR_{day1}}}{\frac{median_{day}}{IQR_{day}} + \frac{median_{day1}}{IQR_{day1}}}$$

If the results were both negative, then the results were considered to show increased discrimination between days. If the results were both positive there wasn't increased discrimination between days and if there was one of each, exact median and interquartile range would need to be compared to determine if increased discrimination occurred. A one-way repeated measure ANOVA was performed to determine if there was a significant ($p < 0.05$) difference in response between days. The sorted results also used a one-way repeated measure ANOVA test to compare between the sorted groups to determine if there was a significant difference.

2.2 Aging Effects on IRN Pitch Sweep Discrimination

2.2.1 Subjects

A total of 7 Fisher-344 rats obtained from Envigo were used. Three were young (3-6 months, 1 male and 2 females) and four were aged (21-26 months females). All animals were handled for 3 days prior to use and housed in the animal care facility during the period of the study in relatively quiet and standard conditions with 12 hour light and dark cycles. All protocols were approved by the Purdue Animal Care and Use Committee (PACUC-1111000167)

2.2.2 Acoustic Stimuli

The previously mentioned click stimuli were used for the ABR portion of the EEG recordings. To understand how the brain processes the different IRN perceived pitch sweeps for the EFR portion of the EEG recordings, the following stimuli were used: 100 to 500 Hz, 500 to 100 Hz, 500 to 1000 Hz, 1000 to 500 Hz, 500 Hz, and 1000 Hz. These stimuli were played 200 times at either 40 dB over the hearing threshold determined by the click stimuli or 80 dB, whichever is lower. The IRN pitch sweep from 100 to 500 Hz was the prepulse and the IRN pitch sweep from 1000 to 500 Hz was the background sweep used in the acoustic startle training (Figure 2.5).

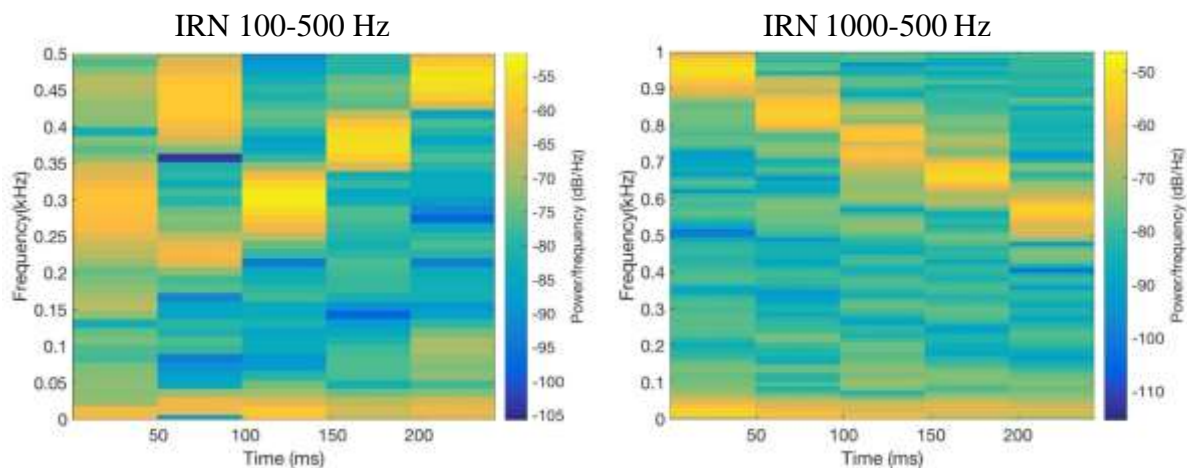


Figure 2.5 Acoustic startle training IRN pitch sweep stimuli (100-500 Hz and 1000-500 Hz) Spectrograms

2.2.3 Electroencephalogram Recordings

The EEG recordings used the standard procedure described above (Section 2.1.2) with only 4 subdermal electrodes. The subdermal electrodes were ground, negative, channel 1, and channel 2 in the locations described in the standard procedure (Figure 2.6). The EEG recordings were done before and after acoustic startle training. After the placement of the electrodes, the ABR and then the EFR were recorded as described in the standard procedure using the stimuli listed above (Section 2.2.2).

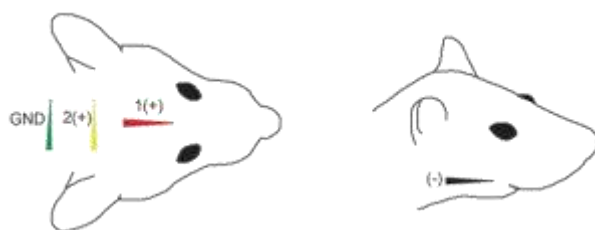


Figure 2.6 EEG 4 Channel Recording Differential Electrode Positioning

2.2.4 Acoustic Startle Training

The acoustic startle training was performed as described in the standard method (Section 2.1.3). There were 3 days of acclimation to the background stimuli, IRN carrier from 1000 to 500 Hz, followed by 3 test days with a spacing of 48 hours between each test day. The test day had the 3 parts to it, acclimation, habituation, and testing (Figure 2.7). The acclimation was similar to the acclimation days for 5 minutes. The habituation was a series of 20 trials where the prepulse, IRN carrier from 100 to 500 Hz, is always played before the SES to create the association between the prepulse and the SES and create PPI. The testing part had a total of 81 trials and was split into 9 blocks of 9 randomized trials each. Each block had the 3 previously mentioned control trials (maximum startle, baseline, and decreased baseline) and 6 PPI trials (Figure 2.7).

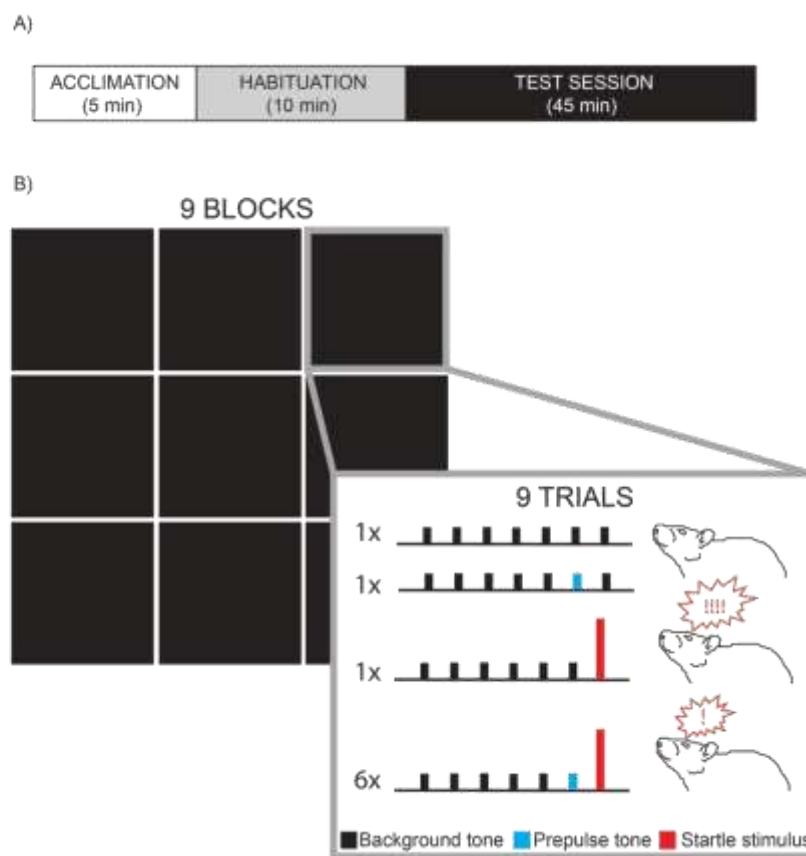


Figure 2.7 Acoustic Startle Training Test Day. A) The different components of a test day with the 5 minutes acclimation, habituation to create PPI, and test session to determine the PPI that was created. B) The test session has 9 blocks of 9 trials with 6 PPI trials and 3 controls. Based on figure [45].

2.3 Aging and Habituation Prepulse Effects on Pitch Sweep Discrimination and Differentiation

2.3.1 Subjects

A total of 7 Fisher-344 rats obtained from Envigo were used. Five were young (3-6 months, 3 males and 2 females) and two were aged (21-26 months females). The animals were split into two groups to determine the better behavioral learning model (Table 2.1). Group 1 had 2 young (1 male and 1 female) and 1 aged female animals. In group 1, 1 young male had type 2 acoustic startle training and 1 young and 1 aged female had type 1 acoustic startle training. Group 2 had 3 young (2 male and 1 female) and 1 aged female animals. In group 2, 2 young male had type 2 acoustic startle training and 1 young and 1 aged female had type 1 acoustic startle training.

Table 2.1 Subject Groups

Group	Young		Aged	
	Type 1	Type 2	Type 1	Type 2
1	1	1	1	0
2	1	2	1	0

All animals were handled for 3 days prior to use and housed in the animal care facility during the period of the study in a relatively quiet and standard conditions with 12 hour light and dark cycles. All protocols were approved by the Purdue Animal Care and Use Committee (PACUC-1111000167)

2.3.2 Acoustic Stimuli

The previously mentioned click stimuli were used for the ABR portion of the EEG recordings (Section 2.1.1). To understand how the brain processes the different pitch sweeps, the stimuli used both IRN and FM/AM stimuli. The IRN stimuli were pitch sweeps from 100 to 500 Hz, 500 to 100 Hz, 500 to 1000 Hz, 1000 to 500 Hz, 500 Hz, and 1000 Hz. The FM/AM stimuli were made from an 8kHz tone with added pitch sweeps from 100 to 500 Hz and 500 to 100 Hz (Figure 2.8).

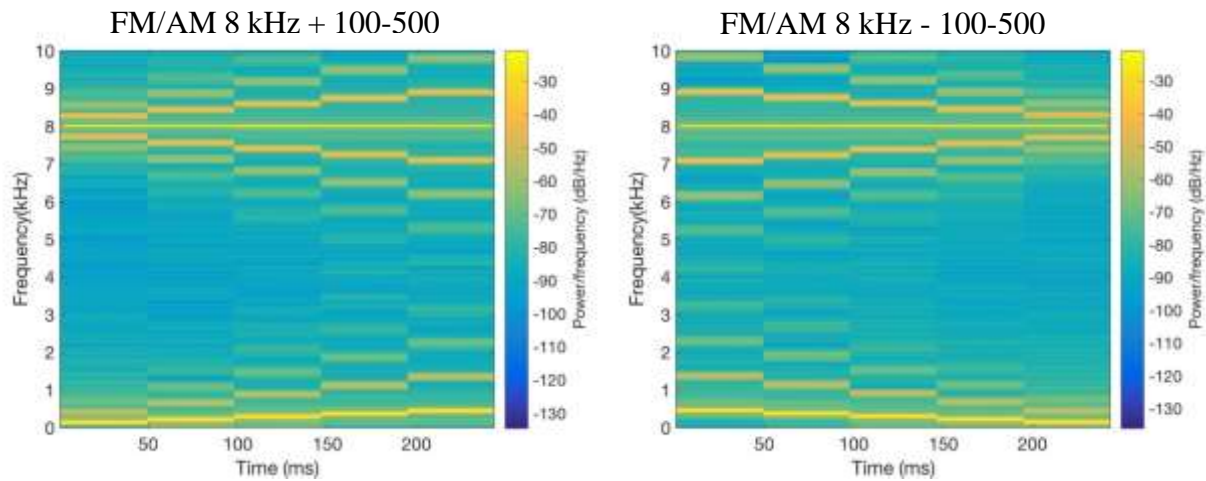


Figure 2.8 FM/AM stimuli (8kHz + 100-500 Hz and 8kHz - 100-500 Hz) spectrogram

These stimuli were played 200 times at either 40 dB over the hearing threshold determined by the click stimuli or 80 dB, whichever is lower. The prepulses for the acoustic startle training were the IRN pitch sweep from 100 to 500 Hz, FM/AM 8 kHz tone with pitch sweep from 100 to 500, FM/AM 8 kHz tone with pitch sweep from 500 to 100, and white gaussian noise at 30, 50, and 70 dB SPL. As the white gaussian noise stimuli are the standard prepulses for startle discrimination, comparing the responses to the noise with the pitch sweeps showed differences in discrimination. The background sweep used in the acoustic startle training was the IRN pitch sweep from 1000 to 500 Hz.

2.3.3 Electroencephalogram Recordings

The EEG recordings used the standard procedure described above with only 4 subdermal electrodes for both group 1 and group 2. The subdermal electrodes were ground, negative, channel 1, and channel 2 in the locations described in the standard procedure (Figure 2.6). The EEG recordings were done before and after acoustic startle training. After the placement of the electrodes, the ABR and then the EFR were recorded as described in the standard procedure using the acoustic stimuli listed above.

2.3.4 Acoustic Startle Training

The acoustic startle training was performed as described in the standard method. There were 3 days of acclimation to the background stimuli, IRN pitch sweep from 1000 to 500 Hz, followed by 3 test days with a spacing of 48 hours between each test day. The test day had the 3 parts to it, acclimation, habituation, and testing (Figure 2.9). The acclimation was similar to the acclimation days for 5 minutes. The habituation was a series of 20 trials where the prepulse is always played before the SES to create the association between the prepulse and the SES and create PPI. For group 1, the habituation prepulse for all trials was the IRN pitch sweep from 100 to 500 Hz. For group 2, the habituation prepulse for 10 trials was the IRN pitch sweep from 100 to 500 Hz and for the other 10 trials was the FM/AM 8kHz tone with pitch sweep from 100 to 500 Hz. The testing part had 7 blocks of 11/12 randomized trials each. Each block had 3 of the previously mentioned control trials (maximum startle, baseline, and decreased baseline or 2 maximum startle, and 1 baseline) and 7/8 PPI trials (Figure 2.9). The responses to the stimuli as well as the stimuli information were recorded.

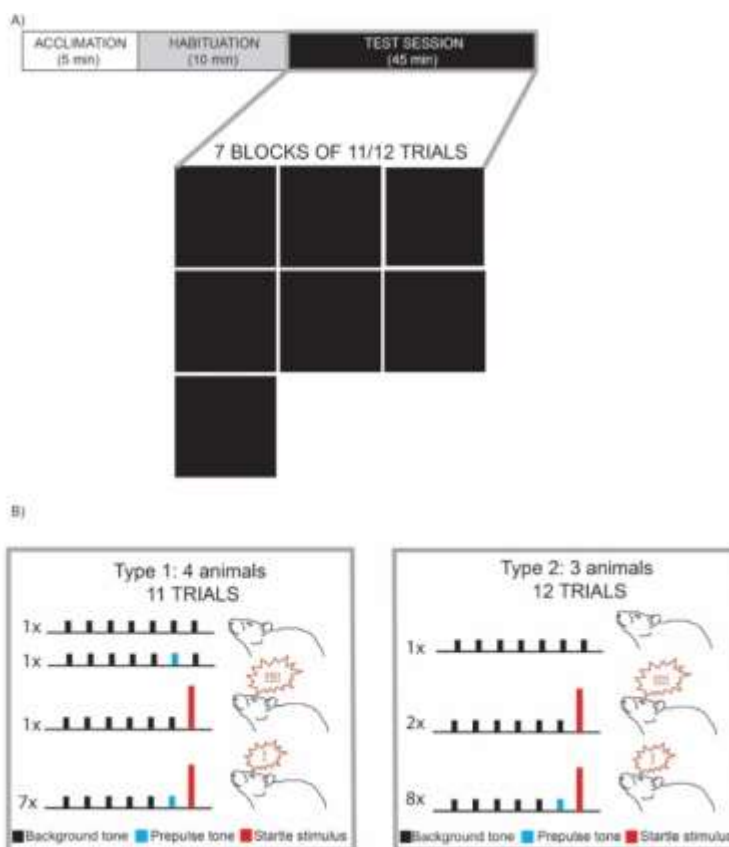


Figure 2.9 Acoustic Startle Training Test Day. A) The different components of a test day with the 5 minutes acclimation, habituation to create PPI, and test session of 7 block with 11 or 12 trials to determine the PPI that was created. B) The two types of test sessions. Type 1 with 7 PPI trials and 3 different controls (maximum startle, baseline, and decreased baseline). Type 2 with 8 PPI and 3 controls (2 maximum startle and 1 baseline)

2.4 Corticofugal Modulation Effects on Pitch Sweep Discrimination and Differentiation

2.4.1 Subjects

A total of 11 young (3-6 months) Fisher-344 rats obtained from Envigo were used for the model. Seven were male and 4 were female. One of the animals was in type 1 of the acoustic startle training, 3 animals were in the type 2 acoustic startle training, and the rest were in type 3 of the acoustic startle training. A total of 2 young (3-6 months) Fisher-344 rats were used to test the surgical approach with dye injections. All animals were handled for 3 days prior to use and housed in the animal care facility during the period of the study in a relatively quiet and standard conditions with 12 hour light and dark cycles. All protocols were approved by the Purdue Animal Care and Use Committee (PACUC-1204000631 and PACUC-1111000167)

2.4.2 Acoustic Stimuli

The previously mentioned click stimuli were used for the ABR portion of the EEG recordings (Section 2.1.1). The previously mentioned IRN and FM/AM stimuli were used (Section 2.3.2) for the EFR and acoustic startle training.

2.4.3 Stereotaxic Viral Injections Surgery

2.4.3.1 Viral Vectors

The stereotaxic viral injections surgery used adeno-associated virus 8 (AAV8) DREADDs vectors to inhibit the primary auditory cortex-inferior colliculus pathway. A Cre-activated inhibitory DREADD, pAAV-hSyn-DIO-hM4D(Gi)-mCherry, and retrograde Cre recombinase, AAV pmSyn1-EBFP-Cre, were used to target only the pathway of interest. The DREADDs vector was injected into layer 5 of A1 and the retrograde Cre vector was injected into ECIC/DCIC region (Figure 2.10). The Cre moved retrogradely to the pyramidal neurons in layer 5 of A1 and uninverted the DREADDs. The uninverted DREADDs then fluoresce with mCherry and the Cre fluoresces with blue fluorescent protein (EBFP) when imaged.

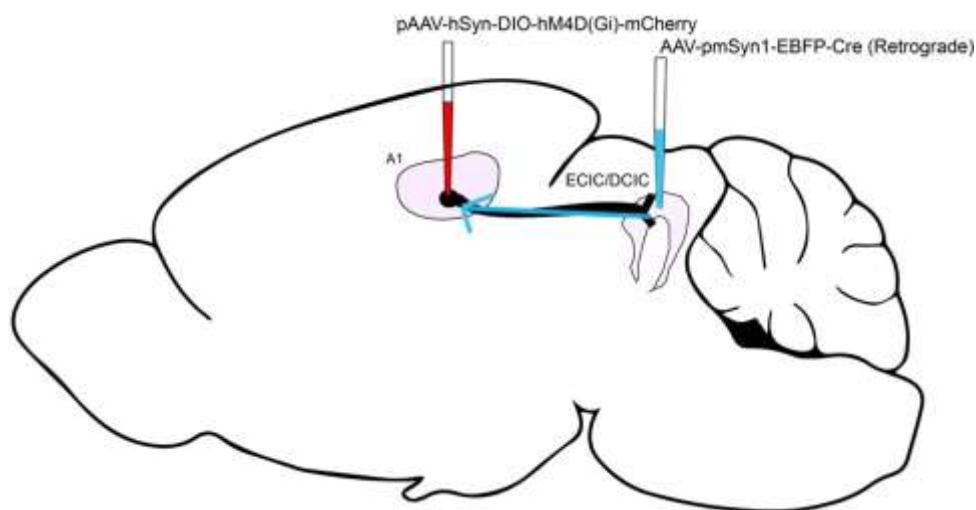


Figure 2.10 DREADDs Injection Pathway

2.4.3.2 Surgical Procedure

The surgical procedure began with an initial 4% isoflurane induction in air in a cylindrical induction chamber until righting reflex was suppressed. The animals were then moved onto a water circulating continuous heating pad at 38 °C to regulate animals body temperature under anesthesia and eye ointment was applied to ensure the eyes didn't dry out. Five of the animals

were then placed on 2% isoflurane induction by nose cone, which was later dropped to 1.5% to maintain the anesthetic plane. After losing several animals during surgery to isoflurane, the next seven animals were given an IM injection of a ketamine (80 mg/kg) - dexmedetomidine (Dexdormitor, 0.2 mg/kg) mixture, updates of 0.1 mL ketamine as needed, and given oxygen through a nose cone. Heart rate and blood oxygenation were measured with a pulse oximeter, intermittent monitoring of respiration rate, and intermittent toe pinch reflex checks were used to monitor and maintain the anesthetic plane.

After ensuring the animal was properly anesthetized using toe pinch reflex, the animal's head was secured with hollowed ear bars. A 1 mL subcutaneous injection (sub-Q) of meloxicam (Metacam, 1 mg/kg) -saline mixture was given as a painkiller and fluid replacement. Then the animal's head was shaved and cleaned 3 times with betadine and ethanol. With the wound site now sterile and aseptic techniques used for the surgeon and the tools, the initial incision was made along midline from around 5 mm anterior to bregma to about 5 mm posterior to lambda. The periosteum was removed and the stereotactic equipment was zeroed at bregma and midline. Any movement in the anterior/posterior (A/P) direction is based on being zeroed at bregma. Any movement in the medial/lateral (M/L) direction is based on being zeroed at midline. Any movement in the dorsal/ventral (D/V) direction is based on being zeroed at the surface of the brain. The desired location of the IC injection was into DCIC and ECIC, which was determined to be A/P -8.3 mm, M/L \pm 1.15 mm, D/V -3.5 mm from the Rat Brain Stereotaxic Coordinates of Wistar rats [81]. However, this location rests right on the lambda suture and therefore a major cerebral artery for Fischer 344 rats. In order to inject into the location of interest, an angled injection anterior to the suture was required between A/P -7.25 mm and -7.8 mm based on the location of the animal's lambda (Figure 2.11). Bilateral craniotomies were drilled in the determined location of the angled injection of IC.

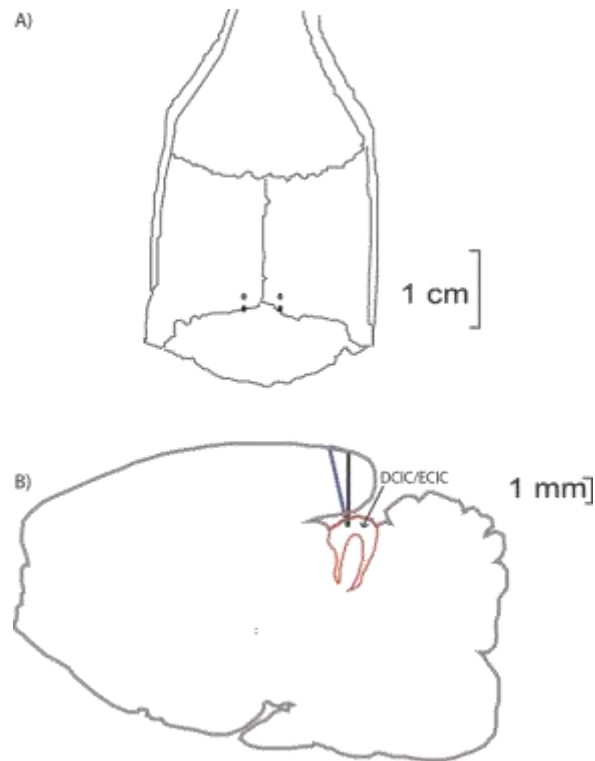


Figure 2.11 ECIC/DCIC Injection Location. A) Sketch of rat skull with the injection site location. B) Sketch of rat brain with the angled injection into ECIC/DCIC

Bilateral injections into primary auditory cortex at A/P -5.28 mm M/L \pm 6.45 mm D/V -4.25 mm was also necessary. However, based on the surgical setup and the curve of the skull drilling through the skull to inject directly into auditory cortex was not possible and another angled injection was required. One landmark on all of the animal's skulls right before the flat top surface of the skull curved was the skull ridge. As the skull ridge was the most lateral flat location of the skull, bilateral craniotomies were made in the skull ridge, varying between M/L \pm 5.4 mm to \pm 6 mm (Figure 2.12).

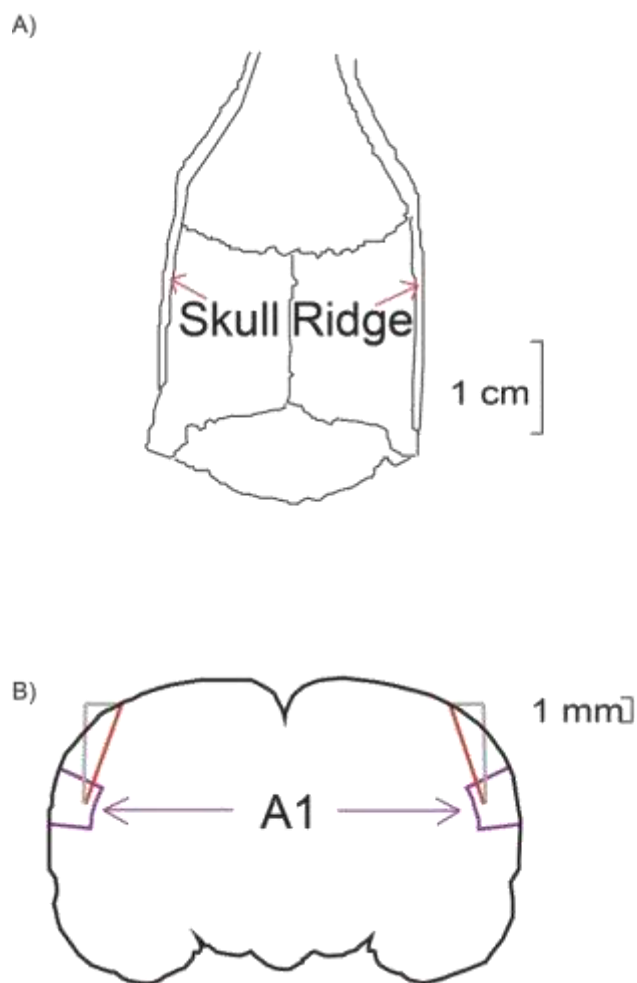


Figure 2.12 Primary Auditory Cortex Injection Location. A) Sketch of rat skull with skull ridge location B) Sketch of rat brain with angled injection into primary auditory cortex (A1)

Two μL of the DREADDs vector was loaded into 5 μL Hamilton syringe using a microsyringe pump controller (World Precision Instruments). Based on the location of the A1 craniotomy, the angle of the syringe (5° - 12°) and the depth of the injection (-4.27 mm to -4.35 mm) was determined. With the tip placed at the surface of the brain, the stereotactic controller was zeroed. A blunted 25 gauge needle was used to burst the dura and then the syringe was moved down into the injection location. The syringe pump then infused $1\mu\text{L}$ at a rate of $.1 \mu\text{L}/\text{min}$. After the infusion was complete, the syringe was left at the site for 5 minutes before being removed and the procedure repeated for the other A1 craniotomy. Two μL of the Cre vector was loaded into a different 5 μL Hamilton syringe. Based on the location of the IC craniotomy, the angle of the syringe (8° - 17°) and the depth of the injection (-3.57 mm to -4.79 mm) was determined. The steps for bursting the

dura and injection were then repeated for the Cre injections. Upon the completion of the injections, the incision site was sutured using 4-0 silk sutures and triple antibiotic ointment was applied. Once the animal recovered from anesthesia, it was returned to its cage to recover. Update sub-Q injections of the meloxicam-saline mixture were given for 5 days following the surgery and the animal's weight was monitored to ensure the animal regained the weight lost from surgery. Based on the rate of wound healing, the sutures were removed 14-21 days after the surgery. In order to ensure the DREADDs have time to activate, no procedures were done to the animals until 4 weeks after the surgery.

2.4.3.3 Dye Injection Test Surgeries

In order to ensure that the angled injection locations of the surgery were successful, several dye injection surgeries were performed using the above surgical procedure without the aseptic technique and wound closure. Instead of injecting the viral vectors, one surgery injected green fluorescent protein (GFP) into two sites, with an angled injection into A1 and a vertical injection into IC. Another surgery injected cresyl violet into two sites, with the same angled injection techniques for all injections.

2.4.4 Electroencephalogram Recordings

The EEG recordings used the standard procedure described above with 6 subdermal electrodes. The subdermal electrodes were ground, negative, channel 1, channel 2, channel 3, and channel 4 in the locations described in the standard procedure (Figure 2.13). The EEG recordings were done before the stereotaxic viral injections, before acoustic startle training, and after acoustic startle training. Before the stereotaxic viral injections only an ABR was recorded. The before acoustic startle training recording took place 4 weeks after the stereotaxic viral injections. For before and after acoustic startle training recordings, the ABR and then the EFR were recorded as described in the standard procedure using the acoustic stimuli listed above. Then an intraperitoneal injection (IP) on CNO at a concentration of 3 mg/kg was injected and waited 40 minutes for the drug to activate. Then another ABR and EFR were recorded using the same procedure as before the CNO injection.

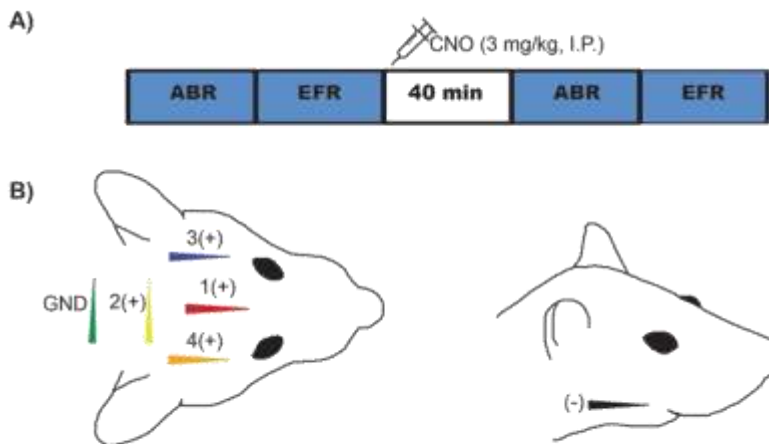


Figure 2.13 DREADDs EEG Recording A) EEG recording schedule B) EEG 6 Channel Recording Differential Electrode Positioning

2.4.5 Acoustic Startle Training

The acoustic startle training was performed as described in the standard method. There were 3 days of acclimation to the background stimuli, IRN carrier pitch sweep from 1000 to 500 Hz, followed by 3/4 test days with a spacing of 48 hours between each test day. The test day had the 3 parts to it, acclimation, habituation, and testing (Figure 2.14). The acclimation was similar to the acclimation days for 5 minutes. The habituation was a series of 20 trials where the prepulse is always played before the SES to create the association between the prepulse and the SES and create PPI. The habituation prepulse for 10 trials was the IRN carrier pitch sweep from 100 to 500 Hz and for the other 10 trials was the FM carrier pitch sweep from 100 to 500 Hz. The testing part had 7 blocks of 11/12 randomized trials each. Each block had 3 of the previously mentioned control trials and either 7/8 PPI trials depending on the type (Figure 2.14). Type 1 test session had 7 PPI trials and 1 maximum startle, 1 baseline, and 1 decreased baseline controls. Type 2 test session had 8 PPI trials and 3 baseline controls. Type 3 had 8 PPI trials and 2 maximum startle and 1 baseline controls.

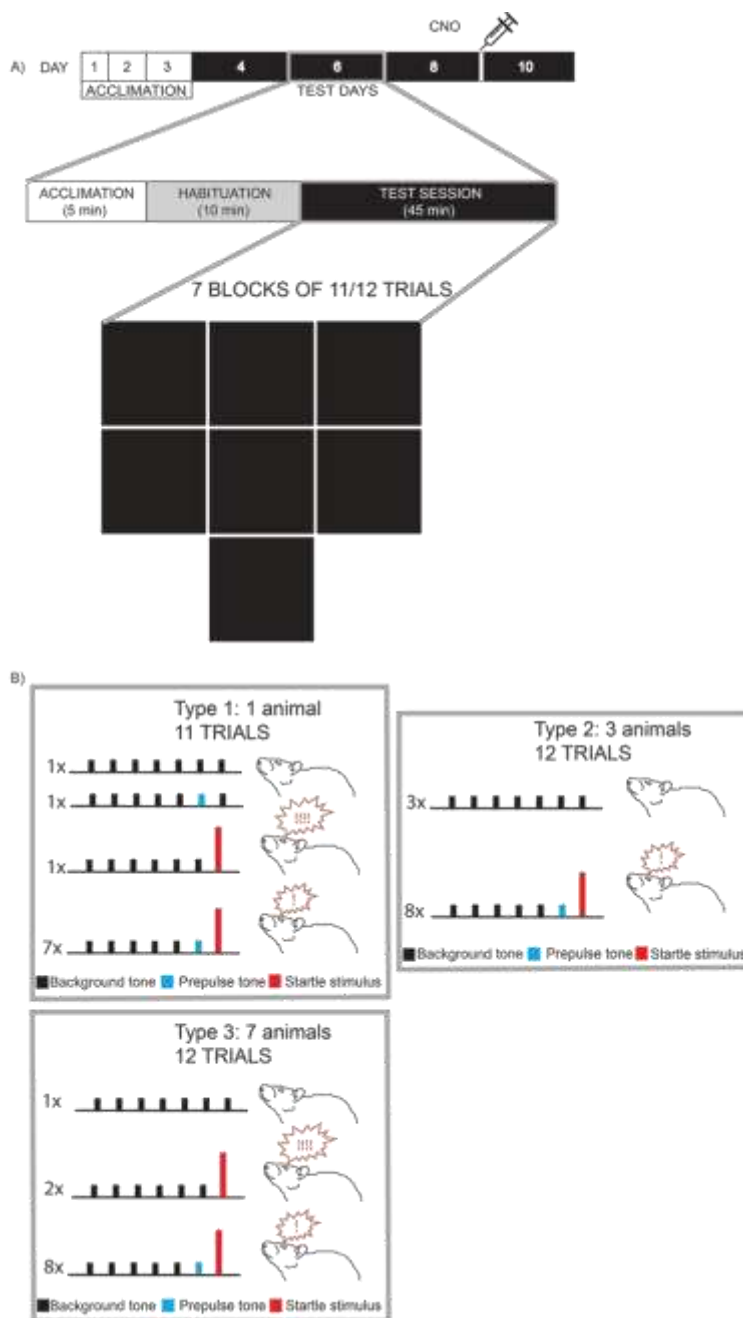


Figure 2.14 Acoustic Startle Training A) Acoustic Startle Training Schedule and breakdown of test day procedures. B) Types of test sessions. Type 1 with 7 PPI trials and 3 different controls (maximum startle, baseline, and decreased baseline). Type 2 with 8 PPI trials and 3 baseline controls. Type 3 with 8 PPI and 3 controls (2 maximum startle and 1 baseline)

2.4.6 Histology

2.4.6.1 Perfusion

Once the acute recordings were completed, the animal was euthanized with an IP injection of Beuthanasia (200 mg/kg). After the vitals dropped and there was no toe pinch response, the animal was moved to the fume hood and transcardially perfused using a variable flow peristaltic pump (Fisher Scientific) with 100 mL of 1M phosphate buffered solution (PBS) and 100 mL of 4% Paraformaldehyde. The brain was then removed and fixed by storing it in 4% Paraformaldehyde for 24 hours. After the 24 hours, the brain was moved to a 30% sucrose solution until the brain sank. The brain was then moved to the -80°C freezer until histology was performed.

2.4.6.2 Tissue Blocking and Sectioning

The brain was block cut to include auditory cortex and IC and moved into optical cutting temperature (OCT) compound solution (Sakura). The brain was then sliced into 40 µm slices using Leica CM3050 Cryostat and slices of A1, IC, and intermittent slices in the corticofugal pathway were kept in the dark in the 4°C fridge in PBS solution in a 16 well plate.

2.4.6.3 Primary Auditory Cortex Histology

2.4.6.3.1 Staining and Mounting

Within 48 hours of slicing the brain, the staining process of the A1 slices began. The primary antibody was anti-VGluT2 anti-Guinea pig and the secondary antibody was anti-guinea pig anti-goat with a fluorescent tag of Alexa Fluor 647. All the slices were protected from light throughout the entire staining and mounting process. First the slices were washed twice for 5 minutes in 1xPBS-0.1% Triton (0.1% PBST) at room temperature. The slices were then incubated in 0.3% PBST at room temperature. Next, the slices were incubated in the immuno buffer, which a 20 mL solution is made of 1 mL goat serum, 0.6 mL bovine serum albumin (BSA), 200 µL sodium azide, and the rest of 0.3% PBST. Afterwards the slices were incubated at 4°C in 1:400 dilution of the primary antibody in immuno buffer. The slices were then washed 3 times for 10 minutes in 0.1% PBST. They were then incubated in 1:400 dilution of the secondary antibody with immuno buffer for an hour. The slices were then washed 3 times for 10 minutes in 0.1% PBST. The slices were then mounted onto microscope slides in PBS in a dark environment. The slices were treated with

20 μ L of the anti-fading agent, Prolong Glass, to preserve the slices. Then they were sealed using coverslips and clear nail polish.

2.4.6.3.2 Confocal Imaging

Within a week of mounting the slices, the slides were brought to the confocal microscope, Zeiss LSM 710, to image. First, the slides were cleaned with ethanol and lens paper and then placed in the scope. Sections containing the auditory cortex were found first visually through the light microscope portion. Then a tile image was taken of the region of the slide with the lasers for mCherry and Alexa Fluor 647 on. If any regions of fluorescence were found, the region was viewed through the light microscope to ensure it was not caused by imperfections in the slide. Then using a range scale, the gain was turned down on both the mCherry and Alexa Fluor 647 to decrease the autofluorescence of the background. If the regions of fluorescence were still evident, a tile-z-stack was taken of the slice. The approximate location of the slice was determined from the structure of the slice compared to the Rat Brain Stereotaxic Coordinates of Wistar rats [81].

2.4.6.4 Dye Injection Surgery Slices

2.4.6.4.1 Mounting

The slices were labeled in order of slicing and mounted onto microscope slides in PBS in a dark environment. The slices were treated with 20 μ L of the anti-fading agent, Prolong Glass, to preserve the slices. Then they were sealed using coverslips and clear nail polish.

2.4.6.4.2 Confocal Imaging

Within a week of mounting the slices, the slides were brought to the confocal microscope, Zeiss LSM 710, to image. First, the slides were cleaned with ethanol and lens paper and then placed in the scope. Region of the brain with auditory cortex or inferior colliculus depending on the slice location were found first visually through the light microscope portion. Then a tile image was taken of the region of the slide with the lasers for GFP or cresyl violet on. If any regions of fluorescence were found, the region was viewed through the light microscope to ensure it was not caused by imperfections in the slide. Then using a range scale, the gain was turned down on both the GFP or cresyl violet to decrease the autofluorescence of the background. Images of the resultant

fluorescence were then saved and the approximate location of the slice was determined from the structure of the slice compared to the Rat Brain Stereotaxic Coordinates of Wistar rats [81].

2.4.6.5 Histological Image Quantification

After the different imaging techniques, the exported images were imported into ImageJ/Fiji software. In ImageJ, the relative optical density (ROD) was measured by normalizing the average pixel intensity value of the region of interest within an unlabeled region. The fluorescence of the region of interest could then be quantified and compared between animals.

3. RESULTS

3.1 Aging Effects on IRN Pitch Sweep Discrimination

3.1.1 Electroencephalogram Recordings

3.1.1.1 Auditory Brainstem Response

The ABRs before and after training were used to test the functionality of the animals' auditory system. The functionality was determined by analyzing two components: the acoustic threshold and the amplitude of peak 1 across sound pressure levels from 95 to 25 dB with 5 dB steps. The thresholds for each animal before and after training is shown in Table 3.1. The averaged change in threshold before and after training was -1.43 dB and the standard deviation was 5.56 dB. The results were then analyzed with a paired t-test, which showed that there was not a significant difference ($p > 0.05$) in thresholds before and after training.

Table 3.1 Aging Effects Model Pre and Post Training Acoustic Hearing Threshold (dB SPL) from Channel 1

	Aged				Young		
	<i>G8A1</i>	<i>G8A2</i>	<i>S1A1</i>	<i>S1A2</i>	<i>G8Y1</i>	<i>S1Y1</i>	<i>S1Y2</i>
Pre-Training	65	65	60	50	30	25	35
Post-Training	65	60	50	55	25	30	35

The amplitude of peak 1 at the varying dB SPL was calculated for each animal an example shown in Figure 3.1. The average change in amplitude of peak 1 at 75 dB was -0.06 and the standard deviation was 0.076. The amplitude of peak 1 at 75 dB SPL before and after training were analyzed (Table B.1) with a paired t-test and with a 95% confidence interval, there was not a significant difference ($p > 0.05$).

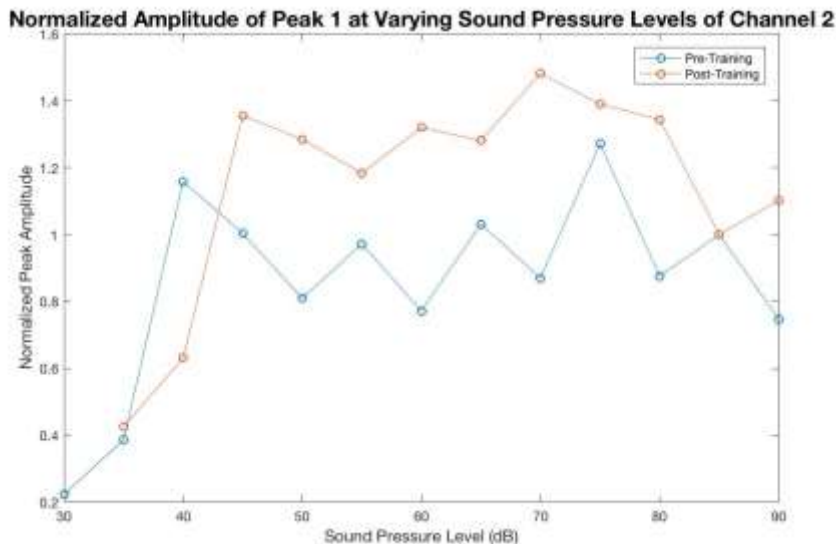


Figure 3.1 Example plot of peak 1 amplitudes from ABR of an animal across varying sound pressure levels before and after training

3.1.1.2 Envelope Following Response

The envelope and temporal fine structures emphasized EFRs were split into two groups: the stimuli that were used in the acoustic startle training and the similar IRN stimuli. The two stimuli used for the prepulse (IRN pitch sweep from 100 to 500) and the background (IRN pitch sweep from 1000 to 500) were the startle stimuli. The other 4 stimuli (IRN pitch sweep from 500 to 100, 500 to 1000, 500 flat tone, and 1000 flat tone) were other related stimuli that weren't directly trained

3.1.1.2.1 Startle Stimuli

The acoustic startle stimuli responses were considered correlated if they were above the threshold correlation of randomized noise (0.0438). The maximum correlation of the responses, both pre and post training, to the prepulse stimulus IRN 100 to 500 Hz are larger than the threshold correlation (Table B.2). As shown in Figure 3.2, the young animals' pre-training envelope emphasized response correlation was higher than the aged animals. However, post-training the young animals' correlation either decreased or remained the same. The aged animals' post-training correlation increased to the correlation range of the young animals. The temporal fine structure response's correlation did not vary as much before and after training. There was no statistically significant difference between the pre and post training correlation coefficients for any of the animals.

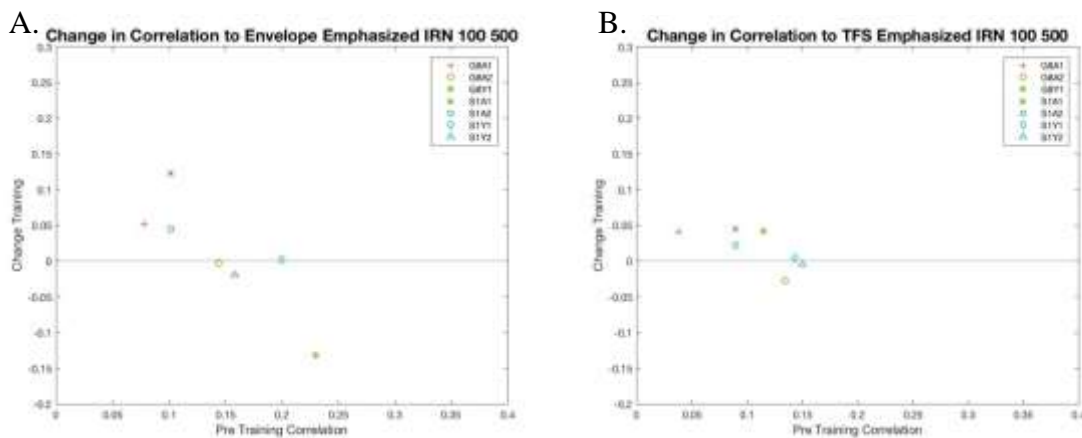


Figure 3.2 Aging Effects on training-related changes to correlation of response to envelope and temporal fine structure of IRN 100-500 stimulus. A) Shows the envelope emphasized pre-training response correlation and change between pre and post training response correlation to IRN 100-500 Hz for young ($N=3$) and aged ($N=4$) animals B) Shows the temporal fine structure emphasized pre-training response correlation and change between pre and post training response correlation to IRN 100-500 Hz for young ($N=3$) and aged ($N=4$) animals

The correlation coefficients of the responses to the background stimulus IRN 1000-500 Hz are greater than the threshold correlation (0.0438) to averaged randomized noise. All of the responses were correlated well above the threshold (Table B.3). Most of the animals had a decrease in correlation after the training and there wasn't a clear difference in the pre-training correlation values (Figure 3.3). There was no significant difference in pre and post correlation values for any of the animals.

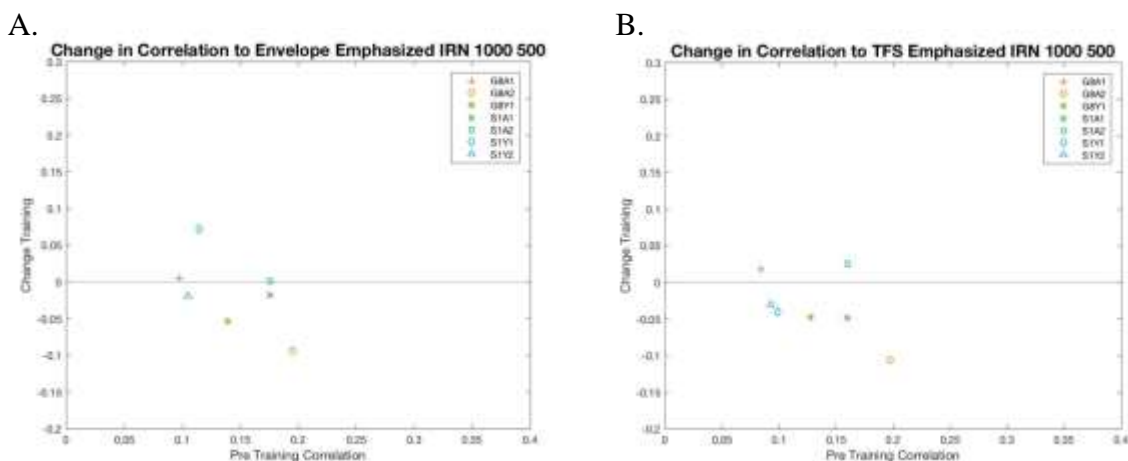


Figure 3.3 Aging Effects on training-related changes to correlation of response to envelope and temporal fine structure of IRN 1000-500 stimulus A) Shows the envelope emphasized pre-training response correlation and change between pre and post training response correlation to IRN 1000-500 Hz for young ($N=3$) and aged ($N=4$) animals B) Shows the temporal fine structure emphasized pre-training response correlation and change between pre and post training response correlation to IRN 1000-500 Hz for young ($N=3$) and aged ($N=4$) animals

3.1.1.2.2 Related IRN Stimuli

The other 4 stimuli still had the significant neural correlation over the threshold of averaged randomized noise correlation, except for G8A1's pre-training response to IRN 500-1000 Hz stimulus and IRN 1000 Hz flat tone stimulus (Table B.4). The envelope emphasized response to the reverse pitch sweep didn't vary for a majority of the animals with training (Figure 3.4). The emphasized response to temporal fine structure showed a decrease after training to the IRN 500-1000 Hz pitch sweep. However, the difference in correlation coefficient was not statistically significant ($p > 0.05$).

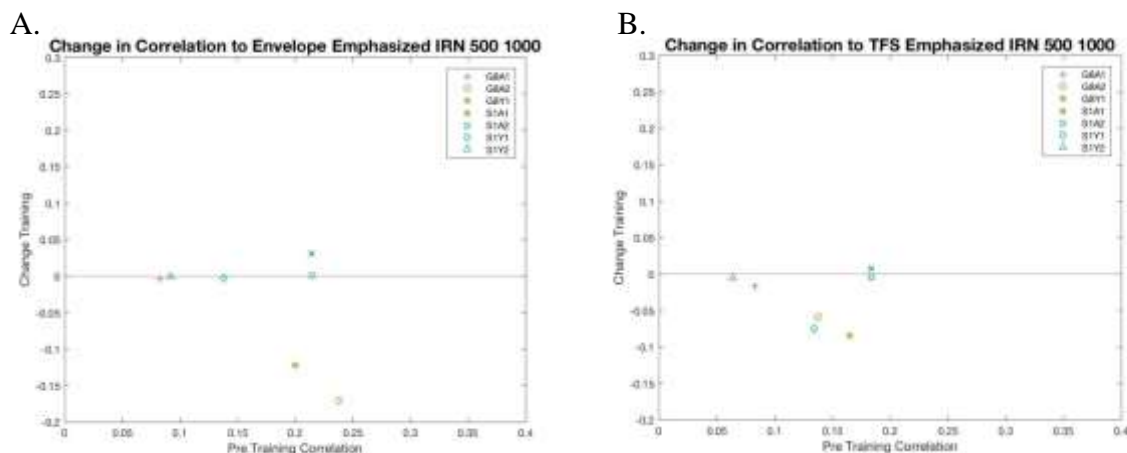


Figure 3.4 Aging Effects on training-related changes to correlation of response to envelope and temporal fine structure of IRN 500-1000 stimulus. A) Shows the envelope emphasized pre-training response correlation and change between pre and post training response correlation to IRN 500-1000 Hz for young ($N=3$) and aged ($N=4$) animals B) Shows the temporal fine structure emphasized pre-training response correlation and change between pre and post training response correlation to IRN 500-1000 Hz for young ($N=3$) and aged ($N=4$) animals

The correlation coefficient for the reversed prepulse IRN stimulus with a pitch sweep from 500 to 100 Hz were all above the threshold (0.0438) for noise correlation (Table B.5). Both young and aged animals didn't show any evidence of changes to the envelope or temporal fine structure emphasized results (Figure 3.5). G8A1 is the only animal that was separate from the cluster and had some apparent variation in response. While there was an apparent difference for G8A1, none of the changes in correlation before and after training were statistically significant.

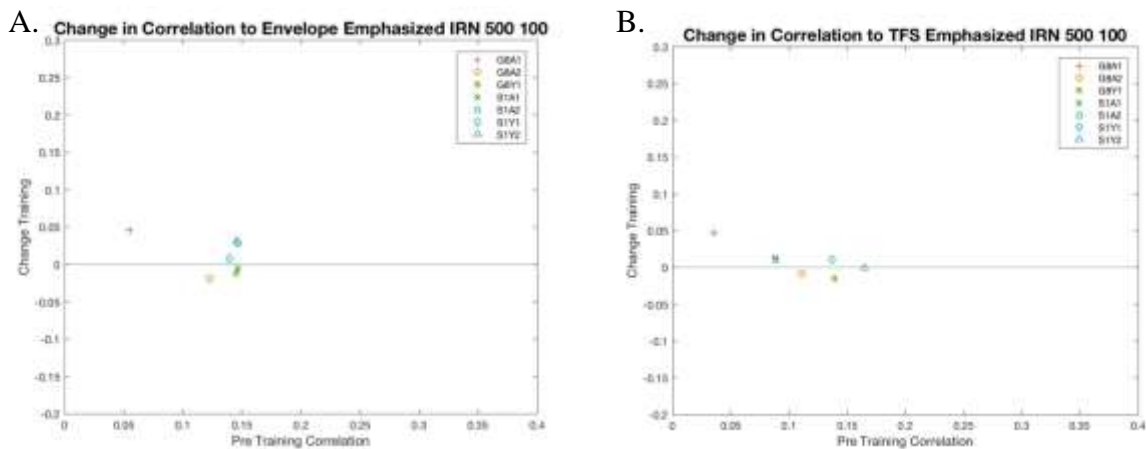


Figure 3.5 Aging Effects on training-related changes to correlation of response to envelope and temporal fine structure of IRN 500-100 stimulus. A) Shows the envelope emphasized pre-training response correlation and change between pre and post training response correlation to IRN 500-100 Hz for young ($N=3$) and aged ($N=4$) animals B) Shows the temporal fine structure emphasized pre-training response correlation and change between pre and post training response correlation to IRN 500-100 Hz for young ($N=3$) and aged ($N=4$) animals

The correlation coefficients for the IRN 1000 Hz flat tone were all above the threshold expected for the pre-training response from G8A1 (Table B.6). There was a group decrease in correlation in envelope emphasized response for the aged animals, except for G8A1 (Figure 3.6). The young animals didn't show a similar change in the emphasized envelope response. The emphasized temporal fine structure response decreased between recordings for the animals, with the exception of G8A1 and S1A2. There was no significant difference between the pre and post training correlations from the paired t-test.

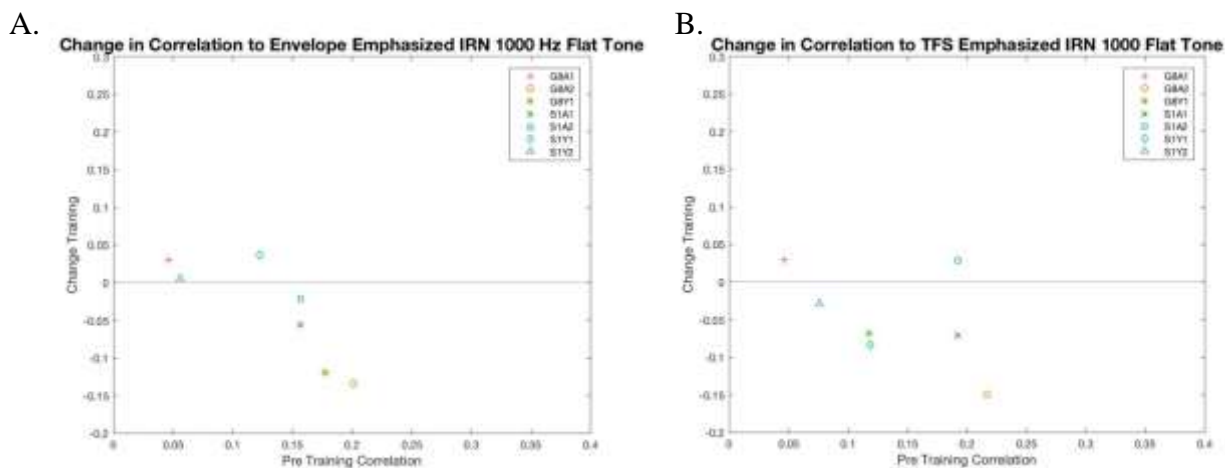


Figure 3.6 Aging Effects on training-related changes to correlation of response to envelope and temporal fine structure of IRN 1000 flat tone stimulus. A) Shows the envelope emphasized pre-training response correlation and change between pre and post training response correlation to IRN 1000 Hz flat tone for young ($N=3$) and aged ($N=4$) animals B) Shows the temporal fine structure emphasized pre-training response correlation and change between pre and post training response correlation to IRN 1000 Hz flat tone for young ($N=3$) and aged ($N=4$) animals

The maximum correlation coefficients for IRN 500 Hz flat tone, except for G8A1 and G8Y1 post-training, were above the threshold correlation of randomized noise (Table B.7). There was a dramatic drop in post-training emphasized envelope correlation for G8A2 and G8Y1 (Figure 3.7). The other animals showed an increased or no change in envelope correlation. The emphasized temporal fine structure showed a decrease in post training correlation for G8A2, G8Y1, and S1A1. All of the other animals showed no change in correlation post training. From the paired t-test, there were no significant ($p > 0.05$) difference between pre and post training correlations.

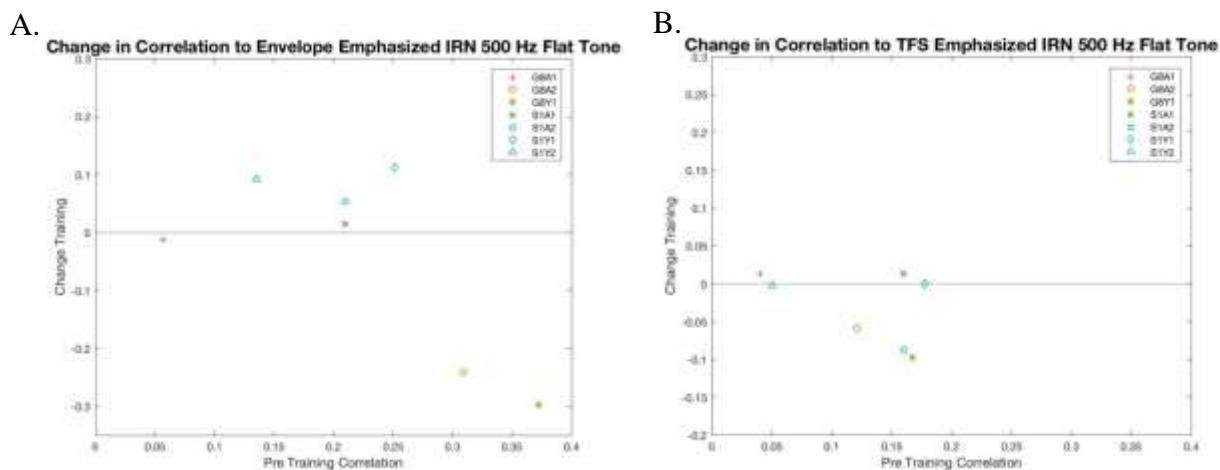


Figure 3.7 Aging Effects on training-related changes to correlation of response to envelope and temporal fine structure of IRN 500 Hz flat tone. A) Shows the envelope emphasized pre-training response correlation and change between pre and post training response correlation to IRN 500 Hz flat tone for young ($N=3$) and aged ($N=4$) animals B) Shows the temporal fine structure emphasized pre-training response correlation and change between pre and post training response correlation to IRN 500 Hz flat tone for young ($N=3$) and aged ($N=4$) animals

3.1.2 Acoustic Startle Response

The acoustic startle response was analyzed by individual days in box plots to effectively convey for each animal whether discrimination occurred. However, this is not plausible to easily compare between many animals with separate box plots. Therefore, the peak variation between day 1 and the other behavioral days was calculated to determine the effectiveness of the animals discrimination of the stimulus (Figure 3.8). These results compared with the paired t-test results of the startle response with the prepulse and the startle response without the prepulse were used to classify the animals as learning, not learning, and potential learning. G8Y1, G8Y2, and G8A2 all had smaller spread of startle response and less median startle than day 1 on at least one of the other days. They were classified as having learned the prepulse. Furthermore, G8Y2 startled significantly ($p < 0.05$) less with the prepulse than the startle response without the prepulse. S1A1 had a smaller median but a slightly larger spread than day 1 on both of the other days and was therefore considered potential magnitude learning. G8A1 had a larger median but a smaller spread than day 1 on both other days and was classified as potential variability learning. S1Y1 had a larger median and spread of startle response than day 1 on both other days. However, S1Y1 startled

significantly less. Also, S1A1's behavior was significantly ($p < 0.05$) larger than the responses on day 1 on the other days. Both of these situations classified them as not learning.

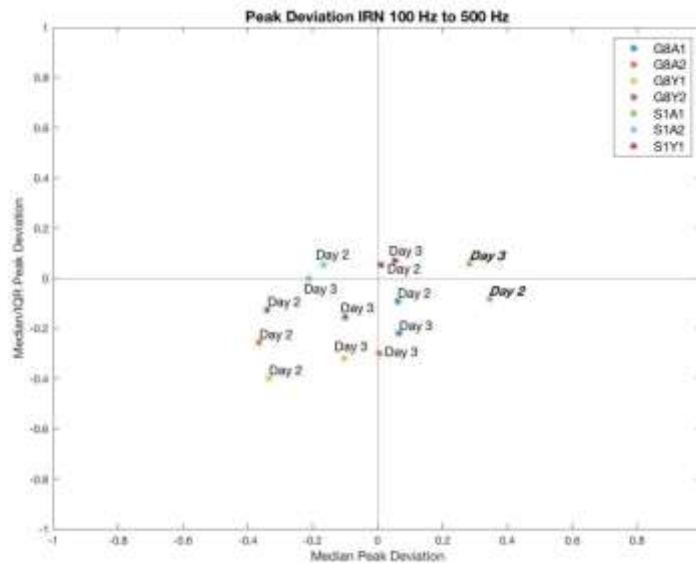


Figure 3.8 Peak Deviation of Startle Response from the first test day of startle in both the median as well as the spread of the response. The bold and italic labels mean that the results were statistically significantly different from the first day from a one-way ANOVA test ($p < 0.05$)

3.2 Aging and Habituation Prepulse Effects Pitch Sweep Discrimination and Differentiation

3.2.1.1 Electroencephalogram Recordings

3.2.1.2 Auditory Brainstem Response

The ABRs for this model were also taken before and after training to test the functionality of the animals' auditory system. The functionality was again determined by analyzing two components: the acoustic threshold and the amplitude of peak 1 across sound pressure levels from 95 to 25 dB with 10 dB steps. The thresholds for each animal before and after training is shown in Table 3.2. The average training-related change in threshold was -0.71 dB and the standard deviation was 5.56 dB.

Table 3.2 Aging and Habituation Prepulse Effects Model Pre and Post Training Acoustic Hearing Threshold (dB SPL) from Channel 1

	Aged		Young				
	S2A1	S2A2	S2Y1	S3Y3	S2Y2	S3Y1	S3Y2
# Habituation Prepulses	1	2	1	1	2	2	2
Pre-Training	60	65	35	35	30	35	30
Post-Training	70	60	35	35	25	35	25

The amplitude of peak 1 at the varying dB SPL was calculated for each animal an example shown in Figure 3.9. The average change in amplitude of peak 1 at 75 dB was 0.17 and the standard deviation was 0.30. The amplitude of peak 1 at 75 dB SPL before and after training were analyzed with a paired t-test and there was not a significant difference ($p > 0.05$).

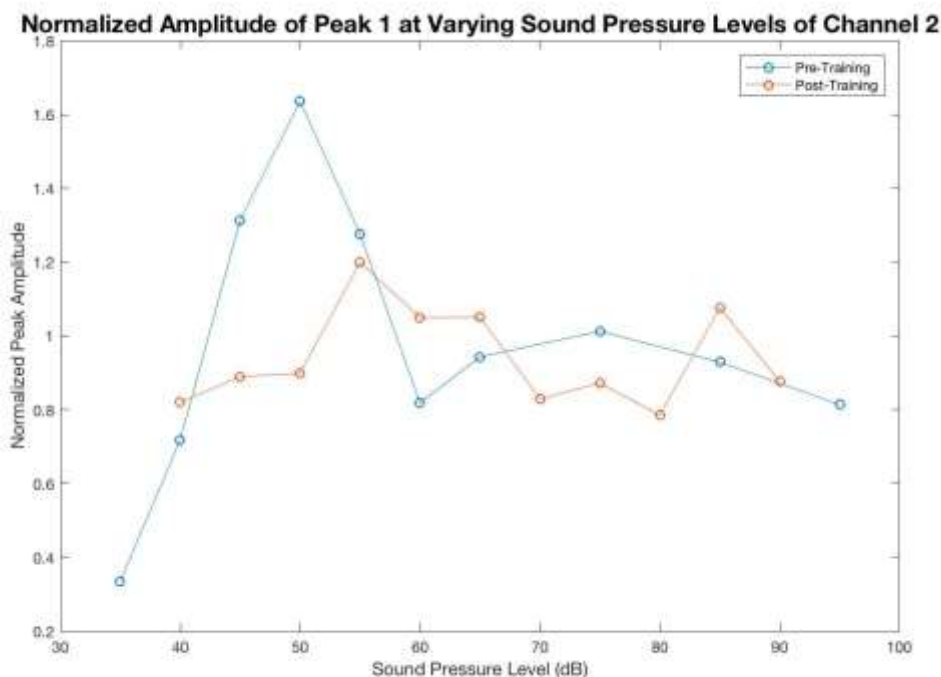


Figure 3.9 Example plot of peak 1 amplitudes from ABR of an animal across varying sound pressure levels before and after training

3.2.1.3 Envelope Following Response

The EFR stimuli were split into two groups: the stimuli that were used in the acoustic startle training and the similar IRN stimuli. The three stimuli used for the prepulse (IRN pitch sweep from

100 to 500, 8 kHz FM carrier plus pitch sweep from 100 to 500, and 8 kHz FM carrier pitch sweep minus pitch sweep from 100 to 500) and the one stimulus for the background (IRN pitch sweep from 1000 to 500) as well as their inverted polarity responses were the startle stimuli. The other 4 stimuli (IRN pitch sweep from 500 to 100, 500 to 1000, 1000 flat tone, and 125 flat tone) and their inverted polarity responses were other related stimuli that weren't directly trained

3.2.1.3.1 Startle Stimuli

The acoustic startle stimuli responses were considered correlated if they were above the threshold correlation of randomized noise (0.0438). The maximum correlation of the responses, both pre and post training, to the prepulse stimulus IRN 100 to 500 Hz are larger than the threshold correlation (Table B.8). S2A1 and S3Y3 had increased correlation coefficients post-training for both the envelope of the IRN 100-500 Hz stimulus (Figure 3.10). All of the other animals decreased slightly during the post-training recording. The emphasized temporal fine structure had an increased correlation post-training for S3Y1. It remained approximately the same for S2A2, S2A1, and S3Y3 and decreased for S2Y1 and S3Y2. The paired t-test between the pre and post training correlations showed that there were no significant ($p > 0.05$) differences between correlations.

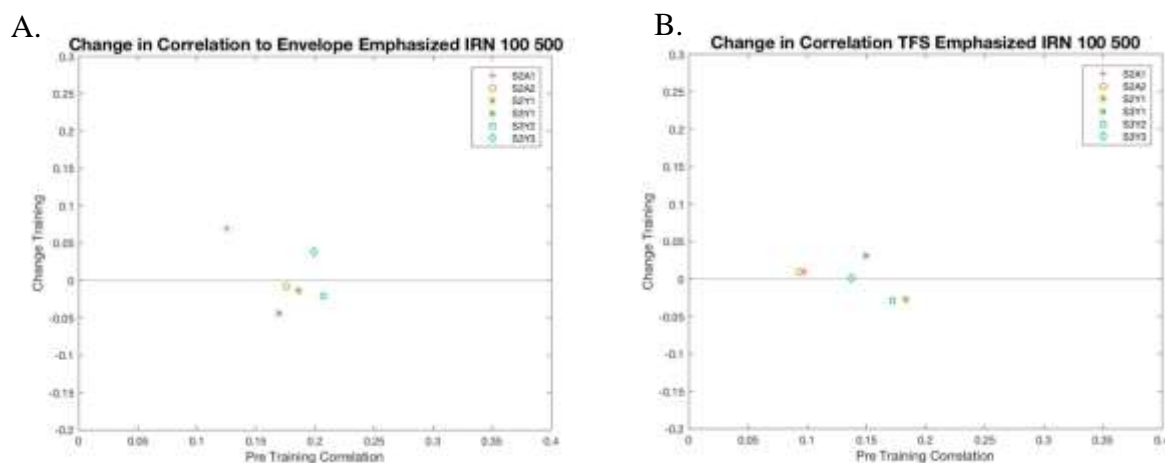


Figure 3.10 Aging and habituation effects on training-related changes to correlation of response to envelope and temporal fine structure of IRN 100-500 stimulus. A) Shows the envelope emphasized pre-training response correlation and change between pre and post training response correlation to IRN 100-500 Hz for young ($N=4$; 1 prepulse $N:2$; 2 prepulse $N:2$) and aged ($N=2$; 1 prepulse $N:1$; 2 prepulse $N:1$) animals B) Shows the temporal fine structure emphasized pre-training response correlation and change between pre and post training response correlation to IRN 100-500 Hz for young ($N=4$; 1 prepulse $N:2$; 2 prepulse $N:2$) and aged ($N=2$; 1 prepulse $N:1$; 2 prepulse $N:1$) animals.

For the correlation to FM 8 kHz + 100-500 Hz sweep, all of the responses were more correlated than the noise threshold correlation (Table B.9). There was an increase in the correlation post-training of S2A1, S2Y1, and S3Y1 for the envelope of the IRN (Figure 3.11). The other animals correlation coefficient decreased post-training. The temporal fine structure correlation had an increase for S2A2 and S2Y1 with a decrease for the rest of the animals. The paired t-test for the difference in correlation coefficients for FM 8 kHz + 100-500 Hz showed that there was no significance ($p > 0.05$) before and after training.

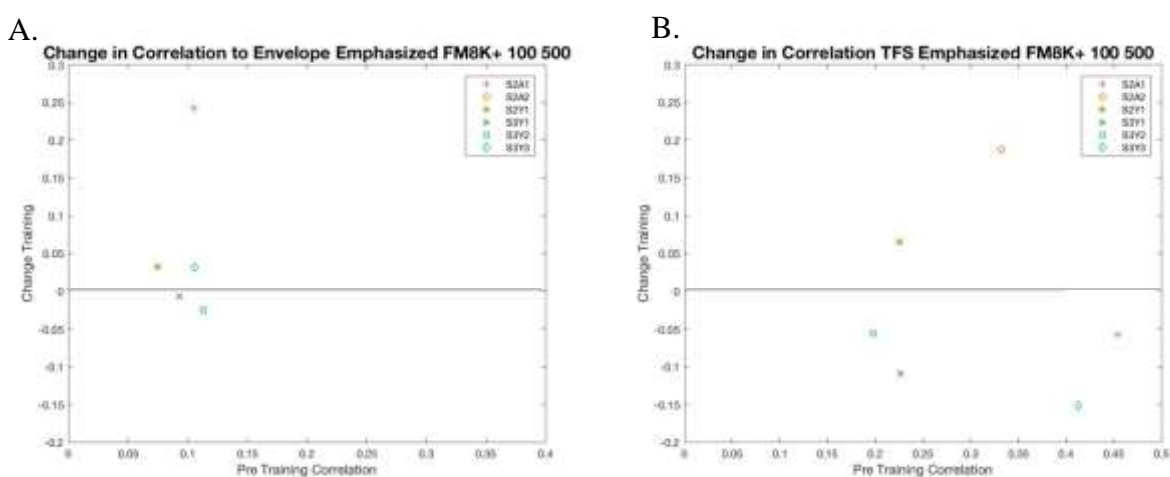


Figure 3.11 Aging and habituation effects on training-related changes to correlation of response to envelope and temporal fine structure of FM 8 kHz + 100-500. A) Shows the envelope emphasized pre-training response correlation and change between pre and post training response correlation to FM 8 kHz + 100-500 Hz for young ($N=4$; 1 prepulse $N:2$; 2 prepulse $N:2$) and aged ($N=2$; 1 prepulse $N:1$; 2 prepulse $N:1$) animals B) Shows the temporal fine structure emphasized pre-training response correlation and change between pre and post training response correlation to FM 8 kHz + 100-500 Hz for young ($N=4$; 1 prepulse $N:2$; 2 prepulse $N:2$) and aged ($N=2$; 1 prepulse $N:1$; 2 prepulse $N:1$) animals.

The correlation of responses to FM 8 kHz – 100-500 Hz prepulse was above the noise threshold correlation for all of the animals and conditions (Table B.10). S2A1, S2Y1, and S2A1 increased the correlation to the envelope of the stimulus post training (Figure 3.12). S2Y1 was the only animal with an increased correlation to the temporal fine structure as well. All of the other animals had negative correlation post training. There was no significant ($p > 0.05$) difference between pre-training and post-training correlation.

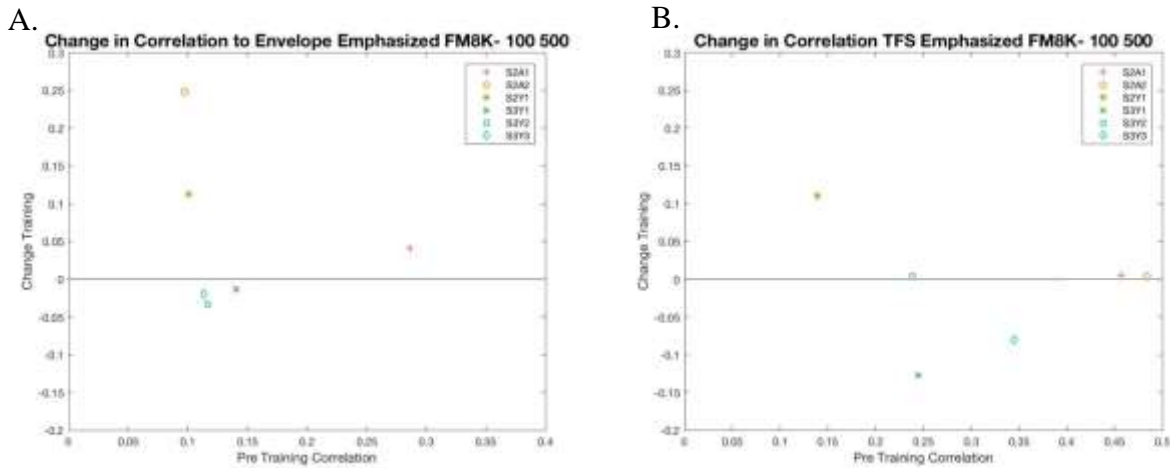


Figure 3.12 Aging and habituation effects on training-related changes to correlation of response to envelope and temporal fine structure of FM 8 kHz - 100-500. A) Shows the envelope emphasized pre-training response correlation and change between pre and post training response correlation to FM 8 kHz - 100-500 Hz for young ($N=4$; 1 prepulse $N:2$; 2 prepulse $N:2$) and aged ($N=2$; 1 prepulse $N:1$; 2 prepulse $N:1$) animals B) Shows the temporal fine structure emphasized pre-training response correlation and change between pre and post training response correlation to FM 8 kHz - 100-500 Hz for young ($N=4$; 1 prepulse $N:2$; 2 prepulse $N:2$) and aged ($N=2$; 1 prepulse $N:1$; 2 prepulse $N:1$) animals.

The correlation of responses to IRN 1000-500 Hz background was above the noise threshold correlation for all of the animals and conditions (Table B.II). S3Y2, S3Y3, S2A1, and S2A2 increased the correlation to both the envelope and temporal fine structure of the stimulus post-training (Figure 3.13). S3Y1 had an increase in correlation to the envelope post-training, but not the temporal fine structure. S2Y1 had a decrease in correlation to both the envelope and temporal fine structure post training. The paired t-test showed that there was no significant difference ($p>0.05$) between pre and post training recordings.

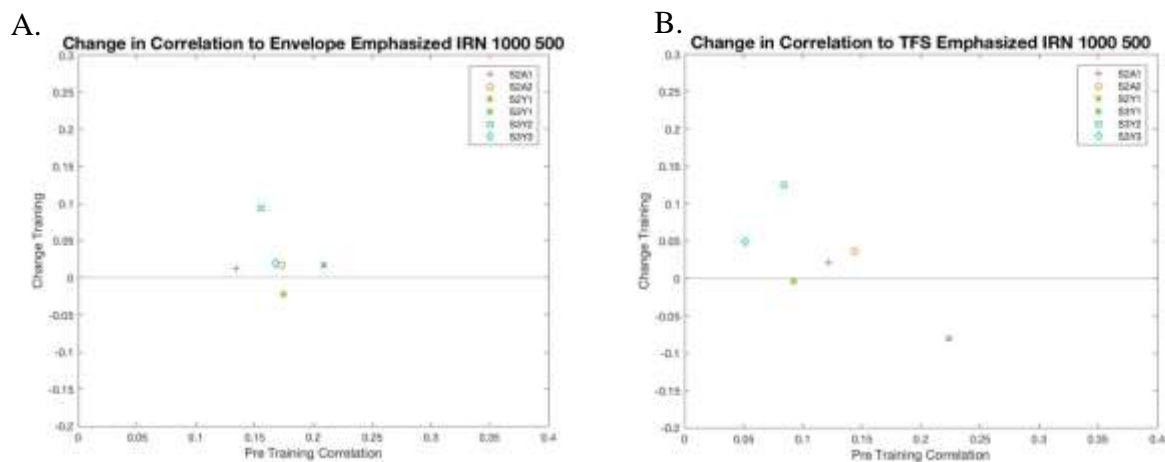


Figure 3.13 Aging and habituation effects on training-related changes to correlation of response to envelope and temporal fine structure of IRN 1000-500 stimulus. A) Shows the envelope emphasized pre-training response correlation and change between pre and post training response correlation to IRN 1000-500 Hz for young ($N=4$; 1 prepulse $N:2$; 2 prepulse $N:2$) and aged ($N=2$; 1 prepulse $N:1$; 2 prepulse $N:1$) animals B) Shows the temporal fine structure emphasized pre-training response correlation and change between pre and post training response correlation to IRN 1000-500 Hz for young ($N=4$; 1 prepulse $N:2$; 2 prepulse $N:2$) and aged ($N=2$; 1 prepulse $N:1$; 2 prepulse $N:1$) animals.

3.2.1.3.2 Related Stimuli

All of the responses to the related stimuli still had the significant neural correlation over the threshold of averaged randomized noise correlation. The change in correlation to the envelope of IRN 500-100 sweep post-training was positive for S2A1. S3Y2 and S3Y3 had a positive change in correlation post-training to the temporal fine structure of the stimulus. All of the other animals had a decreased correlation post training. The paired t-test showed that there was no significant difference ($p>0.05$) between pre-training and post-training correlations.

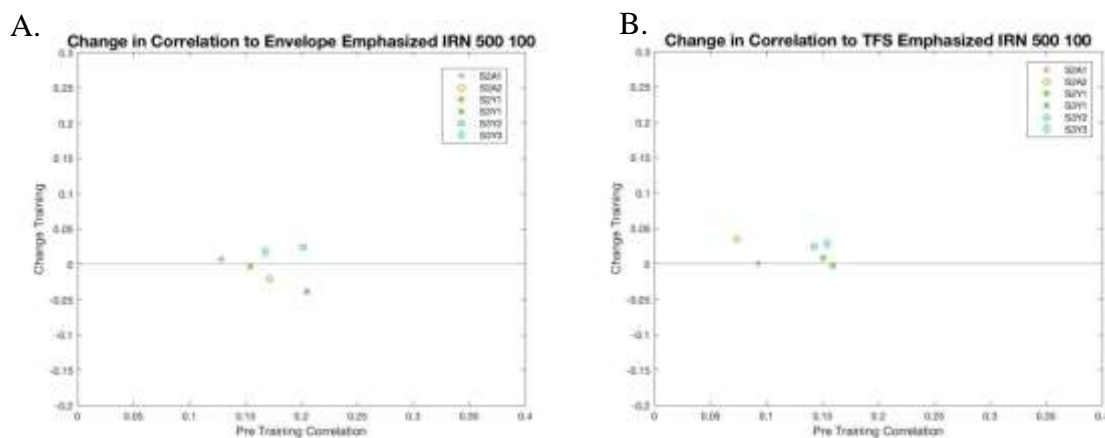


Figure 3.14 Aging and habituation effects on training-related changes to correlation of response to envelope and temporal fine structure of IRN 500-100 stimulus. A) Shows the envelope emphasized pre-training response correlation and change between pre and post training response correlation to IRN 500-100 Hz for young ($N=4$; 1 prepulse $N:2$; 2 prepulse $N:2$) and aged ($N=2$; 1 prepulse $N:1$; 2 prepulse $N:1$) animals B) Shows the temporal fine structure emphasized pre-training response correlation and change between pre and post training response correlation to IRN 500-100 Hz for young ($N=4$; 1 prepulse $N:2$; 2 prepulse $N:2$) and aged ($N=2$; 1 prepulse $N:1$; 2 prepulse $N:1$) animals.

All of the correlations were above the noise correlation threshold (Table B.12). The increased correlation post training to the envelope of IRN 500-1000 Hz pitch sweep was found for all animals, except S2Y1 and S2A1 (Figure 3.15). The temporal fine structure increased for all of the animals, except S3Y2. The paired t-test showed that there was no significant ($p > 0.05$) difference between the pre-training and post-training correlation.

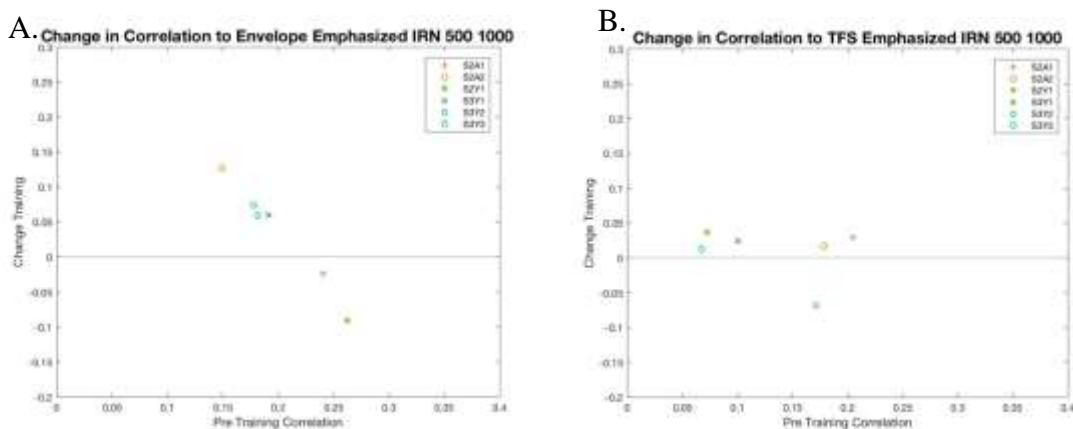


Figure 3.15 Aging and habituation effects on training-related changes to correlation of response to envelope and temporal fine structure of IRN 500-1000 stimulus. A) Shows the envelope emphasized pre-training response correlation and change between pre and post training response correlation to IRN 500-1000 Hz for young ($N=4$; 1 prepulse $N=2$; 2 prepulse $N=2$) and aged ($N=2$; 1 prepulse $N=1$; 2 prepulse $N=1$) animals B) Shows the temporal fine structure emphasized pre-training response correlation and change between pre and post training response correlation to IRN 500-1000 Hz for young ($N=4$; 1 prepulse $N=2$; 2 prepulse $N=2$) and aged ($N=2$; 1 prepulse $N=1$; 2 prepulse $N=1$) animals.

The correlations to the IRN 1000 Hz flat tone were larger than the average threshold noise response (0.0438) (Table B.13). S2A2's correlation increases for both envelope and temporal fine structure post training recordings (Figure 3.16). S3Y1 and S3Y3 had increased correlation post training to both the normal and inverted IRN 1000 flat tone. S2A2 had increased correlation post training only to the normal IRN 1000 flat tone. All of the other animals had decreased correlation post training. The paired t-test showed that there was no significant difference ($p>0.05$) between the pre-training and post-training correlation coefficients.

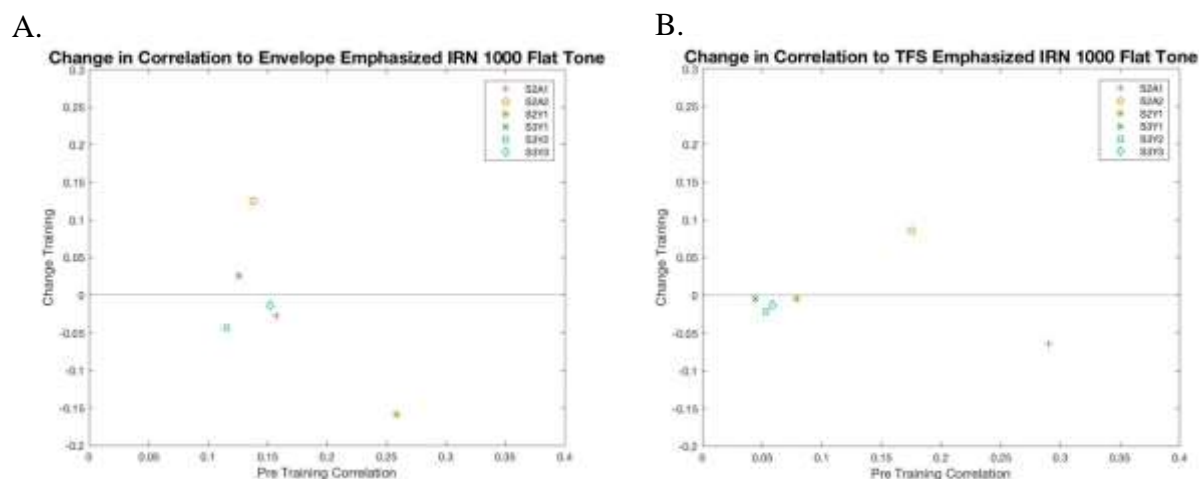


Figure 3.16 Aging and habituation effects on training-related changes to correlation of response to envelope and temporal fine structure of IRN 1000 Hz flat tone stimulus. A) Shows the envelope emphasized pre-training response correlation and change between pre and post training response correlation to IRN 1000 Hz flat tone for young ($N=4$; 1 prepulse $N:2$; 2 prepulse $N:2$) and aged ($N=2$; 1 prepulse $N:1$; 2 prepulse $N:1$) animals B) Shows the temporal fine structure emphasized pre-training response correlation and change between pre and post training response correlation to IRN 1000 Hz flat tone for young ($N=4$; 1 prepulse $N:2$; 2 prepulse $N:2$) and aged ($N=2$; 1 prepulse $N:1$; 2 prepulse $N:1$) animals.

All of the correlation coefficients for the animals' pre-training and post-training recordings were larger than the noise correlation threshold and therefore were correlated to the stimulus (Table B.14). S2A1 and S3Y3 had an increase in correlation post training for the emphasized envelope IRN 125 Hz flat tone recording (Figure 3.17). All of the other animals had decreased or no change in correlation post training. The temporal fine structure response correlation decreased or remained about the same for all animals post-training. The paired t-test showed that there was no significant difference ($p>0.05$) between pre-training and post-training correlation coefficients.

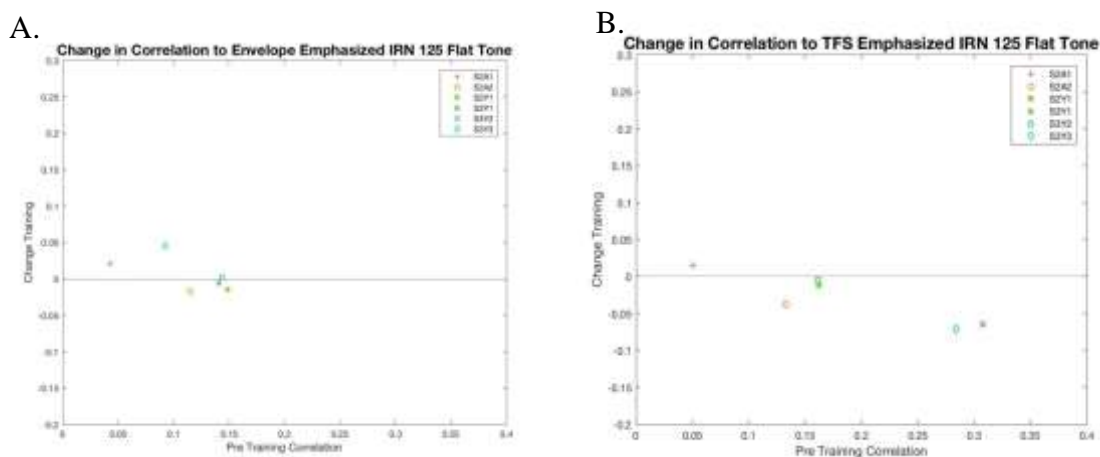


Figure 3.17 Aging and habituation effects on training-related changes to correlation of response to envelope and temporal fine structure of IRN 125 Hz flat tone stimulus. A) Shows the envelope emphasized pre-training response correlation and change between pre and post training response correlation to IRN 125 Hz flat tone for young ($N=4$; 1 prepulse $N=2$; 2 prepulse $N=2$) and aged ($N=2$; 1 prepulse $N=1$; 2 prepulse $N=1$) animals B) Shows the temporal fine structure emphasized pre-training response correlation and change between pre and post training response correlation to IRN 125 Hz flat tone for young ($N=4$; 1 prepulse $N=2$; 2 prepulse $N=2$) and aged ($N=2$; 1 prepulse $N=1$; 2 prepulse $N=1$) animals.

3.2.2 Acoustic Startle Response

The acoustic startle response was analyzed for all 7 of the prepulse stimuli. The peak variation between day 1 and the other behavioral days for each stimulus was calculated to determine the effectiveness of the animals' discrimination of the stimulus. As well as the ability to compare between the stimuli, the animals' overall ability to discriminate. Furthermore, results from paired t-test and repeated measure ANOVAs were used to support these comparisons.

For the IRN 100-500 pitch sweep prepulse (Figure 3.18), S3Y1 and S3Y2 for both days had a smaller median and IQR than day 1 and was therefore classified as learning. S2A2 both had a day with a smaller median but a larger spread and were classified as potential magnitude learning. S3Y3 also had a day where the median was smaller and the spread was larger, however, the paired t-test between startles with prepulses and startle without prepulses showed a significant difference ($p < 0.05$) between the two. Therefore, S3Y3 was classified as learning. S2Y2 had one day with a larger median but a smaller spread and was classified as potential variation learning. S2A1 had a smaller median but the repeated measure ANOVA that was used to compare between days showed that there was a significantly ($p < 0.05$) larger spread than day 1 and was therefore classified as not

learning. The repeated measure ANOVA for the impacts of aging and habituation showed that there was a significant ($p < 0.05$) change in responses between days for all groups, there was not one between groups ($p > 0.05$). However, there was a significant difference ($p < 0.05$) between how the aged animals changed across days and how their young counterparts changed across days.

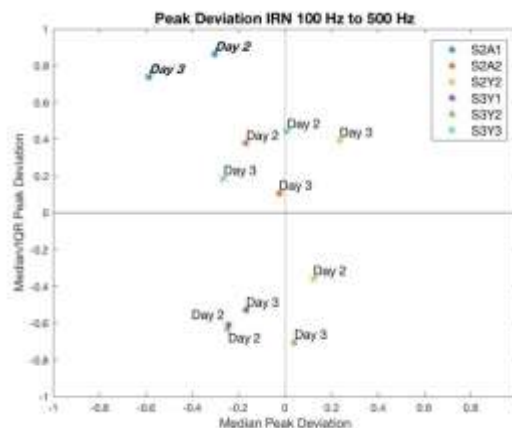


Figure 3.18 Peak Deviation of Startle Response to IRN 100-500 Hz pitch sweep prepulse and IRN 1000-500 Hz pitch sweep background stimulus from the first test day of startle in both the median as well as the spread of the response. The bold and italic labels mean that the results were statistically significantly different from the first day from a one-way ANOVA test ($p < 0.05$)

In Figure 3.18, the FM 8 kHz pitch sweeps showed different trends based on the direction of the sweep. For the FM 8 kHz – 100 Hz to 500 Hz (negative), a small cluster of S2Y2, S2A2, S3Y1, and S3Y2 with smaller median and spread than on day 1 and therefore was classified as learning. For the same region of the plot for FM 8 kHz + 100-500 Hz (positive), only S3Y2 had a smaller median and spread than day 1. For both plots S3Y3, had a larger spread and generally larger median, which qualified as the animal not learning. S2A1's startle response with prepulse was significantly less than the startle response without the prepulse and was therefore classified as learning. S2Y2 for the positive pitch sweep had a smaller median but larger spread and had a statically significant difference between the startle with a prepulse and the startle response without a prepulse. The positive pitch sweep showed that S3Y1 had a larger median but a smaller spread and was labeled as potential variability learning. The repeated measure ANOVA showed that there was a significant difference ($p < 0.05$) between the positive and negative sweeps as the animals discriminated better with the positive sweep than with the negative. The repeated measure

ANOVA between aged groups showed that like with the IRN 100-500 Hz sweep there is a significant difference in how the aged discriminate across days in comparison to their young counter parts.

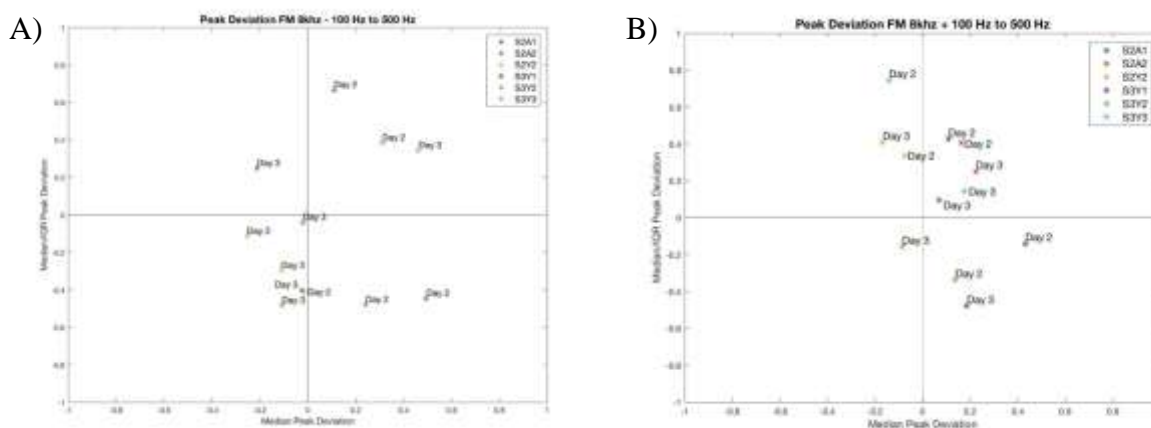


Figure 3.19 Peak Deviation of Startle Response to FM 8 kHz pitch sweeps prepulses and IRN 1000-500 Hz pitch sweep background stimulus from the first test day of startle in both the median as well as the spread of the response. The bold and italic labels mean that the results were statistically significantly different from the first day from a one-way ANOVA test ($p < 0.05$) A) Peak deviation of startle response from FM 8 kHz – 100-500 Hz prepulse. B) Peak deviation of startle response from FM 8 kHz + 100-500 Hz prepulse.

The 4 white gaussian noise (WGN) prepulses showed some interesting trends at the varying sound levels and with or without background noise (Figure 3.20). For all 4 stimuli and both days, S3Y1 and S3Y2 had smaller medians and spreads than day 1. Furthermore, S3Y1 day 2 and day 3 were significantly different from day 1 for WGN with background, at 30, and at 70 dB. S3Y2 day 2 and day 3 were significantly different from day 1 for WGN at 50 dB. They were both classified as learning the 4 stimuli. S2Y2 had a significant decrease in startle response prepulse when compared to startle without prepulse for all of the WGN prepulses and was therefore classified as learning all of them. The other animals were less consistent across the 4 prepulses. S2A1 day 2 and day 3 for WGN with background, at 30, and at 70 dB had a smaller median and larger spread than day 1. Also S2A1 was significantly different from day 1 and had a significant decrease in startle response prepulse when compared to startle without prepulse for WGN with background and at 70 dB. Therefore, classified S2A1 as learning those two stimuli and potential magnitude learning for the other. S2A2 had a larger spread and median than day 1 on both days for the standard prepulse

at 30 and 50 dB and was labeled at not having learned either stimuli. For the WGN with the background, S2A2 had a smaller median and spread for one of the days and was classified as learning. S2A2 for the WGN at 70 dB had a slightly smaller median but a larger spread one day and a larger median but a smaller spread for the other and was classified as both potential magnitude learning and potential variation learning. S3Y3 had a smaller median than day 1 by day 3 for all WGN prepulses (potential magnitude learning) and had both a smaller median and spread for day 3 70 dB (learning). When comparing between the aged and young groups, the repeated measure ANOVA showed that there was a significant difference in the change in discrimination across days between the young and aged animals. Furthermore, there was a significant difference ($p < 0.05$) between the response to WGN with background and the WGN at 50 or 70 dB, but not between the other startle responses.

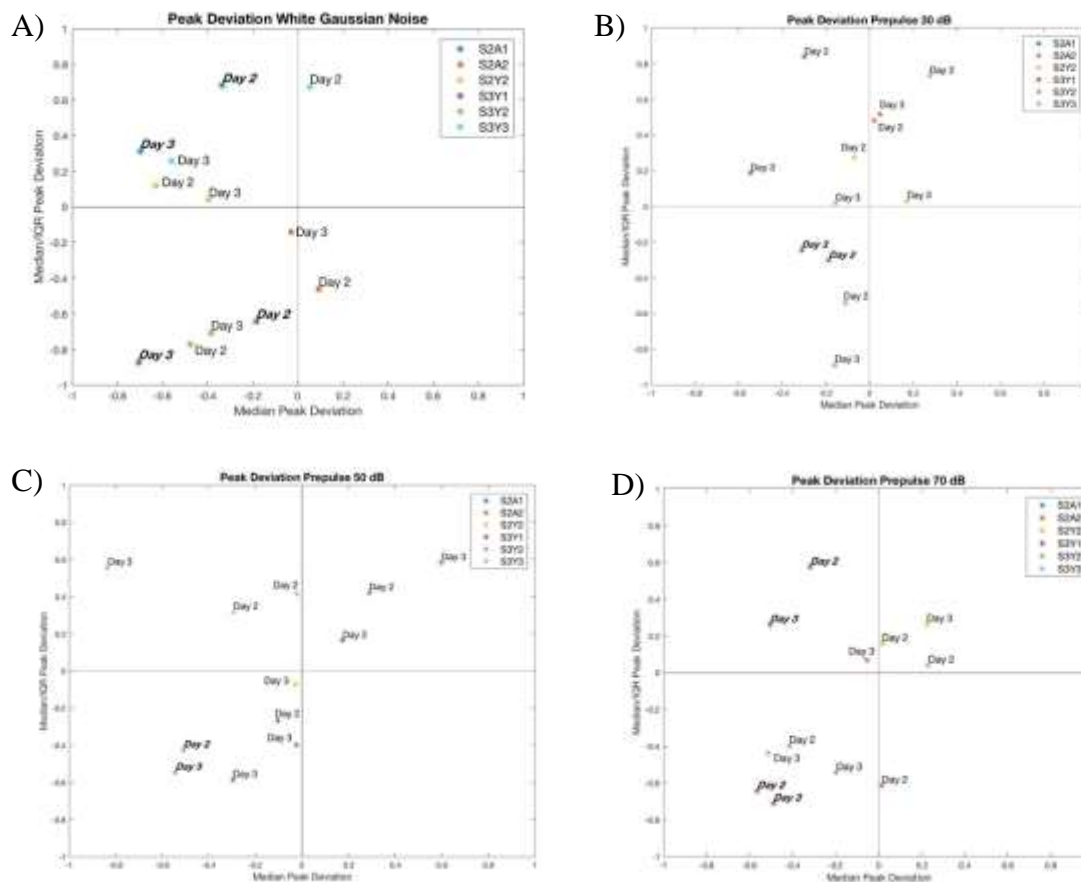


Figure 3.20 Peak Deviation of Startle Response to white gaussian noise from the first test day of startle in both the median as well as the spread of the response. The bold and italic labels mean that the results were statistically significantly different from the first day from a one-way ANOVA test ($p < 0.05$) A) Peak deviation of startle response from white gaussian noise 40 dB above threshold or at 80 dB with a background stimulus of IRN 1000-500 Hz. B) Peak deviation of startle response from whit gaussian noise 30 dB prepulse without a background stimulus. C) Peak deviation of startle response from whit gaussian noise 50 dB prepulse without a background stimulus. D) Peak deviation of startle response from whit gaussian noise 70 dB prepulse without a background stimulus.

3.3 Corticofugal Modulation Effects on Pitch Sweep Discrimination and Differentiation

3.3.1 Dye Injection Surgery

The dye injection surgeries were used to ensure that the angled injections were targeting the regions of interest in the brain. As shown in Figure 3.21, the fluorescence of the cresyl violet injection is in the top of the IC slice. The angled injection is visually shown to reach DCIC/ECIC from this slice. The ranged image of Figure 3.22 shows an increased intensity around the injection

location of viral GFP in auditory cortex in gray. There is a clear indentation where the needle entered the brain in visual cortex and continued down towards auditory cortex.

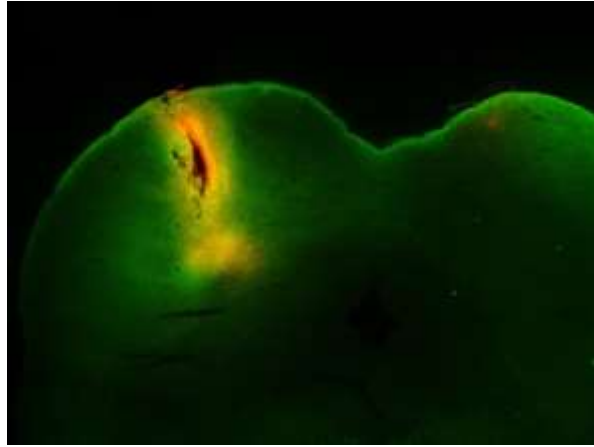


Figure 3.21 IC Injection Site with Cresyl Violet dye injection (orange) and background fluorescence to show structure of slice (green)

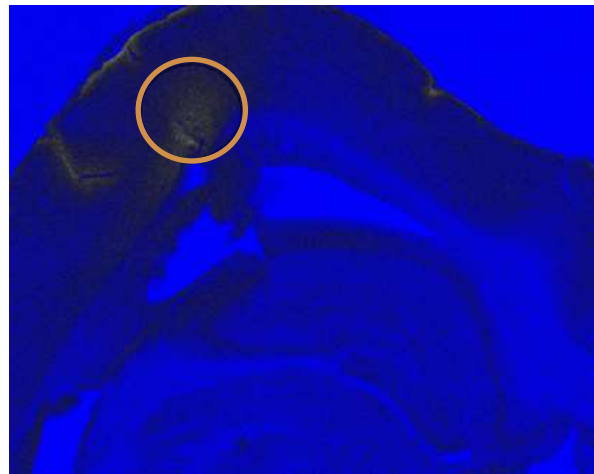


Figure 3.22 A1 Injection Site Ranged Image of GFP fluorescence (gray)

3.3.2 Electroencephalogram Recordings

3.3.2.1 Auditory Brainstem Response

The ABRs were taken before and after each part of the experiment (pre-surgery, pre-training pre-CNO, pre-training post-CNO, post-training pre-CNO, and post-training post-CNO) to test the functionality of the animals' auditory system throughout the experiment. The continued

functionality of the system throughout the experiment was shown by analyzing two components: the acoustic threshold and the amplitude of peak 1 across sound pressure levels from 95 to 25 dB with 5 dB steps. The thresholds for each animal and each part of the experiment is shown in Table 3.3. The average surgery-related change (pre-surgery and pre-training pre-CNO) was 0 and the standard deviation was 8.06. The average training-related change (pre-training pre-CNO and post training pre-CNO) was 4.55 and the standard deviation was 7.56. The average CNO-related change (pre-training pre-CNO compared with pre-training post-CNO and post-training pre-CNO compared with post training post-CNO) was -0.28 and the standard deviation was 7.15. The results were then analyzed with a paired t-test for each portion of the experiment, which showed that there was not a significant difference ($p > 0.05$) in thresholds from any part of the experiment.

Table 3.3 *Acoustic Hearing Thresholds (dB SPL) throughout Experiment from Channel 1*

	DR01	DR02	DR03	DR04	DR05	DR08	DR09	DR10	DR11	DR13	DR14
Pre-Surgery	35	25	25	25	40	35	35	25	35	35	35
Pre-Training Pre-CNO	45	35	30	35	35	25	35	25	25	25	35
Pre-Training Post-CNO	35	35	35	35	35	35	35	35	35	35	35
Post-Training Pre-CNO	30	45	35	40	35	35	40	35	35	35	35
Post-Training Post-CNO	35	35	25	25	35	35	40	35	25	35	35

The amplitude of peak 1 at the varying dB SPL was calculated for each animal an example shown in Figure 3.23. The average surgery related change in amplitude of peak 1 at 75 dB was -0.03 and the standard deviation was 0.26. The average training related change in amplitude of peak 1 at 75 dB was 0.02 and the standard deviation was 0.25. The average surgery related change in amplitude of peak 1 at 75 dB was 0.02 and the standard deviation was 0.34. The change in amplitude of peak 1 at 75 dB SPL for each portion of the experiment were analyzed with a paired t-test and there was not a significant difference ($p > 0.05$).

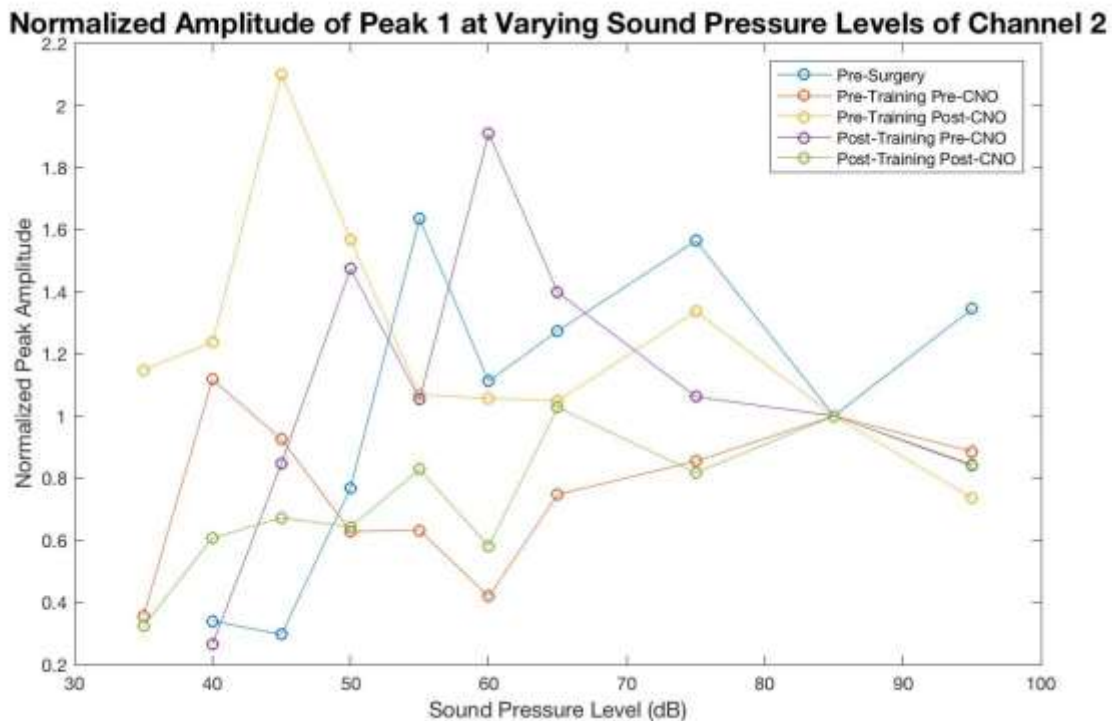


Figure 3.23 Example plot of peak 1 amplitudes from ABR of an animal across varying sound pressure levels throughout experiment

3.3.2.2 Envelope Following Response

The EFR stimuli were split into two groups: the stimuli that were used in the acoustic startle training and the similar IRN stimuli. The three stimuli used for the envelope and temporal fine structure's prepulse (IRN pitch sweep from 100 to 500, 8 kHz FM carrier plus pitch sweep from 100 to 500, and 8 kHz FM carrier pitch sweep minus pitch sweep from 100 to 500) and the one stimulus for the background (IRN pitch sweep from 1000 to 500). The other 4 stimuli (IRN pitch sweep from 500 to 100, 500 to 1000, 1000 flat tone, and 125 flat tone) were related to stimuli that were used but weren't directly trained

3.3.2.2.1 Startle Stimuli

The acoustic startle stimuli responses were considered correlated if they were above the threshold correlation of randomized noise (0.0438). The maximum correlation of the 3 responses (pre-training, post-training, post CNO) to the prepulse stimulus IRN 100 to 500 Hz are larger than the threshold correlation (Table B.16). The change in correlation to the envelope from training and

CNO is shown in **Figure 3.24**, with DR05, DR08, DR09, and DR10 showing an increase in correlation to the envelope post-training and DR01, DR03, DR08, DR11, and DR14 showing a decrease in correlation post CNO. The temporal fine structure changes in correlation were smaller so only DR08 and DR13 were shown to have an increase in correlation post-training and DR08 decreased in temporal fine structure post CNO. There was no significant ($p>0.05$) differences between the pre-training and post-training correlations found from the paired t-test.

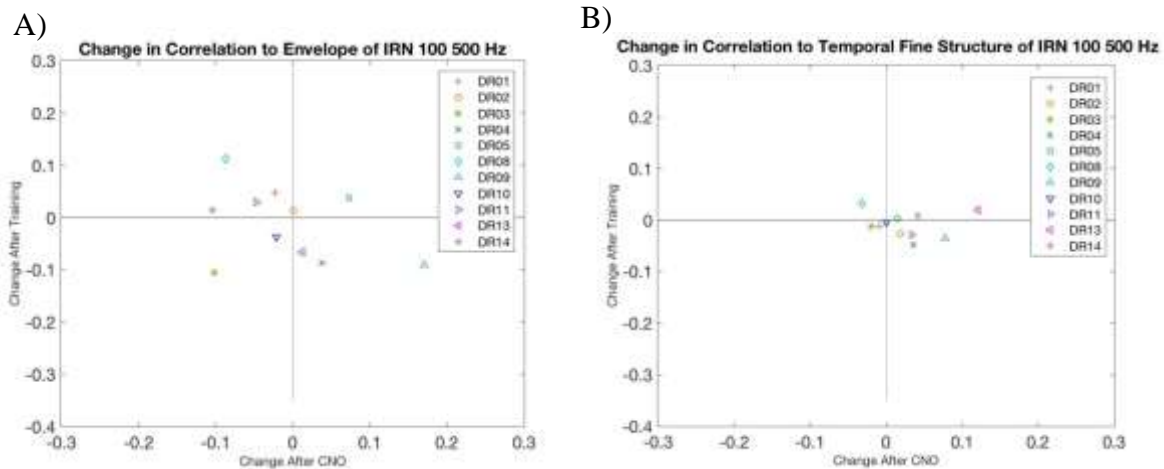


Figure 3.24 Corticofugal Inhibition effects on training-related changes to correlation of response to envelope and temporal fine structure of IRN 100-500 Hz stimulus. A) Shows the envelope emphasized change between pre and post training response correlation and change between pre and post CNO response correlation to IRN 100-500 Hz stimulus for young ($N=11$) animals B) Shows the temporal fine structure emphasized change between pre and post training response correlation and change between pre and post CNO response correlation to IRN 100-500 Hz stimulus tone for young ($N=11$) animals.

The maximum correlation of the 3 responses (pre-training, post-training, post CNO) to the prepulse stimulus FM 8 kHz + 100-500 Hz are larger than the threshold correlation (Table B.18). The change in correlation from training and CNO is shown in Figure 3.25. There was an increase in envelope correlation post training and decrease in correlation post CNO for DR02 and DR04. There was an increase in correlation post CNO for DR11, DR13, and DR14. The temporal fine structure correlation was more spread out with changes in both training and CNO correlations. DR03, DR05, DR08, DR09, and DR13 all had their post training temporal fine structure increase. Only DR03, DR04, and DR09 had a decrease in temporal fine structure correlation post CNO.

There was no significant difference between pre-training and post training as well as pre-CNO and post-CNO.

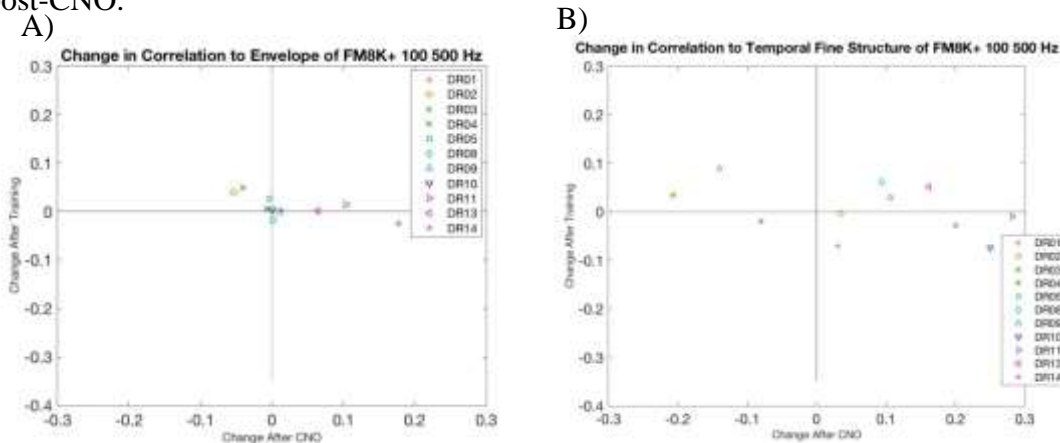


Figure 3.25 Corticofugal Inhibition effects on training-related changes to correlation of response to envelope and temporal fine structure of FM 8 kHz + 100-500 Hz stimulus. A) Shows the envelope emphasized change between pre and post training response correlation and change between pre and post CNO response correlation to FM 8 kHz + 100-500 Hz stimulus for young ($N=11$) animals B) Shows the temporal fine structure emphasized change between pre and post training response correlation and change between pre and post CNO response correlation to FM 8 kHz + 100-500 Hz stimulus tone for young ($N=11$) animals.

The maximum correlation coefficients for the FM 8 kHz – 100-500 Hz prepulse are all over the threshold of randomized noise (Table 0.20). The changes in correlation from training and CNO is shown in Figure 3.26. There was an increase in correlation to envelope of stimulus after training for DR04, DR05, DR09, DR11, DR13, and DR14. There was a decrease in correlation to the envelope after CNO injection for DR01, DR03, DR04, and DR09. For the temporal fine structure correlation most of the animals had minimal to no change in correlation in relation to training and CNO injection. Only DR09, DR11, and DR14 were spread out with a large change in correlation, DR09 had a large increase in correlation post training and decrease in correlation after the CNO injection. DR11 and DR14 had minimal training related changes in correlation but had a large increase correlation after the CNO injection. There was no significant differences between correlations before and after training as well as before and after the CNO injection

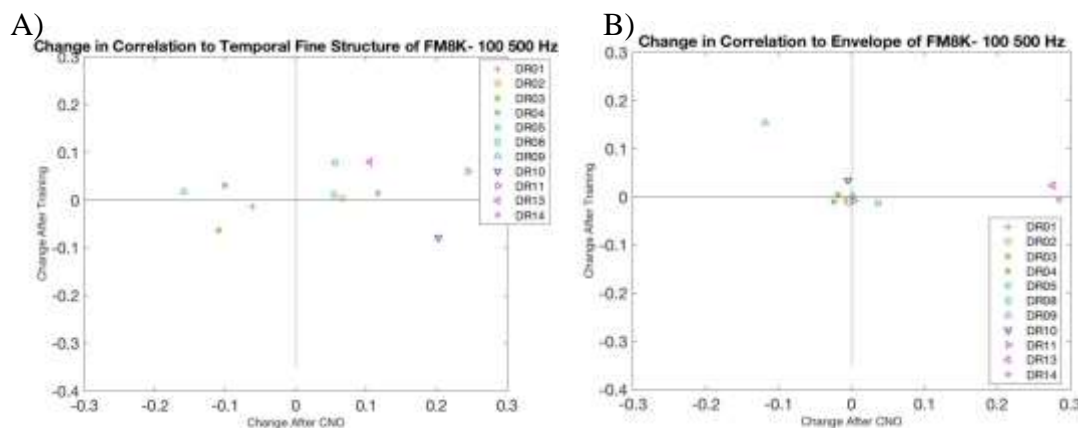


Figure 3.26 Corticofugal Inhibition effects on training-related changes to correlation of response to envelope and temporal fine structure of FM 8 kHz - 100-500 Hz stimulus. A) Shows the envelope emphasized change between pre and post training response correlation and change between pre and post CNO response correlation to FM 8 kHz - 100-500 Hz stimulus for young ($N=11$) animals B) Shows the temporal fine structure emphasized change between pre and post training response correlation and change between pre and post CNO response correlation to FM 8 kHz - 100-500 Hz stimulus tone for young ($N=11$) animals.

The maximum correlation coefficients for the IRN 1000-500 Hz background stimulus are all over the threshold of randomized noise (Table 0.22). The changes in correlation after training and after CNO injection is shown below in Figure 3.27. There was an increase in the correlation coefficient to the envelope after training for DR04, DR09, DR10, and DR13. There was a decrease in the correlation coefficient to the envelope response for DR03, DR04, DR09, DR10, DR11, DR13, and DR14 after the CNO injection. The temporal fine structure response was more clustered and only DR04, DR09, DR11, and DR13 were increased with after training. Only DR04 and DR09 decreased after the CNO injection. There was no significant difference between the pre-training and post-training or pre and post CNO correlation coefficients.

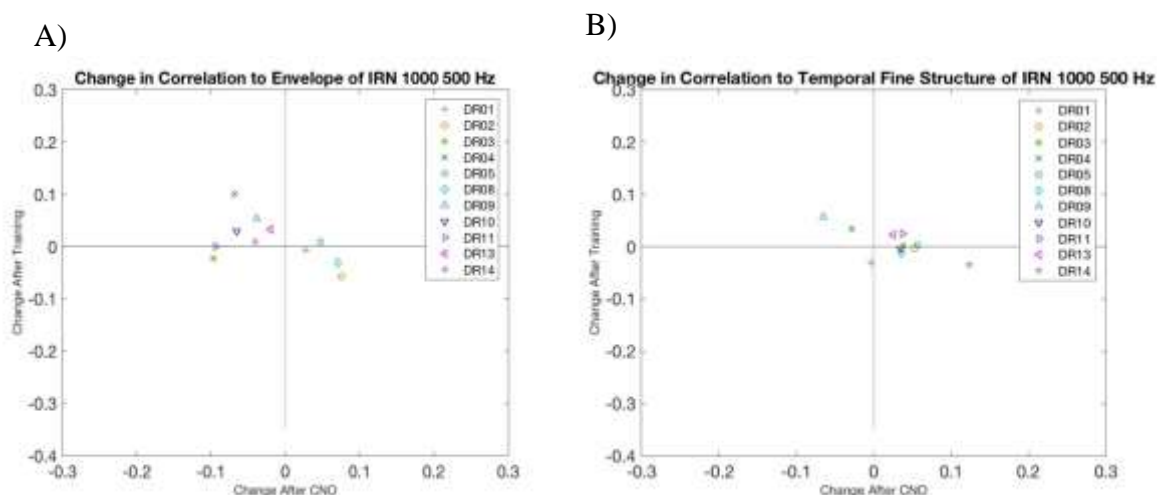


Figure 3.27 Corticofugal Inhibition effects on training-related changes to correlation of response to envelope and temporal fine structure of IRN 1000-500 Hz stimulus. A) Shows the envelope emphasized change between pre and post training response correlation and change between pre and post CNO response correlation to IRN 1000-500 Hz stimulus for young ($N=11$) animals B) Shows the temporal fine structure emphasized change between pre and post training response correlation and change between pre and post CNO response correlation to IRN 1000-500 Hz stimulus tone for young ($N=11$) animals.

3.3.2.2.2 Related Stimuli

The 4 related stimuli were IRN 500-100 Hz pitch sweep, IRN 500-1000 Hz pitch sweep, IRN 1000 Hz flat tone, and IRN 125 Hz flat tone. All the other related stimuli still had the significant neural correlation over the threshold of averaged randomized noise correlation, except for DR03 Post Training Pre CNO response to IRN 1000 Hz flat tone (Table 0.24). For the IRN 500-100 Hz pitch sweep (Figure 3.29), the correlation coefficients for envelope response that increased after training were DR04, DR05, DR08, and DR13. The correlation coefficients in response to the envelope of IRN 500-100 Hz pitch sweep decreased after CNO injection for DR01, DR03, DR05, DR08, DR10, and DR13. The temporal fine structure emphasized response had an increased correlation after training for DR02, DR04, DR11, and DR13. The emphasized temporal fine structure had a decrease after CNO for DR02, DR03, DR10, DR11, DR13, and DR14. There was no significant ($p>0.05$) difference between the pre and post training or pre and post CNO correlation.

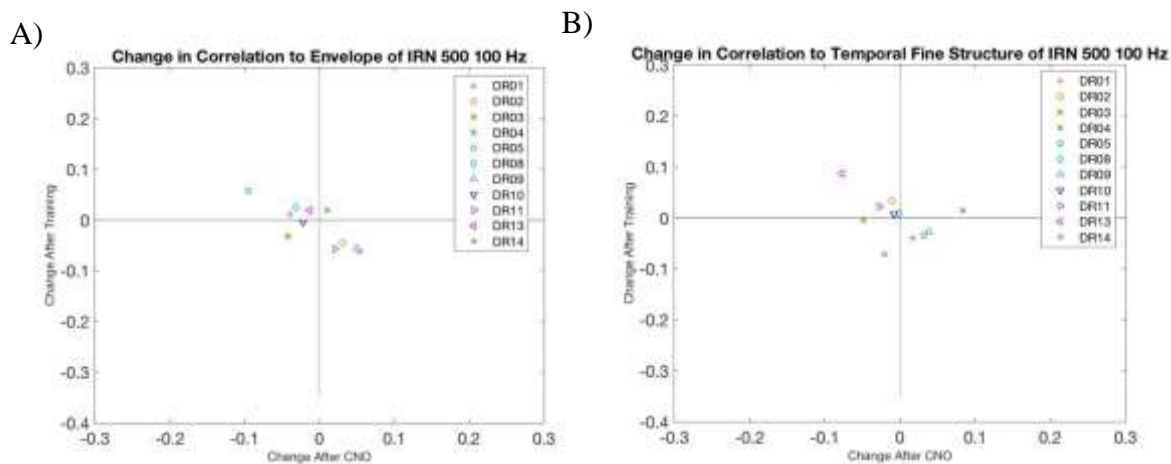


Figure 3.28 Corticofugal Inhibition effects on training-related changes to correlation of response to envelope and temporal fine structure of IRN 500-100 Hz stimulus. A) Shows the envelope emphasized change between pre and post training response correlation and change between pre and post CNO response correlation to IRN 500-100 Hz stimulus for young ($N=11$) animals B) Shows the temporal fine structure emphasized change between pre and post training response correlation and change between pre and post CNO response correlation to IRN 500-100 Hz stimulus tone for young ($N=11$) animals.

The maximum correlation coefficients in response to IRN 500-1000 Hz were all above the average threshold correlation of noise (Table 0.26 **Error! Reference source not found.**). DR04, DR08 and DR09 had an increase in correlation to the envelope of IRN 500-1000 Hz pitch sweep after training (Figure 3.30). DR02, DR04, DR08, DR09, DR11, and DR14 had a decrease in correlation to the envelope of the pitch sweep after CNO injection. DR03, DR04, DR05, DR08, DR09, DR13, and DR14 all had an increase in correlation to the temporal fine structure of the sweep after training. DR03, DR04, DR08, DR09, and DR10 had a decrease in correlation to the temporal fine structure of the sweep after the CNO injection. There was no significant difference between the pre and post training and CNO correlation coefficients.

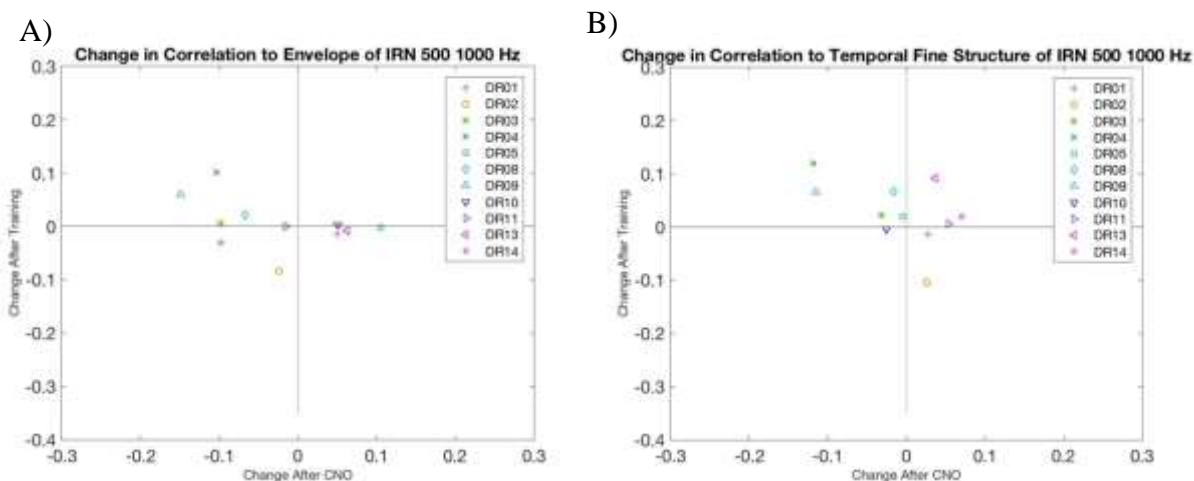


Figure 3.29 Corticofugal Inhibition effects on training-related changes to correlation of response to envelope and temporal fine structure of IRN 500-1000 Hz stimulus. A) Shows the envelope emphasized change between pre and post training response correlation and change between pre and post CNO response correlation to IRN 500-1000 Hz stimulus for young ($N=11$) animals B) Shows the temporal fine structure emphasized change between pre and post training response correlation and change between pre and post CNO response correlation to IRN 500-1000 Hz stimulus tone for young ($N=11$) animals

The maximum correlation coefficients in response to IRN 1000 Hz were all above the average threshold correlation of noise, except the DR03 Post Training Pre CNO response (Table 0.28). DR05, DR08, DR09, DR10 and DR13 had an increase in correlation to the envelope of IRN 1000 Hz flat tone after training and a decrease in the correlation to the envelope of the sweep after the CNO injection (Figure 3.31). DR03 and DR04 also had a decrease in correlation to the envelope of the pitch sweep after CNO injection. DR04, DR09, DR11, DR13, and DR14 all had an increase in correlation to the temporal fine structure of the sweep after training. DR03, DR05, DR09, and DR11 all had a decrease in correlation to the temporal fine structure after CNO injection. There was no significant ($p>0.05$) difference between correlation groups.

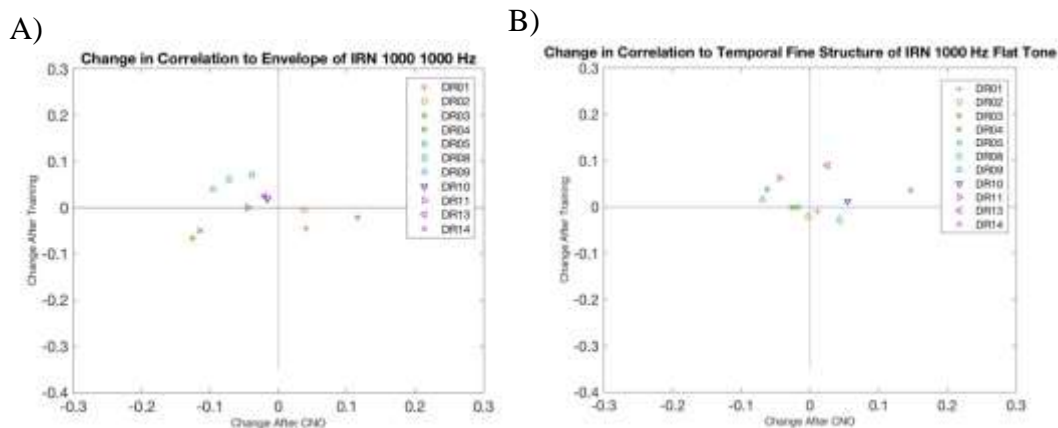


Figure 3.30 Corticofugal Inhibition effects on training-related changes to correlation of response to envelope and temporal fine structure of IRN 1000 Hz flat tone stimulus. A) Shows the envelope emphasized change between pre and post training response correlation and change between pre and post CNO response correlation to IRN 1000 Hz flat tone stimulus for young ($N=11$) animals B) Shows the temporal fine structure emphasized change between pre and post training response correlation and change between pre and post CNO response correlation to IRN 1000 Hz flat tone stimulus for young ($N=11$) animals

The maximum correlation coefficients in response to IRN 125 Hz were all above the average threshold correlation of noise (Table 0.30). DR02, DR08, and DR13 had an increase in correlation to envelope for IRN 125 Hz flat tone after training (Figure 3.31). DR01, DR02, DR03, DR05, DR09, DR10, and DR13 had a decrease in correlation to the envelope of the pitch sweep after CNO injection. DR03, DR08, DR09, and DR11 had an increase in correlation to the temporal fine structure of IRN 125 Hz flat tone after training. DR01, DR03, DR10, and DR11 had a decrease in correlation to the temporal fine structure of the pitch sweep after CNO injection. There was no significant ($p>0.05$) differences between correlation groups.

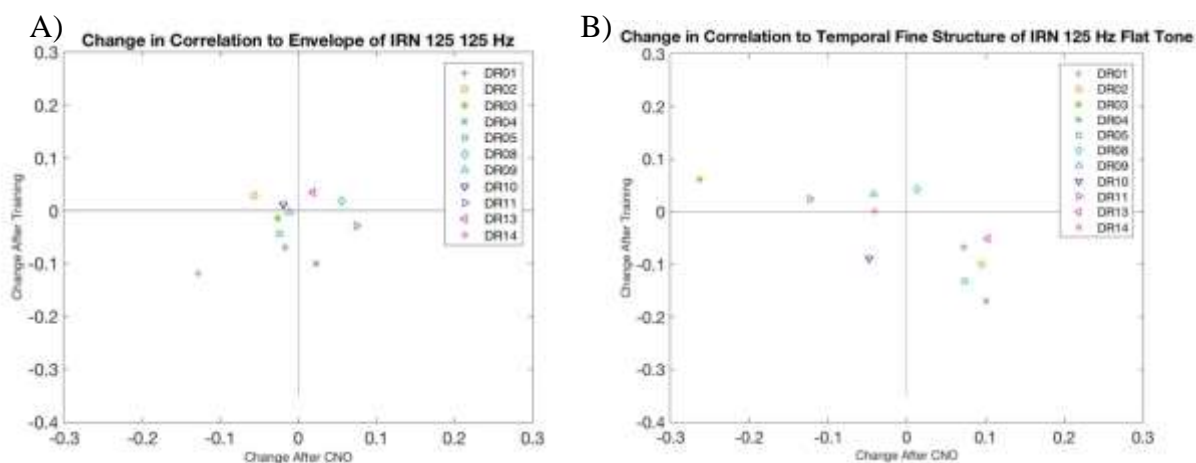


Figure 3.31 Corticofugal Inhibition effects on training-related changes to correlation of response to envelope and temporal fine structure of IRN 125 Hz flat tone stimulus. A) Shows the envelope emphasized change between pre and post training response correlation and change between pre and post CNO response correlation to IRN 125 Hz flat tone stimulus for young ($N=11$) animals B) Shows the temporal fine structure emphasized change between pre and post training response correlation and change between pre and post CNO response correlation to IRN 125 Hz flat tone stimulus tone for young ($N=11$) animals

3.3.3 Acoustic Startle Response

The acoustic startle response was analyzed for all 7 of the prepulse stimuli. The peak variation between day 1 and the other behavioral days for each stimulus was calculated to determine the effectiveness of the animals' discrimination of the stimulus. As well as the ability to compare between the stimuli, the animals' overall ability to learn. The paired t-test and repeated measure ANOVAs were also used to compare between stimuli and show discrimination

For the IRN 100-500 Hz prepulse pitch sweep (Figure 3.32), DR05, DR08, DR11, DR13, and DR14 had either day 2 or day 3 with a smaller median and smaller spread than their day 1 responses. The paired t-test showed that DR05, DR08, DR10, DR11, and DR13 significantly discriminated between the startle with a prepulse and the startle without a prepulse. They were all therefore classified as having learned this stimulus. DR09 responses were significantly ($p < 0.05$) different median and spread from day 1 with a lower median and larger spread. DR01 had a larger median but smaller spread than day 1 and was classified as potential variation learning.

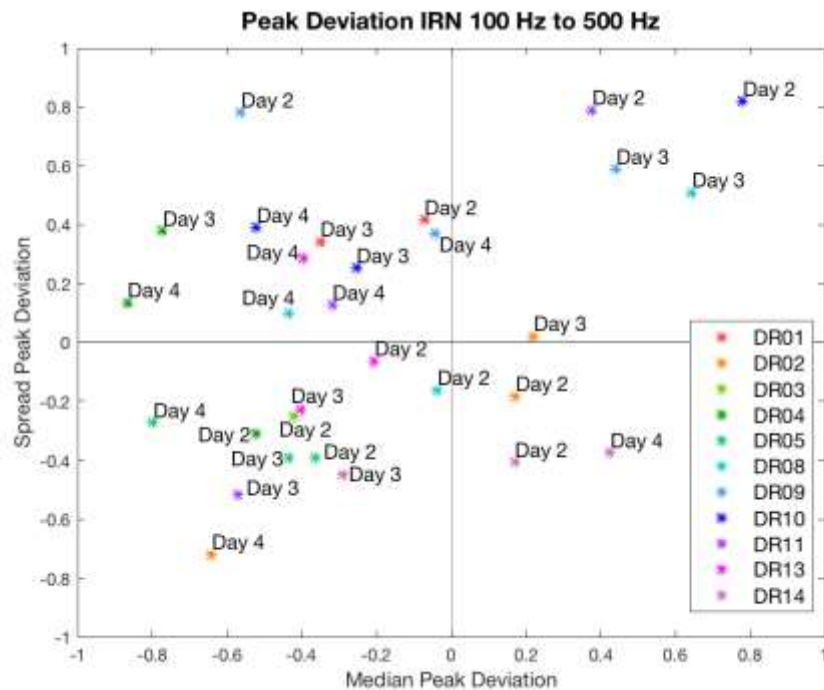


Figure 3.32 Peak Deviation of Startle Response to IRN 100-500 Hz pitch sweep prepulse and IRN 1000-500 Hz pitch sweep background stimulus from the first test day of startle in both the median as well as the spread of the response. The bold and italic labels mean that the results were statistically significantly different from the first day from a one-way ANOVA test ($p < 0.05$)

In Figure 3.33, the FM 8 kHz pitch sweeps showed different trends based on the direction of the sweep. The FM 8 kHz – 100-500 Hz (negative) showed a cluster of animals that had a lower median and spread on day 2 and day 3 than on day 1. DR01, DR02, DR05, DR08, DR10, and DR14 all have at least one day where their median and spread of their startle was less than the first day and therefore were classified as learning the stimulus. DR03, DR09, and DR11 startled less but had a larger spread of startle response. They were classified as potential magnitude learning. DR04, DR08, and DR13 had a larger median but smaller spread than day 1 and therefore were classified as potential variation learning. The FM 8 kHz + 100-500 (positive) seemed to have two polarizing groups: those that learned and those that didn't. DR01, DR02, DR03, DR04, DR05, DR09, DR11, and DR13 all had a smaller median and spread than their first day and therefore were classified as learning the positive stimulus. DR14 had a smaller median but a larger spread than the first day and was classified as potential magnitude learning. DR08 and DR10 had a larger median and spread than the first day and were classified as not learning.

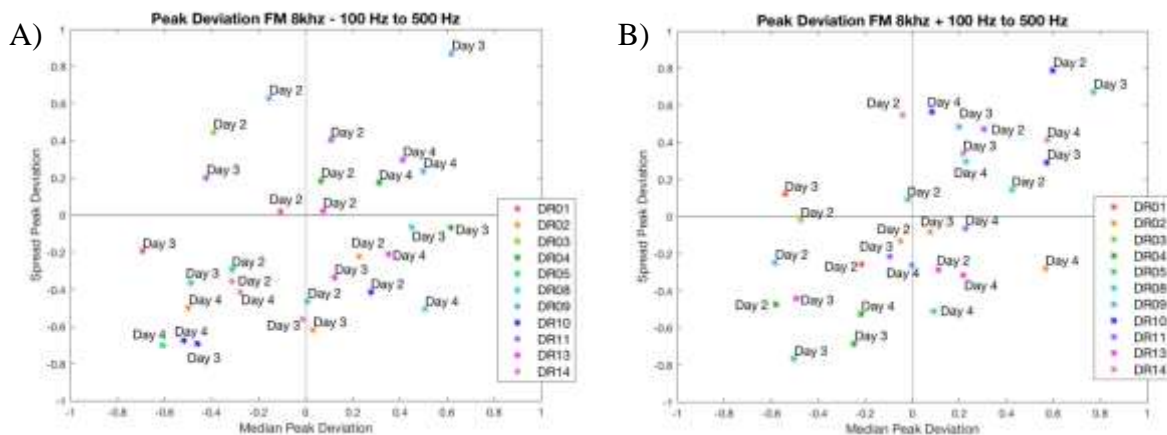


Figure 3.33 Peak Deviation of DREADDs animal Startle Response to FM 8 kHz pitch sweeps prepulses and IRN 1000-500 Hz pitch sweep background stimulus from the first test day of startle in both the median as well as the spread of the response. The bold and italic labels mean that the results were statistically significantly different from the first day from a one-way ANOVA test ($p < 0.05$) A) Peak deviation of startle response from FM 8 kHz – 100-500 Hz prepulse. B) Peak deviation of startle response from FM 8 kHz + 100-500 Hz prepulse.

The 4 white gaussian noise (WGN) prepulses showed some interesting trends at the varying sound levels and with or without background noise (Figure 3.34). For all 4 stimuli, DR03, DR05, DR11, and DR14 showed a smaller median and spread than day 1 and were classified as learning. The other animals were less consistent. DR01 had a smaller median and spread than day 1 for the WGN with background, WGN at 70 dB without background, and WGN at 30 dB without background, but had a smaller median and a larger spread for WGN at 50 dB and was therefore classified as learning 3 stimuli and potential magnitude learning of WGN at 50 dB. DR02 had a smaller median and spread for the WGN with background, a larger median but a smaller spread for WGN at 30 dB, a larger median and spread for WGN at 50 dB, and the same median but larger spread for WGN at 70 dB. DR02 was classified as learning WGN with background, potential variation learning for WGN at 30 dB, no learning for WGN at 50 dB, and potential magnitude learning for WGN at 70 dB. DR04 had a smaller median and spread for WGN with background and at 50 and 70 dB but had a smaller median and larger variation for WGN at 30 dB. DR04 was therefore classified as having learned the 3 stimuli and potential median learning for WGN at 30 dB. DR08 had a smaller median and variation for WGN at 30, 50, and 70 dB, but had a smaller median and larger spread for WGN with background. DR08 was classified as learning WGN without a background at 30, 50, and 70 dB and potential magnitude learning for WGN with a background.

DR09 had a smaller median and spread for WGN at 30 and 50 dB but had a smaller median and larger spread for WGN with background and at 70 dB. DR09 was classified as learning WGN at 30 and 50 dB and potential magnitude learning WGN with background and at 70 dB. DR10 had a smaller median and peak spread for WGN with background and a smaller median and larger spread for WGN at 30, 50, and 70 dB. DR01 was therefore classified as learning WGN with background and potential magnitude learning WGN at 30, 50, and 70 dB. DR13 had a smaller median and spread for WGN at 30 and 50 dB and a smaller median and a larger spread for WGN with background and at 70 dB. Therefore, DR13 was classified as learning WGN at 30 and 50 dB and potential median learning WGN with background and at 70 dB.

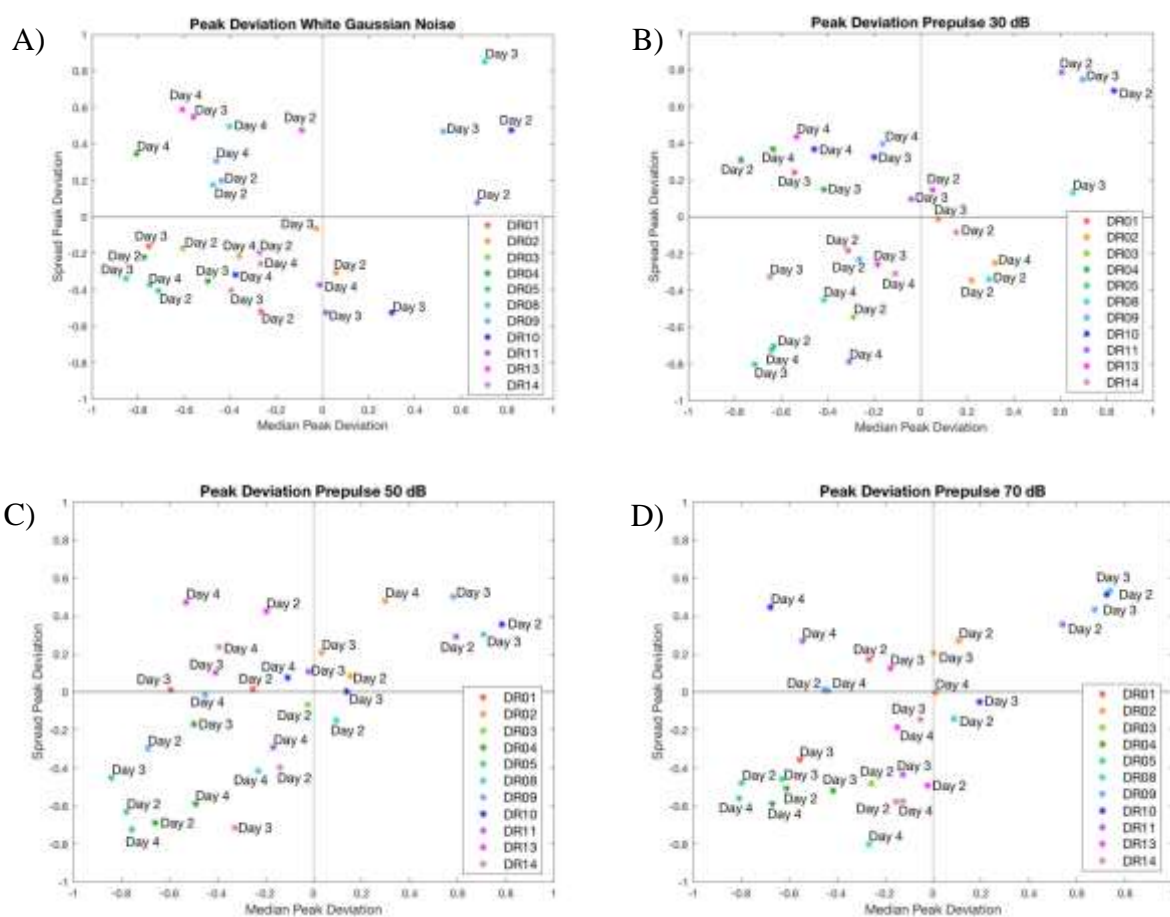


Figure 3.34 Peak deviation of DREADDs animal startle response to white gaussian noise from the first test day of startle in both the median and spread of the response. A) Peak deviation of startle response from white gaussian noise 40 dB above threshold or at 80 dB with a background stimulus of IRN 1000-500 Hz. B) Peak deviation of startle response from white gaussian noise 30 dB prepulse without a background stimulus. C) Peak deviation of startle response from white gaussian noise 50 dB prepulse without a background stimulus. D) Peak deviation of startle response from white gaussian noise 70 dB prepulse without a background stimulus.

3.3.4 Histology

The histology was used after the completion of the behavioral and electrophysiological portions of the study, the animals' brains were imaged to determine whether the DREADDs successfully activated. An example of DREADDs activation is shown below in Figure 3.35 and a stained image of activation is shown in Figure 3.36. The rest of the images of successful DREADDs activation is shown in Appendix C.

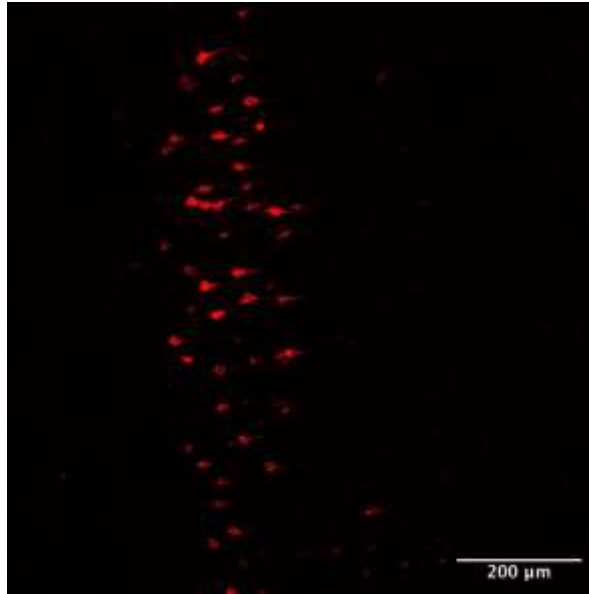


Figure 3.35 Example of DREADDs mCherry fluorescence showing activation in auditory cortex

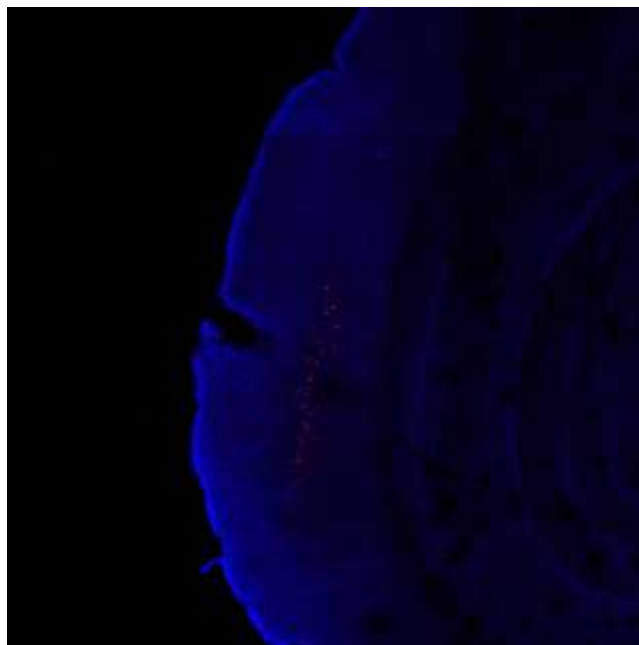


Figure 3.36 Example of DREADDs mCherry fluorescence showing activation in auditory cortex and stained slice with VGlut2 highlighting layers 3 and 6 of auditory cortex.

From these images, the DREADDs animals can be sorted into groups based on the fluorescent activation (Table 3.4). DR01, DR09, and DR13 had no activation and were therefore controls. DR03 and DR08 had bilateral activation. DR02, DR04, DR05, DR10, DR11, and DR14 all had unilateral activation.

Table 3.4 DREADDs Activation Hemisphere

	DR01	DR02	DR03	DR04	DR05	DR08	DR09	DR10	DR11	DR13	DR14
Right	No	Yes	Yes	Yes	Yes	Yes	No	Yes	Yes	No	Yes
Left	No	No	Yes	No	No	Yes	No	No	No	No	No

The fluorescence of the area was also quantified for each of the animals to compare amount of activation between animals (Table 3.5). All of the fluorescence was between 9.3 and 18.9 when normalized to the background fluorescence.

Table 3.5 DREADDs Quantification of Activation by Hemisphere

	DR02	DR03	DR04	DR05	DR08	DR10	DR11	DR14
Right	11	17.4	11.73	18	16.7	11.3	18.9	13.1
Left	N/A	9.3	N/A	N/A	13.7	N/A	N/A	N/A

4. DISCUSSION

4.1 Aging Effects on IRN Pitch Sweep Discrimination

In this study, we investigated the effects of aging on IRN linear pitch sweep learning by evaluating behavioral changes to acoustic startle response as well as neural potential changes in EFR before and after the behavioral testing. As summarized in Table 4.2, behaviorally the young animals mitigated the ASR more than that of their aged counterparts. However, the aged animals had more improved correlation to the EFR. This can be explained by a number of reasons. The pretraining correlation for the aged animals was lower than that of the younger animals and therefore had more potential correlation. There does appear to be a trend of increased correlation in the EFR and animals that were classified as having learned the IRN pitch sweep stimulus. Furthermore, it also appears that the young animals learned the IRN pitch sweep better than the aged animals.

Table 4.1 Learning Results Legend

	= Learning
	= Potential Learning
	= No Learning
	= Recording Issues

Table 4.2 Summary of Aging Effects on Learning Results for IRN Pitch Sweep. Legend: Table 4.1

Group	Young				Aged			
Animal	G8Y1	G8Y2	S1Y1	S1Y2	G8A1	G8A2	S1A1	S1A2
Startle								
EFR								

4.2 Aging and Habituation Prepulse Effects on Pitch Sweep Discrimination and Differentiation

4.2.1 Aging and Habituation Prepulse Effects on Combination of Acoustic Startle Response and Envelope Following Response

In this study, we investigated the effects of aging and habituation prepulse on pitch sweep learning and differentiation by evaluating behavioral changes to acoustic startle response as well as neural potential changes in EFR before and after the behavioral testing. The classification of learning by

the different methods are shown in Table 4.3. The IRN pitch sweep from 100 to 500 Hz was discriminated equally by both young and aged animals as well as by exposure to 1 or 2 habituation prepulses. The FM 8 kHz + 100-500 Hz pitch sweep was better discriminated by both the young and the 2 habituation prepulses groups. The FM 8 kHz –100-500 Hz pitch sweep was discriminated better by both the young and 2 habituation prepulses groups as well.

Table 4.3 Summary of Aging and Habituation Prepulse Effects on Learning and Pitch Sweep Differentiation. Legend: Table 4.1

Stimulus	Group	Aged		Young				
	# Prepulses	1	2	1	2	2	2	1
	Animal	S2A1	S2A2	S2Y1	S2Y2	S3Y1	S3Y2	S3Y3
IRN 100-500 Hz	Startle	Green	Yellow	Grey	Yellow	Green	Green	Yellow
	EFR	Green	Green	Green	Grey	Yellow	Yellow	Green
FM 8 kHz +100-500	Startle	Yellow	Green	Grey	Green	Green	Green	Red
	EFR	Yellow	Green	Green	Grey	Red	Yellow	Red
FM 8 kHz – 100-500	Startle	Red	Red	Grey	Yellow	Yellow	Green	Yellow
	EFR	Green	Yellow	Green	Grey	Red	Yellow	Red

4.2.2 Aging and Habituation Prepulse Effects on Acoustic Startle Response

The behavior model included the above mentioned prepulses (Section 4.2.1) as well as other prepulses to compare the learning and differentiation to the standard startle response (Table 4.4). The young animals had more consistent learning of the standard prepulse (WGN without background) than that of the aged animals. The young 1 habituation prepulse animal did not to discriminate between any of the stimuli other than the standard prepulse at 70 dB. There was a difference in amount of discrimination between WGN with and without background. However, the WGN with background was still discriminated but not as much as those without the background. There is significantly more learning of the standard prepulse than the other stimuli. The 2 habituation prepulse group (both young and aged animals) appears to learn the FM carrier sweeps better than their counter parts. The young within the group discriminate the sweeps better in noise than their aged counterparts.

Table 4.4 Aging and Habituation Prepulse Effects on Acoustic Startle Response. Legend: Table 4.1

# Prepulses	Aged		Young				
	1	2	1	2	2	2	1
Animals	S2A1	S2A2	S2Y1	S2Y2	S3Y1	S3Y2	S3Y3
IRN 100-500	Green	Yellow	Grey	Yellow	Green	Green	Yellow
FM 8 kHz + 100-500	Yellow	Green	Grey	Green	Green	Green	Red
FM 8 kHz - 100-500	Red	Red	Grey	Yellow	Yellow	Green	Yellow
WGN with Background	Yellow	Green	Grey	Yellow	Green	Green	Yellow
WGN at 30 dB	Yellow	Red	Grey	Yellow	Green	Green	Yellow
WGN at 50 dB	Green	Red	Grey	Green	Green	Green	Yellow
WGN at 70 dB	Yellow	Yellow	Grey	Red	Green	Green	Green

4.2.3 Aging and Habituation Prepulse Effects on Envelope Following Response

The electrophysiological model included the above mentioned prepulses (Section 4.2.1) as well as other prepulses to compare the learning and differentiation to the untrained pitch sweep response (Table 4.5). The aged animals have more increase in envelope following responses to the prepulses post training. The 1 habituation prepulse seem to have increase more between the pre and post EFRs. The young animals have more of an increase to the background (IRN 1000-500) pitch sweep post training. The young animals also have an increase associated with time reversed pitch sweeps from the prepulses. Only the young animals have an increase in correlation to the flat IRN 1000 Hz tone.

Table 4.5 Aging and Habituation Prepulse Effects on Envelope Following Response. Legend:
Table 4.1

# Prepulses	Aged		Young				
	1	2	1	2	2	2	1
Animals	S2A1	S2A2	S2Y1	S2Y2	S3Y1	S3Y2	S3Y3
IRN 100-500	Green	Green	Green	Grey	Yellow	Yellow	Green
FM 8 kHz + 100-500	Yellow	Green	Green	Grey	Red	Yellow	Red
FM 8 kHz - 100-500	Green	Yellow	Green	Grey	Red	Yellow	Red
IRN 1000-500	Green	Red	Green	Grey	Yellow	Green	Green
IRN 500-100	Green	Green	Green	Grey	Yellow	Green	Green
IRN 500-1000	Green	Yellow	Red	Grey	Yellow	Green	Green
IRN 125	Green	Red	Red	Grey	Green	Yellow	Red
IRN 1000	Red	Yellow	Red	Grey	Green	Red	Green

4.3 Corticofugal Modulation Effects on Pitch Sweep Discrimination and Differentiation

4.3.1 Corticofugal Modulation Effects on Combination of Acoustic Startle Response and Envelope Following Response

In this study, we investigated the effects of corticofugal modulation on pitch sweep learning and differentiation by evaluating behavioral changes to acoustic startle response as well as neural potential changes in EFR before and after the behavioral testing. The classification of learning by the different methods are shown in Table 4.6. The IRN pitch sweep from 100 to 500 Hz appears to have been learned by a majority of the animals, both behaviorally and electro physiologically. There was also a decrease in the apparent learning with CNO in both the behavior and electrophysiological data. The FM 8 kHz + 100-500 pitch sweep from the both responses appear to have been learned by most of the animals. There was also a decrease in the apparent learning with CNO for the majority of animals. The FM 8 kHz – 100-500 appeared to be learned from the electrophysiological data for most animals, but from the behavioral data did not appear to have been learned. There was a decrease in apparent learning from CNO injection from the EFR response.

Table 4.6 Corticofugal Modulation Effects on Learning and Pitch Sweep Differentiation. Legend: Table 4.1

Stimulus	Type	CNO	Ideal	Bilateral Activation		Unilateral Activation						Controls			
				DR03	DR08	DR05	DR04	DR14	DR11	DR02	DR10	DR09	DR01	DR13	
IRN 100-500	Startle	Pre	Green	Green	Green	Green	Green	Green	Green	Green	Yellow	Yellow	Yellow	Yellow	Green
		Post	Red	Green	Yellow	Green	Yellow	Yellow	Green	Yellow	Yellow	Yellow	Yellow	Yellow	Yellow
	EFR	ΔT	Green	Red	Green	Green	Green	Green	Red	Green	Yellow	Green	Red	Red	Red
		ΔC	Red	Green	Yellow	Red	Red	Red	Green	Yellow	Green	Red	Green	Yellow	Yellow
FM 8 kHz + 100-500	Startle	Pre	Green	Green	Red	Green	Green	Yellow	Green	Green	Red	Green	Green	Green	
		Post	Red	Green	Red	Yellow	Green	Red	Yellow	Yellow	Red	Yellow	Yellow	Yellow	
	EFR	ΔT	Green	Red	Green	Green	Red	Red	Green	Green	Green	Red	Red	Green	
		ΔC	Red	Green	Green	Red	Green	Red	Red	Red	Green	Red	Yellow	Yellow	
FM 8 kHz - 100-500	Startle	Pres	Green	Yellow	Green	Green	Red	Green	Yellow	Yellow	Green	Yellow	Yellow	Yellow	
		Post	Red	Yellow	Yellow	Green	Red	Green	Red	Green	Green	Red	Green	Yellow	
	EFR	ΔT	Green	Red	Red	Green	Red	Green	Green	Green	Green	Yellow	Red	Green	
		ΔC	Red	Green	Green	Red	Yellow	Green	Red	Red	Green	Yellow	Yellow	Red	

4.3.2 Corticofugal Modulation Effects on Acoustic Startle Response

The behavior model included the above mentioned prepulses (Section 4.3.1) as well as other prepulses to compare the learning and differentiation to the standard startle response (**Error! Reference source not found.**). More than half of the animals learned each of the variations of the standard prepulse (WGN without background). The CNO injection didn't decrease the number of animals that learned the variations and in the case of WGN at 50 and 70 dB the number of animals that learned the stimulus increase after the CNO injection. There does not appear to be a difference between the WGN with background and the standard prepulse response learning. The majority of the animals appeared to learn the IRN 100-500 pitch sweep and FM 8kHz + 100-500 pitch sweep, but not the FM 8 kHz – 100-500 pitch sweep.

Table 4.7 Corticofugal Modulation Effects on Acoustic Startle Response. Legend: Table 4.1

Stimulus	CNO Inj.	Ideal	Bilateral Activation		Unilateral Activation						Controls		
			DR03	DR08	DR05	DR04	DR11	DR14	DR02	DR10	DR09	DR01	DR13
IRN 100-500	Pre												
	Post												
FM 8 kHz + 100-500	Pre												
	Post												
FM 8 kHz – 100-500	Pre												
	Post												
WGN with Background	Pre												
	Post												
WGN 30 dB	Pre												
	Post												
WGN 50 dB	Pre												
	Post												
WGN 70 dB	Pre												
	Post												

4.3.3 Corticofugal Modulation Effects on Envelope Following Response

The electrophysiological model included the above mentioned prepulses (Section 4.3.1) as well as other prepulses to compare the learning and differentiation to the untrained pitch sweep response (Table 4.8). The IRN 1000-500 pitch sweep was the background tone and 4 of the 11 animals had an increase in correlation post training. However, there was not a decrease in the number after the CNO injection. The time reversal pitch sweeps (IRN 500-100 and 500-1000) did not have a large increase correlation post training or CNO. The IRN 125 flat tone was similar to the time reversals with minimal changes post training or CNO. The IRN 1000 Hz tone didn't have a lot of increase in correlation post training but a majority of the animals had an increase post CNO injection.

Table 4.8 Corticofugal Modulation Effects on Envelope Following Response. Legend: Table 4.1

Stimulus	Type	Ideal	Bilateral Activation		Unilateral Activation						Controls			
			DR08	DR03	DR05	DR04	DR02	DR14	DR10	DR11	DR09	DR13	DR01	
IRN 100-500	ΔT	Green	Green	Red	Green	Green	Green	Green	Green	Yellow	Red	Green	Red	Red
	ΔC	Red	Yellow	Green	Red	Red	Yellow	Red	Green	Green	Red	Yellow	Red	Red
FM 8 kHz + 100-500	ΔT	Green	Green	Red	Green	Red	Green	Red	Green	Green	Red	Green	Red	Red
	ΔC	Red	Green	Green	Red	Green	Red	Red	Green	Red	Red	Yellow	Yellow	Yellow
FM 8 kHz - 100-500	ΔT	Green	Red	Red	Green	Red	Green	Green	Green	Green	Yellow	Green	Red	Red
	ΔC	Red	Green	Green	Red	Yellow	Red	Green	Green	Red	Yellow	Red	Red	Yellow
IRN 1000-500	ΔT	Green	Green	Red	Green	Green	Red	Red	Red	Red	Red	Green	Red	Red
	ΔX	Red	Green	Green	Yellow	Yellow	Red	Green	Green	Red	Red	Yellow	Yellow	Yellow
IRN 500-100	ΔT	Green	Red	Red	Red	Green	Green	Red	Red	Red	Red	Yellow	Red	Red
	ΔC	Red	Green	Green	Green	Red	Red	Yellow	Red	Green	Yellow	Red	Yellow	Yellow
IRN 500-1000	ΔT	Green	Red	Red	Green	Red	Red	Red	Green	Yellow	Red	Green	Red	Red
	ΔC	Red	Yellow	Green	Green	Green	Red	Yellow	Red	Yellow	Red	Yellow	Yellow	Green
IRN 125	ΔT	Green	Yellow	Red	Yellow	Red	Red	Red	Red	Red	Green	Red	Green	Red
	ΔC	Red	Yellow	Green	Green	Red	Red	Yellow	Green	Yellow	Red	Red	Red	Red
IRN 1000	ΔT	Green	Red	Red	Green	Red	Yellow	Green	Red	Red	Red	Red	Red	Red
	ΔC	Red	Green	Green	Yellow	Green	Green	Red	Green	Yellow	Green	Green	Green	Green

5. CONCLUSION

5.1 Aging Effects on Behavioral and Electrophysiological IRN Pitch Sweep Learning

Based on the overall results of the study, there is IRN pitch sweep learning in rats shown both with behavioral and electrophysiological response to training. Behaviorally the young animals performed better than their aged counterparts. The electrophysiological response supported the behavioral data for learning but didn't clearly distinguish between young and aged learning. Further study is needed to more clearly determine the differences in young and aged rats pitch sweep learning.

5.2 Aging and Habituation Prepulses Effects on Behavioral and Electrophysiological Pitch Sweep Learning and Differentiation

Based on the overall results of this study, there is an age-related impact on pitch sweep learning and differentiation in rats shown both with behavioral and electrophysiological response to training. There also is contradictory behavioral and electrophysiological data on the effect of habituation prepulse in pitch sweep learning and differentiation. When comparing young and aged animals, behaviorally the young animals performed better than their aged counterparts. The electrophysiological response from the aged and young animals generally supported learning trend shown by the behavioral data but didn't clearly distinguish between young and aged learning. The behavior data showed increased learning by the 2 habituation prepulse group. However, the electrophysiological data suggested the opposite was true and that the 1 habituation prepulse group had increased learning. By expanding this study to include more animals and recording and analyzing the habituation period of the behavioral training more differences in young and aged animals pitch sweep discrimination can be more clearly determined.

5.3 Corticofugal Modulation Effects on Behavioral and Electrophysiological Pitch Sweep Learning and Differentiation

Based on the overall results of this study, there is pitch sweep learning and differentiation in rats shown both with behavioral and electrophysiological response to training. There was a decrease in learned behavior and electrophysiological changes after the CNO injection in DREADDs

activated animals. The bilateral activated animals showed a decrease in discrimination for the perceived pitch sweep prepulses and it didn't effect their discrimination of the WGN prepulses. This shows preliminary evidence of the role of A1/IC in maintaining pitch sweep learning. The unilateral activated animals showed similar results to the bilaterally activated animals showing the significance of either A1/IC pathways. The control animals did show some variation in behavior due to the CNO injection. However, the changes were less than those of the bilateral or unilateral DREADDs activation. Further study of the bilateral activation of the pathway is needed to better show the role of it in maintaining pitch sweep learning and discrimination.

APPENDIX A. INCOMPLETE DATA

1. Single-unit Recordings

a. Acute Surgery

The surgical procedure began with an initial 4% isoflurane induction in air in a cylindrical induction chamber until righting reflex was suppressed. The animals were then moved onto a water circulating continuous heating pad at 38 °C to regulate animals body temperature under anesthesia and eye ointment was applied to ensure the eyes didn't dry out. They were given an IM injection of a ketamine (VetaKet, 80 mg/kg) -dexmedetomidine (Dexdormitor, 0.2 mg/kg) mixture, updates of 0.1 mL ketamine as needed, and given oxygen through a nose cone. Heart rate and blood oxygenation were measured with a pulse oximeter, intermittent monitoring of respiration rate, and intermittent toe pinch reflex checks were used to monitor and maintain the anesthetic plane.

After ensuring the animal was properly anesthetized using toe pinch reflex, the animal's head was secured with hollowed ear bars and then shaved. The initial incision was made along midline from around 3 mm anterior to bregma to about 3 mm posterior to lambda. The periosteum was removed and the stereotactic equipment was zeroed at bregma and midline. A craniotomy over IC from A/P -7 to -9 and M/L -1 to -2 was marked in the skull using a ___ mm drill bit (Figure 2.11). Then using a 1 mm drill bit a craniotomy was made and a bone screw was placed about 1 mm into the skull along midline anterior to bregma. The headpost was positioned and a craniotomy was made and a bone screw was placed about 1 mm into the skull on the left side of the skull. The third craniotomy was made on the right side of the skull based on the positioned headpost. Using the smaller drill bit again the craniotomy over IC was drilled. The ground screw was then placed 1.25 mm into the skull to touch the brain. The skull between the screws was scored with the scalpel blade and the headpost was superglued to the skull. Dental cement (Depsly) was used to secure the headpost to the ground screws.

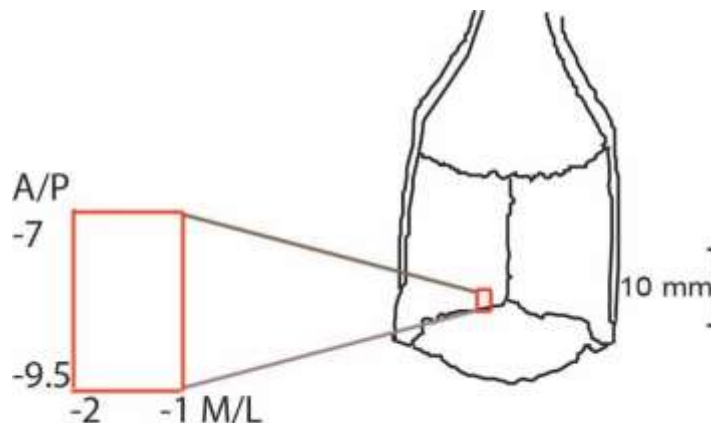


Figure A.1 Acute Recording Craniotomy

b. Electrode Placement and Recording

After the surgery, the animal was moved into the 9' by 9' anechoic chamber (Industrial Acoustic Corporation) used for the EEG recordings and placed on oxygen through a nose cone. Heart rate and blood oxygenation were measured with a pulse oximeter, intermittent monitoring of respiration rate, and intermittent toe pinch reflex checks were used to monitor and maintain the anesthetic plane. The animal's head was secured level using the headpost placed previously described in the surgery. A parylene-C insulated Tungsten electrode (AM Systems, 2 M Ω) encased in a glass capillary tube was secured into an electrode holder on a hydraulic manipulator (Narishige). Prior to insertion into the brain, the electrode was submerged in a DMSO- red fluorescent dye 1,1'-dioctadecyl-3,3,3',3'-tetramethylindocarbocyanine perchlorate (DiI) (Invitrogen) solution for histological localization [82]. The electrode was then lowered into the brain and resubmerged before each subsequent track. The outputs of the electrode was measured by connecting it and the ground screw to a headstage (RA4, TDT) and amplifying the signal using 1 channel of the 4 channel preamplifier (RA4PA preamplifier, TDT) used in EEG recordings. The amplified signal was then recorded with an RZ5 (TDT) at a sampling rate of 24.42 kHz. The signal was then sent to the computer where it was filtered from 500 to 5000 Hz and spike-sorted using OpenEx and RpvdsEx software (TDT). While advancing the track the electrode was on, the bandpass noise (BPN) and noise amplitude modulated (NAM) were played to find auditory responses. Once auditory responses were confirmed .the responses to BPN, NAM, IRN, and tuning stimuli were recorded. Then an IP injection of CNO (3 mg/kg) was given and there was a 10 minute

pause in the recordings. The same 4 stimuli were repeated and the responses recorded for the 145-165 minutes after the injection.

2. Inferior Colliculus and Corticofugal Pathway

a. Mounting

The IC and corticofugal pathway slices were labeled in order of slicing and mounted onto microscope slides in PBS in a dark environment. The slices were treated with 20 μ L of the anti-fading agent, Prolong Glass, to preserve the slices. Then they were sealed using coverslips and clear nail polish.

b. Fluorescence Imaging

The slices were then imaged with the DAPI wavelengths (excitation 350 nm and emission 455 nm) to find the fluorescence of EBFP. The gain was adjusted to image the slice without excessive autofluorescence of the background. The approximate location of the slice was determined from the structure of the slice compared to the Rat Brain Stereotaxic Coordinates of Wistar rats [81].

APPENDIX B. EEG DATA TABLES

1. ABR Peak 1 Amplitude Results

Table B.1 Effects of Aging on Discrimination Model Normalized Channel 2 Peak 1 Amplitude at 75 dB SPL

	Aged				Young		
	G8A1	G8A2	S1A1	S1A2	G8Y1	S1Y1	S1Y2
Pre-Training	1.1232	0.8988	0.8109	1.0763	0.8109	1.442	1.3223
Post-Training	1.0380	0.8863	0.6995	0.9590	0.6995	1.5349	1.2618

2. EFR Correlation Coefficient Results

Table B.2 Effects of Aging on Discrimination Model Maximum Correlation Coefficients of IRN 100 - 500 Hz Normal and Inverted Polarity Pitch Sweeps

Stimulus	Correlation Condition	Animal						
		G8A1	G8A2	G8Y1	S1A1	S1A2	S1Y1	S1Y2
IRN 100-500 Hz	Pre-Training	0.0477	0.1512	0.1921	0.1011	0.0969	0.1760	0.18831
	Post-Training	0.0924	0.1373	0.1215	0.1813	0.1412	0.1663	0.15237
	Post - Pre	0.0447	-0.0139	-0.0706	0.0802	0.0443	-0.0098	-0.03594
IRN 100-500 Hz Inverted	Pre-Training	0.0543	0.1370	0.1582	0.0898	0.0932	0.1476	0.1806
	Post-Training	0.1022	0.1125	0.1099	0.1323	0.1237	0.1669	0.1432
	Change	0.0479	-0.0245	-0.0483	0.0425	0.0307	0.0193	-0.0374

Table B.3 Effects of Aging on Discrimination Model Maximum Correlation Coefficients of IRN 1000 - 500 Hz Normal and Inverted Polarity Pitch Sweeps

Stimulus	Correlation Conditions	Animal						
		G8A1	G8A2	G8Y1	S1A1	S1A2	S1Y1	S1Y2
IRN 1000-500 Hz	Pre-Training	0.0963	0.1952	0.1467	0.1681	0.1655	0.1263	0.1417
	Post-Training	0.0933	0.0788	0.0829	0.1281	0.1806	0.1708	0.0940
	Change	-0.0030	-0.1164	-0.0638	-0.0400	0.0151	0.0445	-0.0477
IRN 1000-500 Hz Inverted	Pre-Training	0.0794	0.1343	0.1742	0.2069	0.1928	0.2142	0.1149
	Post-Training	0.1012	0.1043	0.0789	0.1951	0.2112	0.1683	0.1320
	Change	0.0218	-0.0299	-0.0952	-0.0117	0.0183	-0.0459	0.0171

Table B.4 Effects of Aging on Discrimination Model Maximum Correlation Coefficients of IRN 500 - 1000 Hz Normal and Inverted Polarity Pitch Sweeps

Stimulus	Correlation Condition	Animal						
		G8A1	G8A2	G8Y1	S1A1	S1A2	S1Y1	S1Y2
IRN 500 – 1000 Hz	Pre-Training	0.0416	0.1369	0.1438	0.1482	0.1340	0.1392	0.1383
	Post-Training	0.1059	0.1071	0.1441	0.1620	0.1450	0.1593	0.2381
	Change	0.0643	-0.0298	0.0003	0.0138	0.0110	0.0201	0.0997
IRN 500 – 1000 Hz Inverted	Pre-Training	0.0422	0.1143	0.1326	0.1170	0.1220	0.1321	0.1553
	Post-Training	0.0900	0.1056	0.1232	0.1499	0.1294	0.1585	0.1913
	Change	0.0478	-0.0087	-0.0094	0.0329	0.0075	0.0265	0.0360

Table B.5 Effects of Aging on Discrimination Model Maximum Correlation Coefficients of IRN 500 - 100 Hz normal and inverted polarity Pitch Sweeps

Stimulus	Correlation Condition	Animal						
		G8A1	G8A2	G8Y1	S1A1	S1A2	S1Y1	S1Y2
IRN 500 – 100 Hz	Pre-Training	0.1024	0.1610	0.1733	0.1455	0.1532	0.1190	0.0976
	Post-Training	0.0797	0.0792	0.0929	0.1869	0.1907	0.1298	0.1052
	Change	-0.0227	-0.0817	-0.0805	0.0415	0.0375	0.0108	0.0076
IRN 500 – 100 Hz Inverted	Pre-Training	0.0827	0.2038	0.1534	0.1749	0.1958	0.1591	0.0896
	Post-Training	0.0650	0.0818	0.0965	0.1534	0.1963	0.1066	0.0816
	Change	-0.0177	-0.1220	-0.0570	-0.0215	0.0004	-0.0526	-0.0080

Table B.6 Effects of Aging on Discrimination Model Maximum Correlation Coefficients of IRN 1000 Hz normal and inverted polarity Flat Tone

Stimulus	Correlation Condition	Animal						
		G8A1	G8A2	G8Y1	S1A1	S1A2	S1Y1	S1Y2
IRN 1000 Hz Flat Tone	Pre-Training	0.0385	0.2017	0.1447	0.1805	0.2632	0.1281	0.1084
	Post-Training	0.0597	0.0395	0.0452	0.1023	0.1749	0.1350	0.0856
	Change	0.0212	-0.1622	-0.0996	-0.0782	-0.0883	0.0069	-0.0227
IRN 1000 Hz Flat Tone Inverted	Pre-Training	0.0319	0.1922	0.1608	0.0937	0.1042	0.1326	0.0656
	Post-Training	0.0665	0.0698	0.0415	0.0971	0.1832	0.1142	0.0948
	Change	0.0345	-0.1223	-0.1193	0.0033	0.0789	-0.0184	0.0292

Table B.7 Effects of Aging on Discrimination Model Maximum Correlation Coefficients of IRN 500 Hz Normal and Inverted Polarity Flat Tone

Stimulus	Correlation Condition	Animal						
		G8A1	G8A2	G8Y1	S1A1	S1A2	S1Y1	S1Y2
IRN 500 Hz Flat Tone	Pre-Training	0.0460	0.2352	0.3097	0.1847	0.2427	0.2731	0.1662
	Post-Training	0.0311	0.0450	0.0361	0.2037	0.2186	0.3481	0.2087
	Change	-0.0149	-0.1902	-0.2737	0.0190	-0.0241	0.0750	0.0425
IRN 500 Hz Flat Tone	Pre-Training	0.0512	0.2695	0.2780	0.1383	0.2163	0.2485	0.1336
	Post-Training	0.0520	0.0552	0.0671	0.1704	0.1431	0.3613	0.1847
	Change	0.0008	-0.2143	-0.2109	0.0321	-0.0732	0.1128	0.0511

Table B.8 Effects of Aging and Habituation Prepulse Model Maximum Correlation Coefficients of IRN 100 - 500 Hz Prepulse Normal and Inverted Polarity Pitch Sweeps

Stimulus	Correlation Conditions	Animal					
		S2A1	S2A2	S2Y1	S3Y1	S3Y2	S3Y3
IRN 100-500 Hz	Pre-Training	0.1211	0.1399	0.1624	0.1587	0.1663	0.1492
	Post-Training	0.1427	0.1258	0.1887	0.1381	0.1350	0.2606
	Change	0.0215	-0.0141	0.0263	-0.0205	-0.0313	0.1114
IRN 100-500 Hz Inverted	Pre-Training	0.1089	0.09844	0.1292	0.1916	0.2025	0.1572
	Post-Training	0.1491	0.1297	0.1637	0.1537	0.1447	0.1591
	Change	0.0402	0.03122	0.0345	-0.0379	-0.0578	0.0019

Table B.9 Effects of Aging and Habituation Prepulse Model Maximum Correlation Coefficients of FM 8 kHz + 100-500 Hz Prepulse Normal and Inverted Polarity Pitch Sweeps

Stimulus	Correlation Conditions	Animal					
		S2A1	S2A2	S2Y1	S3Y1	S3Y2	S3Y3
FM 8kHz + 100- 500 Hz	Pre-Training	0.4049	0.3521	0.1251	0.1423	0.1046	0.2881
	Post-Training	0.3834	0.4254	0.2188	0.0990	0.1061	0.0947
	Change	-0.021	0.0733	0.0938	-0.0432	0.0015	-0.1934
FM 8kHz + 100- 500 Hz Inverted	Pre-Training	0.4273	0.3874	0.1564	0.2126	0.1746	0.2952
	Post-Training	0.4343	0.4519	0.2318	0.1009	0.0902	0.1535
	Change	0.007	0.0645	0.0753	-0.1117	-0.0844	-0.1417

Table B.10 Effects of Aging and Habituation Prepulse Model Maximum Correlation Coefficients of FM 8 kHz - 100-500 Hz Prepulse Normal and Inverted Polarity Pitch Sweeps

Stimulus	Correlation Conditions	Animal					
		S2A1	S2A2	S2Y1	S3Y1	S3Y2	S3Y3
FM 8kHz - 100- 500 Hz	Pre-Training	0.4488	0.4234	0.1226	0.1567	0.1306	0.2471
	Post-Training	0.4490	0.4174	0.2055	0.1138	0.1245	0.1197
	Change	0.0002	-0.0059	0.0829	-0.0429	-0.0061	-0.1274
FM 8kHz - 100- 500 Hz Inverted	Pre-Training	0.4170	0.4040	0.1301	0.1259	0.1829	0.2712
	Post-Training	0.4537	0.4629	0.1939	0.0923	0.1436	0.1520
	Change	0.0367	0.0589	0.0639	-0.0336	-0.0394	-0.1191

Table B.11 Effects of Aging and Habituation Prepulse Model Maximum Correlation Coefficients of IRN 1000-500 Hz Background Normal and Inverted Polarity Pitch Sweeps

Stimulus	Correlation Conditions	Animal					
		S2A1	S2A2	S2Y1	S3Y1	S3Y2	S3Y3
IRN 1000- 500 Hz	Pre-Training	0.1285	0.1754	0.1614	0.2477	0.1471	0.1618
	Post-Training	0.1449	0.1734	0.1570	0.2374	0.2418	0.1482
	Change	0.0163	-0.0021	-0.0044	-0.0104	0.0947	-0.0137
IRN 1000- 500 Hz Inverted	Pre-Training	0.1922	0.1989	0.1466	0.1927	0.1355	0.1332
	Post-Training	0.1738	0.1510	0.1719	0.1933	0.1950	0.1740
	Change	-0.0184	-0.0479	0.0253	0.0006	0.0595	0.0408

Table B.12 Effects of Aging and Habituation Prepulse Model Maximum Correlation Coefficients of IRN 500-100 Hz Normal and Inverted Polarity Pitch Sweeps

Stimulus	Correlation Conditions	Animal					
		S2A1	S2A2	S2Y1	S3Y1	S3Y2	S3Y3
IRN 500- 100 Hz	Pre-Training	0.0959	0.1163	0.1632	0.1571	0.2426	0.1886
	Post-Training	0.1134	0.1215	0.1658	0.1492	0.2273	0.1769
	Change	0.0174	0.0052	0.0026	-0.0078	-0.0153	-0.0117
IRN 500- 100 Hz Inverted	Pre-Training	0.1073	0.1233	0.1335	0.1834	0.1692	0.1543
	Post-Training	0.1106	0.1379	0.1328	0.1670	0.2233	0.1841
	Change	0.0033	0.0146	-0.0008	-0.0164	0.0542	0.0298

Table B.13 Effects of Aging and Habituation Prepulse Model Maximum Correlation Coefficients of IRN 500-1000 Hz Normal and Inverted Polarity Pitch Sweeps

Stimulus	Correlation Conditions	Animal					
		S2A1	S2A2	S2Y1	S3Y1	S3Y2	S3Y3
IRN 500-1000 Hz	Pre-Training	0.1625	0.1888	0.2189	0.1608	0.2044	0.1353
	Post-Training	0.1987	0.1951	0.1374	0.1876	0.2267	0.1931
	Change	0.0361	0.0063	-0.0815	0.0268	0.0224	0.0577
IRN 500-1000 Hz Inverted	Pre-Training	0.2071	0.2311	0.1929	0.1898	0.1878	0.1586
	Post-Training	0.1677	0.2010	0.1673	0.1914	0.2299	0.1798
	Change	-0.0394	-0.0301	-0.0256	0.0016	0.0420	0.0212

Table B.14 Effects of Aging and Habituation Prepulse Model Maximum Correlation Coefficients of IRN 1000 Hz Normal and Inverted Polarity Flat Tone

Stimulus	Correlation Conditions	Animal					
		S2A1	S2A2	S2Y1	S3Y1	S3Y2	S3Y3
IRN 1000 Hz Flat Tone	Pre-Training	0.2889	0.1850	0.2197	0.1062	0.0960	0.1215
	Post-Training	0.2635	0.1943	0.1394	0.1182	0.0585	0.1293
	Change	-0.0253	0.0093	-0.0803	0.0120	-0.0375	0.0078
IRN 1000 Hz Flat Tone Inverted	Pre-Training	0.1787	0.1519	0.1988	0.0968	0.1019	0.1034
	Post-Training	0.1167	0.1285	0.0761	0.1242	0.0787	0.1141
	Change	-0.0618	-0.0234	-0.1227	0.0274	-0.0232	0.0107

Table B.15 Effects of Aging and Habituation Prepulse Model Maximum Correlation Coefficients of IRN 125 Hz Normal and Inverted Polarity Flat Tone

Stimulus	Correlation Conditions	Animal					
		S2A1	S2A2	S2Y1	S3Y1	S3Y2	S3Y3
IRN 125 Hz Flat Tone	Pre-Training	0.0557	0.1786	0.1603	0.1877	0.1690	0.1751
	Post-Training	0.0949	0.1271	0.0966	0.2132	0.1481	0.1518
	Change	0.0392	-0.0515	-0.0637	0.0255	-0.0208	-0.0233
IRN 125 Hz Flat Tone Inverted	Pre-Training	0.0438	0.1437	0.1417	0.1378	0.1127	0.1829
	Post-Training	0.0818	0.1271	0.1422	0.1475	0.1292	0.1478
	Change	0.0379	-0.0166	0.0005	0.0098	0.0165	-0.0352

Table B.16 DREADDs Animal Maximum Correlation Coefficients of IRN 100 - 500 Hz Prepulse Normal and Inverted Polarity Pitch Sweeps

Stim	Condition	Animal										
		DR01	DR02	DR03	DR04	DR05	DR08	DR09	DR10	DR11	DR13	DR14
IRN 100 – 500 Hz	Pre Training	0.1846	0.1705	0.2213	0.1734	0.1472	0.1653	0.1773	0.1426	0.2070	0.2580	0.2158
	Post Training Pre CNO	0.1350	0.1964	0.1338	0.2133	0.1403	0.1532	0.1504	0.1773	0.1426	0.1729	0.1947
	Post Training Post CNO	0.1572	0.1822	0.2148	0.1562	0.1527	0.2030	0.1530	0.1805	0.1541	0.1830	0.1686
IRN 100 – 500 Hz Inv.	Pre Training	0.1332	0.1556	0.1974	0.1798	0.1583	0.1331	0.1703	0.1886	0.1811	0.2319	0.1628
	Post Training Pre CNO	0.1525	0.1582	0.1333	0.1899	0.2289	0.1997	0.2215	0.1353	0.1604	0.2212	0.2284
	Post Training Post CNO	0.1592	0.1849	0.1702	0.1709	0.1658	0.1762	0.1638	0.1820	0.1545	0.1991	0.1661

Table B.17 DREADDs Animal Changes from Training and CNO in Correlation Coefficients of IRN 100 - 500 Hz Prepulse Normal and Inverted Polarity Pitch Sweeps

Stim	Co	Animal										
		DR01	DR02	DR03	DR04	DR05	DR08	DR09	DR10	DR11	DR13	DR14
Nor	ΔT	-0.0496	0.0259	-0.0876	0.0399	-0.0069	-0.0121	-0.0269	0.0347	-0.0644	-0.0851	-0.0211
	ΔC	-0.0222	0.0143	-0.0811	0.0571	-0.0124	-0.0499	-0.0026	-0.0033	-0.0115	-0.0097	0.0262
Inv.	ΔT	0.0192	0.0026	-0.0641	0.0101	0.0706	0.0667	0.0512	-0.0533	-0.0207	-0.0107	0.0655
	ΔC	-0.0067	-0.0267	-0.0369	0.0190	0.0631	0.0235	0.0577	-0.0467	0.0060	0.0222	0.0622

Table B.18 DREADDs Animal Maximum Correlation Coefficients of FM 8 kHz + 100 - 500 Hz Prepulse Normal and Inverted Polarity Pitch Sweeps

Stim	Condition	Animal										
		DR01	DR02	DR03	DR04	DR05	DR08	DR09	DR10	DR11	DR13	DR14
FM 8 kHz + 100 - 500 Hz	Pre Training	0.1403	0.0908	0.1688	0.1399	0.0964	0.1125	0.1801	0.1616	0.1614	0.1746	0.1843
	Post Training Pre CNO	0.1249	0.0965	0.1135	0.0902	0.2518	0.1678	0.1214	0.2334	0.3467	0.3239	0.3036
	Post Training Post CNO	0.0902	0.1200	0.1649	0.1633	0.1666	0.3108	0.1061	0.3482	0.2023	0.3349	0.3733
FM 8 kHz + 100 - 500 Hz Inv	Pre Training	0.0942	0.0919	0.1182	0.1237	0.1076	0.1335	0.1852	0.1039	0.0928	0.2012	0.2190
	Post Training Pre CNO	0.0865	0.1761	0.0926	0.1099	0.2296	0.1519	0.1364	0.1914	0.3471	0.3242	0.3031
	Post Training Post CNO	0.1225	0.1090	0.2310	0.1943	0.1712	0.3080	0.1221	0.3366	0.2658	0.3402	0.4166

Table B.19 DREADDs Animal Changes from Training and CNO in Correlation Coefficients of FM 8 kHz + 100 - 500 Hz Prepulse Normal and Inverted Polarity Pitch Sweeps

Stim	Co	Animal										
		DR01	DR02	DR03	DR04	DR05	DR08	DR09	DR10	DR11	DR13	DR14
Nor	ΔT	-0.0154	0.0056	-0.0553	-0.0498	0.1553	0.0553	-0.0587	0.0718	0.1853	0.1494	0.1193
	ΔC	0.0347	-0.0236	-0.0515	-0.0731	0.0852	-0.1430	0.0153	-0.1148	0.1444	-0.0110	-0.0697
Inv.	ΔT	-0.0077	0.0842	-0.0256	-0.0138	0.1220	0.0184	-0.0488	0.0876	0.2543	0.1229	0.0842
	ΔC	-0.0360	0.0671	-0.1384	-0.0843	0.0584	-0.1560	0.0143	-0.1452	0.0814	-0.0161	-0.1135

Table B.20 DREADDs Animal Maximum Correlation Coefficients of FM 8 kHz - 100 - 500 Hz Prepulse Normal and Inverted Polarity Pitch Sweeps

Stim	Condition	Animal										
		DR01	DR02	DR03	DR04	DR05	DR08	DR09	DR10	DR11	DR13	DR14
FM 8 kHz - 100 - 500 Hz	Pre Training	0.1374	0.0935	0.1311	0.1356	0.1306	0.1722	0.1442	0.1350	0.0985	0.2266	0.2220
	Post Training Pre CNO	0.0999	0.1624	0.0872	0.1024	0.2269	0.1431	0.1519	0.2676	0.3368	0.2970	0.2797
	Post Training Post CNO	0.1052	0.1368	0.2062	0.1197	0.2135	0.2766	0.1796	0.3547	0.1922	0.3041	0.4006
FM 8 kHz - 100 - 500 Hz Inv	Pre Training	0.1414	0.1132	0.1644	0.1484	0.1146	0.1284	0.1724	0.1245	0.0939	0.2249	0.2126
	Post Training Pre CNO	0.1143	0.1185	0.0969	0.1096	0.2429	0.1854	0.1209	0.1834	0.3409	0.3178	0.2911
	Post Training Post CNO	0.1352	0.1039	0.2405	0.1151	0.1798	0.3222	0.1053	0.3364	0.2419	0.3181	0.3834

Table B.21 DREADDs Animal Changes from Training and CNO in Correlation Coefficients of FM 8 kHz - 100 - 500 Hz Prepulse Normal and Inverted Polarity Pitch Sweeps

Stim	Co	Animal										
		DR01	DR02	DR03	DR04	DR05	DR08	DR09	DR10	DR11	DR13	DR14
Nor	ΔT	-0.0374	0.0689	-0.0439	-0.0333	0.0963	-0.0291	0.0077	0.1326	0.2383	0.0705	0.0577
	ΔC	-0.0053	0.0256	-0.1190	-0.0173	0.0134	-0.1335	-0.0277	-0.0871	0.1446	-0.0071	-0.1209
Inv.	ΔT	-0.0270	0.0054	-0.0675	-0.0388	0.1283	0.0570	-0.0514	0.0590	0.2471	0.0929	0.0785
	ΔC	-0.0209	0.0146	-0.1436	-0.0055	0.0631	-0.1368	0.0157	-0.1530	0.0990	-0.0003	-0.0922

Table B.22 DREADDs Animal Maximum Correlation Coefficients of IRN 1000 - 500 Hz Background Stimulus Normal and Inverted Polarity Pitch Sweeps

Stim	Condition	Animal										
		DR01	DR02	DR03	DR04	DR05	DR08	DR09	DR10	DR11	DR13	DR14
IRN 1000 - 500 Hz	Pre Training	0.1684	0.1781	0.1781	0.1681	0.1791	0.1386	0.1642	0.2076	0.1991	0.2079	0.2274
	Post Training Pre CNO	0.1525	0.1724	0.1035	0.1424	0.2502	0.2100	0.1461	0.1895	0.2084	0.2944	0.2153
	Post Training Post CNO	0.1701	0.1441	0.2335	0.2749	0.2695	0.2738	0.1331	0.2959	0.1352	0.2122	0.2273
IRN 1000 - 500 Hz Inv.	Pre Training	0.1498	0.1646	0.1716	0.1270	0.1541	0.1243	0.1539	0.1559	0.2015	0.1545	0.2168
	Post Training Pre CNO	0.1445	0.1412	0.1014	0.1735	0.2027	0.1562	0.1523	0.1334	0.1411	0.1753	0.1988
	Post Training Post CNO	0.1985	0.0929	0.1911	0.1628	0.2218	0.1919	0.1369	0.1770	0.1107	0.2151	0.2163

Table B.23 DREADDs Animal Changes from Training and CNO in Correlation Coefficients of IRN 1000-500 Hz Background Stimulus Normal and Inverted Polarity Pitch Sweeps

Stim	Co	Animal										
		DR01	DR02	DR03	DR04	DR05	DR08	DR09	DR10	DR11	DR13	DR14
Nor	ΔT	-0.0159	-0.0058	-0.0746	-0.0257	0.0711	0.0714	-0.0181	-0.0181	0.0093	0.0865	-0.0121
	ΔC	-0.0176	0.0282	-0.1301	-0.1326	-0.0193	-0.0638	0.0130	-0.1064	0.0732	0.0822	-0.0120
Inv.	ΔT	-0.0053	-0.0234	-0.0702	0.0466	0.0486	0.0319	-0.0016	-0.0224	-0.0605	0.0209	-0.0180
	ΔC	-0.0540	0.0483	-0.0897	0.0107	-0.0190	-0.0357	0.0154	-0.0436	0.0303	-0.0398	-0.0175

Table B.24 DREADDs Animal Maximum Correlation Coefficients of IRN 500 – 100 Hz Normal and Inverted Polarity Pitch Sweeps

Stim	Condition	Animal										
		DR01	DR02	DR03	DR04	DR05	DR08	DR09	DR10	DR11	DR13	DR14
IRN 500 – 100 Hz	Pre Training	0.2187	0.1666	0.1507	0.1693	0.2025	0.2021	0.1565	0.1841	0.1546	0.2357	0.2106
	Post Training Pre CNO	0.1694	0.2186	0.1207	0.1523	0.1535	0.1684	0.1632	0.1896	0.1415	0.1600	0.1722
	Post Training Post CNO	0.1611	0.1442	0.1764	0.1423	0.1551	0.2582	0.1428	0.1709	0.1538	0.1377	0.2065
IRN 500 – 100 Hz Inv.	Pre Training	0.2097	0.1810	0.1857	0.1591	0.2364	0.1634	0.1507	0.1897	0.1884	0.1465	0.1962
	Post Training Pre CNO	0.1668	0.1764	0.1279	0.2080	0.1616	0.1766	0.1621	0.1695	0.1519	0.1808	0.1797
	Post Training Post CNO	0.1856	0.1812	0.1707	0.1388	0.2017	0.1688	0.1717	0.1715	0.1881	0.1595	0.1541

Table B.25 DREADDs Animal Changes from Training and CNO in Correlation Coefficients of IRN 500-100 Hz Normal and Inverted Polarity Pitch Sweeps

Stim	Co	Animal										
		DR01	DR02	DR03	DR04	DR05	DR08	DR09	DR10	DR11	DR13	DR14
Nor	ΔT	-0.0493	0.0520	-0.0299	-0.0171	-0.0490	-0.0337	0.0066	0.0054	-0.0131	-0.0757	-0.0384
	ΔC	0.0083	0.0744	-0.0556	0.0100	-0.0016	-0.0898	0.0203	0.0187	-0.0123	0.0223	-0.0343
Inv.	ΔT	-0.0429	-0.0046	-0.0578	0.0488	-0.0748	0.0132	0.0113	-0.0202	-0.0365	0.0343	-0.0165
	ΔC	-0.0188	-0.0049	-0.0428	0.0691	-0.0401	0.0078	-0.0096	-0.0020	-0.0362	0.0213	0.0255

Table B.26 DREADDs Animal Maximum Correlation Coefficients of IRN 500 – 1000 Hz Normal and Inverted Polarity Pitch Sweeps

Stim	Condition	Animal										
		DR01	DR02	DR03	DR04	DR05	DR08	DR09	DR10	DR11	DR13	DR14
IRN 500 – 1000 Hz	Pre Training	0.1699	0.1644	0.1465	0.1836	0.1345	0.1912	0.1642	0.2093	0.1770	0.1720	0.2671
	Post Training Pre CNO	0.1289	0.1210	0.0982	0.1851	0.2037	0.1373	0.1309	0.2062	0.1449	0.1939	0.1885
	Post Training Post CNO	0.1638	0.1208	0.1638	0.1899	0.2091	0.1435	0.1054	0.1950	0.1622	0.2131	0.1908
IRN 500 – 1000 Hz Inv.	Pre Training	0.1807	0.2239	0.1647	0.1924	0.1499	0.1667	0.2030	0.1680	0.1473	0.1886	0.2896
	Post Training Pre CNO	0.1402	0.1349	0.0964	0.1586	0.2093	0.1382	0.1577	0.2025	0.1670	0.2229	0.1908
	Post Training Post CNO	0.1718	0.1069	0.1705	0.2261	0.1756	0.1424	0.1263	0.1930	0.1127	0.1906	0.1971

Table B.27 DREADDs Animal Changes from Training and CNO in Correlation Coefficients of IRN 500-1000 Hz Normal and Inverted Polarity Pitch Sweeps

Stim	Co	Animal										
		DR01	DR02	DR03	DR04	DR05	DR08	DR09	DR10	DR11	DR13	DR14
Nor	ΔT	-0.041	-0.0434	-0.0483	0.0015	0.0691	-0.0539	-0.0333	-0.0032	-0.0321	0.0219	-0.0787
	ΔC	-0.0348	0.0001	-0.0656	-0.0048	-0.0054	-0.0063	0.0255	0.0112	-0.0173	-0.0192	-0.0023
Inv.	ΔT	-0.0404	-0.0890	-0.0684	-0.0338	0.0594	-0.0285	-0.0453	0.0345	0.0198	0.0342	-0.0988
	ΔC	-0.0316	0.0280	-0.0741	-0.0675	0.0337	-0.0042	0.0314	0.0094	0.0544	0.0323	-0.0063

Table B.28 DREADDs Animal Maximum Correlation Coefficients of IRN 1000 Hz Normal and Inverted Polarity Flat Tone

Stim	Condition	Animal										
		DR01	DR02	DR03	DR04	DR05	DR08	DR09	DR10	DR11	DR13	DR14
IRN 1000 Hz Flat	Pre Training	0.1173	0.0819	0.1221	0.2153	0.0954	0.1114	0.0957	0.1133	0.1241	0.1437	0.1430
	Post Training Pre CNO	0.0994	0.0869	0.0312	0.0955	0.1301	0.1043	0.0405	0.0986	0.1239	0.1136	0.1557
	Post Training Post CNO	0.1065	0.1188	0.0930	0.2481	0.1322	0.1393	0.0989	0.1553	0.0979	0.1826	0.1456
IRN 1000 Hz Flat Inv.	Pre Training	0.1312	0.0880	0.1512	0.2317	0.1057	0.1519	0.0976	0.1025	0.1276	0.1484	0.1427
	Post Training Pre CNO	0.0836	0.0841	0.0473	0.0830	0.1249	0.1109	0.0456	0.0886	0.0806	0.1402	0.2385
	Post Training Post CNO	0.1004	0.1146	0.1486	0.2460	0.1160	0.1196	0.0953	0.1888	0.1187	0.1884	0.1805

Table B.29 DREADDs Animal Changes from Training and CNO in Correlation Coefficients of IRN 1000 Hz Normal and Inverted Polarity Flat Tone

Stim	Co	Animal										
		DR01	DR02	DR03	DR04	DR05	DR08	DR09	DR10	DR11	DR13	DR14
Nor	ΔT	-0.0179	0.0049	-0.0909	-0.1198	0.0347	-0.0070	-0.0552	-0.0147	-0.0002	-0.0301	0.0127
	ΔC	-0.0071	-0.0320	-0.0618	-0.1526	-0.0020	-0.0350	-0.0585	-0.0567	0.0260	-0.0690	0.0101
Inv.	ΔT	-0.0476	-0.0039	-0.1039	-0.1487	0.0192	-0.0409	-0.0520	-0.0139	-0.0470	-0.0082	0.0958
	ΔC	-0.0168	-0.0305	-0.1013	-0.1630	0.0089	-0.0087	-0.0497	-0.1002	-0.0381	-0.0482	0.0581

Table B.30 DREADDs Animal Maximum Correlation Coefficients of IRN 125 Hz Normal and Inverted Polarity Flat Tone

Stim	Condition	Animal										
		DR01	DR02	DR03	DR04	DR05	DR08	DR09	DR10	DR11	DR13	DR14
IRN 125 Hz Flat	Pre Training	0.2603	0.1624	0.1625	0.3088	0.2445	0.0918	0.1357	0.1409	0.1104	0.0900	0.2156
	Post Training Pre CNO	0.1687	0.1657	0.0741	0.2849	0.1791	0.1150	0.1643	0.1411	0.1287	0.1857	0.0875
	Post Training Post CNO	0.1700	0.1427	0.1413	0.1031	0.2597	0.1761	0.0680	0.1408	0.1501	0.1179	0.1276
IRN 125 Hz Flat Inv.	Pre Training	0.2913	0.1774	0.1575	0.1735	0.1672	0.1754	0.2153	0.1979	0.137	0.108	0.1738
	Post Training Pre CNO	0.1995	0.1600	0.0728	0.1519	0.2123	0.1633	0.1201	0.0781	0.1648	0.1131	0.1971
	Post Training Post CNO	0.1352	0.0855	0.1362	0.0819	0.2045	0.1344	0.0964	0.1011	0.1122	0.0758	0.1793

Table B.31 DREADDs Animal Changes from Training and CNO in Correlation Coefficients of IRN 125 Hz Normal and Inverted Polarity Flat Tone

Stim	Co	Animal										
		DR01	DR02	DR03	DR04	DR05	DR08	DR09	DR10	DR11	DR13	DR14
Nor	ΔT	-0.0916	0.0033	-0.0884	-0.0239	-0.0654	0.0232	0.0286	0.0002	0.0183	0.0957	-0.1280
	ΔC	-0.0013	0.0230	-0.0671	0.1818	-0.0806	-0.0611	0.0963	0.0003	-0.0215	0.0677	-0.0401
Inv.	ΔT	-0.0918	-0.0174	-0.0847	-0.0215	0.0451	-0.0121	-0.0951	-0.1198	0.0278	0.0051	0.0233
	ΔC	0.0643	0.0745	-0.0634	0.0700	0.0078	0.0289	0.0237	-0.0230	0.0526	0.0373	0.0178

APPENDIX C. HISTOLOGY IMAGES

1. DR02:



Figure C.2 DREADDs mCherry fluorescence showing activation in right auditory cortex of DR02

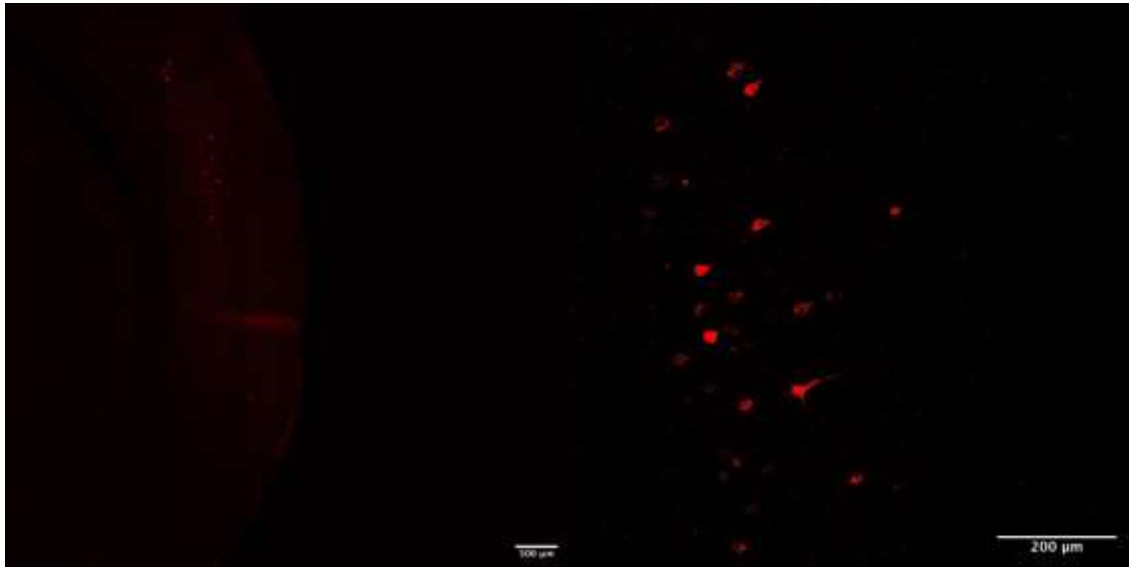
2. DR03**a. Right**

Figure C.3 DREADDs mCherry fluorescence showing activation in right auditory cortex of DR03

b. Left

Figure C.4 DREADDs mCherry fluorescence showing activation in left auditory cortex of DR03

3. DR04

a. Stained

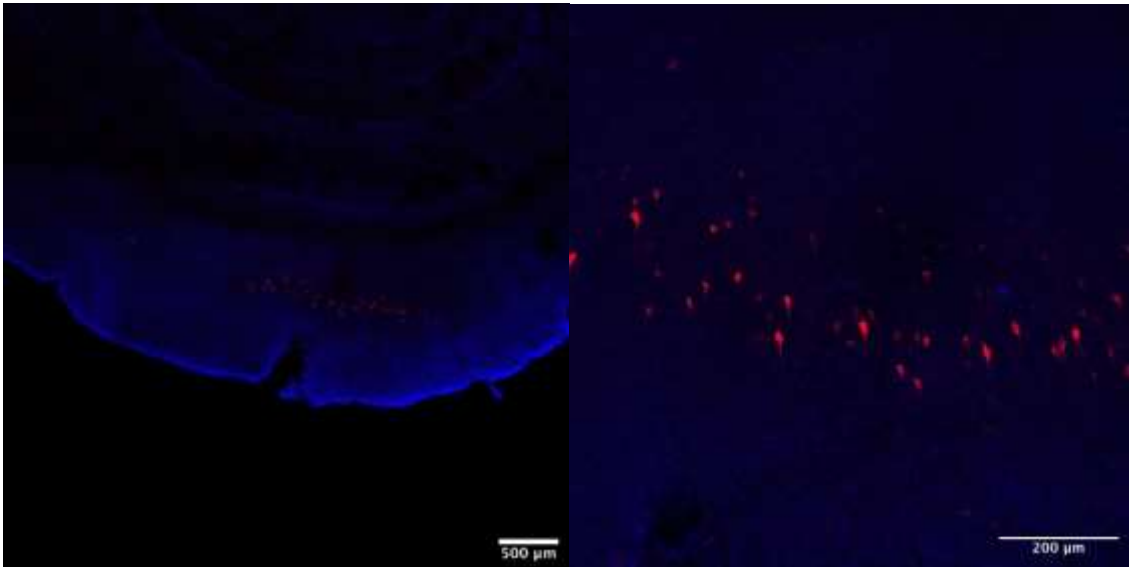


Figure C.5 DREADDs mCherry and VGlut2 Alexa 647 fluorescence showing activation in layer 5 of right auditory cortex of DR04

b. Unstained

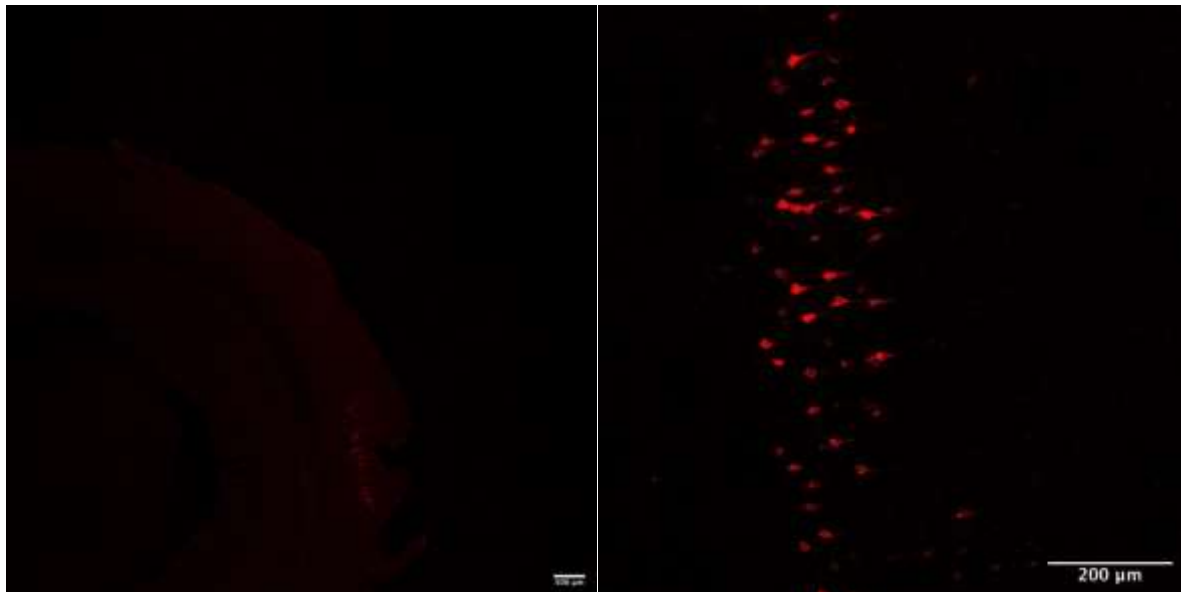


Figure C.6 DREADDs mCherry fluorescence showing activation in right auditory cortex of DR04

4. DR05

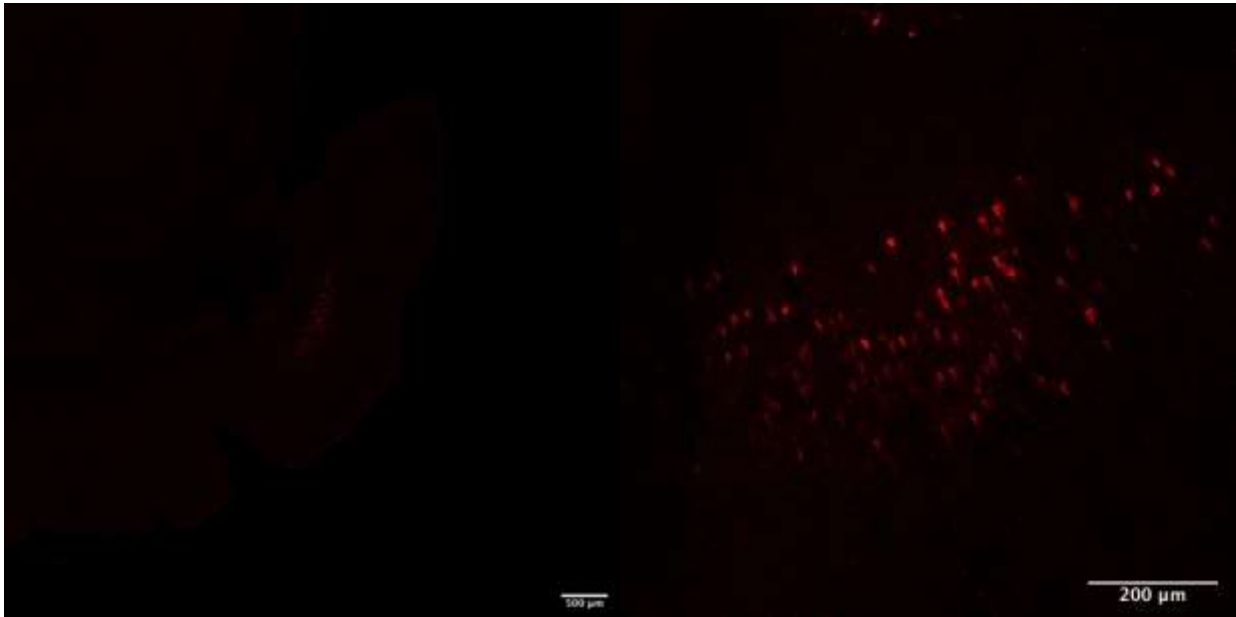


Figure C.7 DREADDs mCherry fluorescence showing activation in right auditory cortex of DR05

5. DR08

a. Right

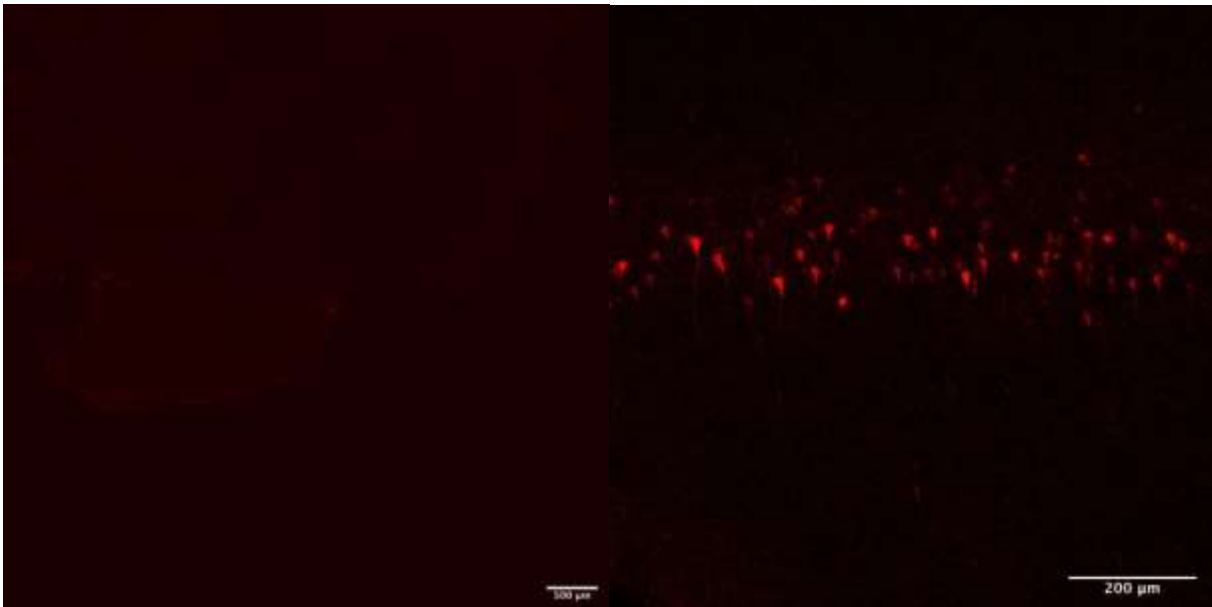


Figure C.8 DREADDs mCherry fluorescence showing activation in right auditory cortex of DR08

b. Left

Figure C.9 DREADDs mCherry fluorescence showing activation in left auditory cortex of DR08

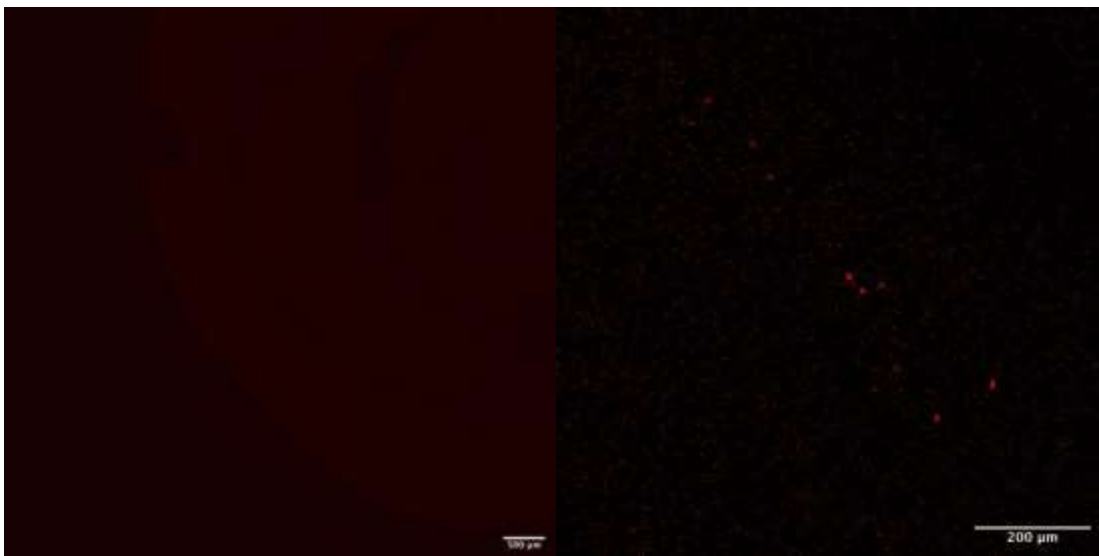
6. DR10

Figure C.10 DREADDs mCherry fluorescence showing activation in right auditory cortex of DR10

7. DR11

Figure C.11 DREADDs mCherry fluorescence showing activation in right auditory cortex of DR11

8. DR14

Figure C.12 DREADDs mCherry fluorescence showing activation in right auditory cortex of DR13

APPENDIX D. DETAILED INSTRUCTIONS

1. Startle Behavior Instructions

Open MATLAB

Open Folder

Open ebartle -> data -> Dowling -> Startle

Acclimation Day 1:

1. Weigh rat
2. Run b0_IRN_acclimation.m -> input animal number -> input 5 minutes -> input threshold -> input 4

Acclimation Day 2:

1. Weigh rat
2. Run b0_IRN_acclimation.m -> input animal number -> input 7 minutes -> input threshold -> input 4

Acclimation Day 3:

1. Weigh rat
2. Run b0_IRN_acclimation.m -> input animal number -> input 10 minutes -> input threshold -> input 4

Startle Test Days 1-3:

1. Weigh rat
2. Run b0_IRN_acclimation.m -> input animal number -> input 5 minutes -> input threshold -> input 4
3. Run b1_IRN_habit.m -> input animal number -> input threshold -> input 4 -> input 2
4. Run b2_IRN.m -> input animal number -> input threshold -> input 4

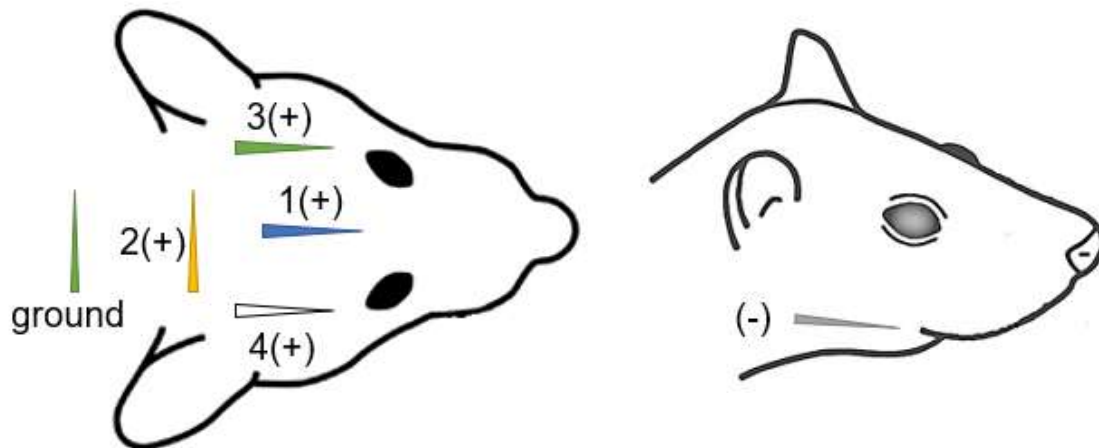
Startle Test Day 4:

1. Weigh rat
2. 1 kg = 1 mL of CNO mixture, concentration = 3 mg/mL, use reconstitution calculator (https://www.tocris.com/products/clozapine-n-oxide_4936) to determine mg of CNO (create 0.1 mL more than needed) (more explanation in the reference sheet)
3. Measure out CNO weight and mix it with (DMSO) and withdraw injection
4. IP injection of CNO mixture in the rat
5. Wait 40 minutes
6. Run b0_IRN_acclimation.m -> input animal number -> input 5 minutes -> input threshold -> input 4

7. Run b1_IRN_habit.m -> input animal number -> input threshold -> input 4 -> input 2
8. Run b2_IRN.m -> input animal number -> input threshold -> input 4

2. PreSurgery EEG Instructions

1. Weigh rat
2. Calculate amount of Dex (0.15 mg/kg) and withdraw amount
3. Calculate amount of Reversal and withdraw amount
4. Ensure heating pad, oxygen, and all TDT equipment are on
5. Get Medusa preamp and connect it to the TDT equipment and the electrode holder
6. Attach electrodes to the electrode holder, clean electrodes with cotton ball and ethanol, and mark a use on the box
7. Check nose cone to ensure it doesn't need to be replaced and place paper towels on heating pad
8. Ensure all oxygen is routed to the iso chamber
9. Put rat in iso chamber with iso set to 4%, remove cage from chamber, and wait about 4 minutes
10. Write on the sheet that the chamber is used for PreSurgery EEG Recordings
11. Decrease iso to anywhere from 2-3% based on animal and route the iso to the nose cone
12. Move rat to the nose cone, check for toe pinch, apply eye ointment, and clean iso chamber
13. Place electrodes as shown in the below figure, use tape to secure them, and press the button for each channel number an electrode is good if only the 1K lights up and lights up clear

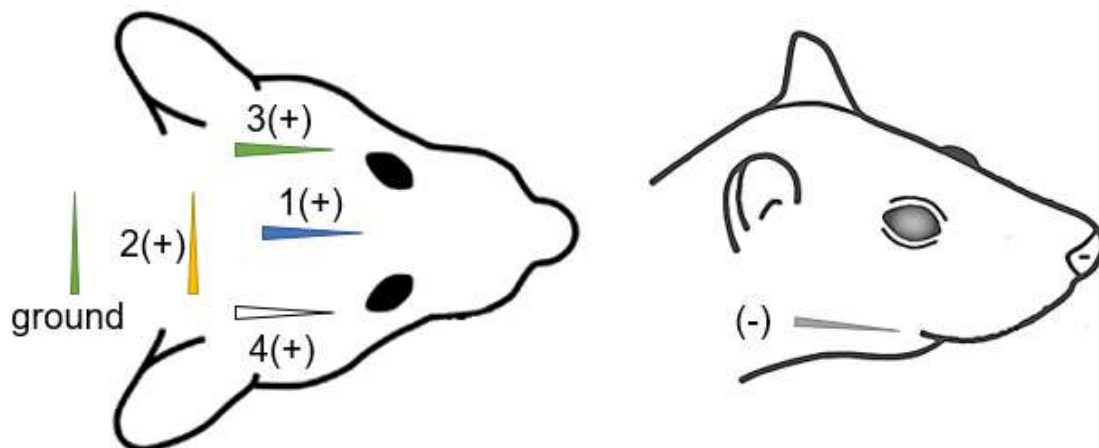


14. Inject Dex using an IM injection
15. Turn off iso, remove nose cone, turn off oxygen, and wait 15 minutes
16. Open BioSig, click open config file-> Windows 7->TDT-> TDT files->ClickABRINS4channelintensity
17. Check stimulis is AgedClickRP_highlo_dense (Same folder as config)
18. Click begin ebartle-> data-> Dowling->folder with animal number->animalNumberPreSurgeryABR and click start and enter animals number and PreSurgery ABR

19. Check that the waveforms look reasonable and select channel 1 trace above threshold and drag it to workspace
20. Filter trace from 80 to 3000 Hz
21. Wait until there appears to be no signal and drag channel 1 from that dB over
22. Filter trace from 80 to 3000 Hz
23. Hold CTRL button to select both waveforms, double click on the above threshold waveform to thicken it then stop pressing control and click above the believed threshold waveform
24. Compare the two waveforms, if there are peaks even delayed peaks above the general noise of the signal then it is not threshold and check on below it.
25. Remove electrodes, clean them with cotton swabs and ethanol, and place them into the box
26. Inject the reversal using an IM injection into the other back leg and move the animal back into the cage
27. Remove paper towels from heating pad and return electrodes to the box
28. Unplug the medusa from inside the chamber and charge it outside of the chamber
29. Turn off the heating pad, turn off the TDT equipment, and log out

3. Pre and Post Training EEG Instructions

1. Weigh rat
2. Calculate amount of Dex (0.25 mg/kg) and withdraw amount
3. Calculate amount of Reversal and withdraw amount
4. Calculate amount of CNO required (weight of the rat in kg + minimum of .1 =mL of CNO, concentration = 3 mg/mL, reconstitution equation to determine mass of CNO:) mix and withdraw CNO
5. Ensure heating pad, oxygen, and all TDT equipment are on
6. Get Medusa preamp and connect it to the TDT equipment and the electrode holder
7. Attach electrodes to the electrode holder, clean electrodes with cotton ball and ethanol, and mark a use on the box
8. Check nose cone to ensure it doesn't need to be replaced and place paper towels on heating pad
9. Ensure all oxygen is routed to the iso chamber
10. Put rat in iso chamber with iso set to 4%, remove cage from chamber, and wait about 4 minutes
11. Write on the sheet that the chamber is used for PreTraining EEG Recordings
12. Decrease iso to anywhere from 2-3% based on animal and route the iso to the nose cone
13. Move rat to the nose cone, check for toe pinch, apply eye ointment, and clean iso chamber
14. Place electrodes as shown in the below figure, use tape to secure them, and press the button for each channel number an electrode is good if only the 1K lights up and lights up clear



15. Inject Dex using an IM injection
16. Turn off iso, remove nose cone, turn off oxygen, and wait 15 minutes
17. Open BioSig, click open config file-> Windows 7->TDT-> TDT files->ClickABRINS4channelintensity
18. Check stimulus is AgedClickRP_highlo_dense (Same folder as config)
19. Click begin ebartle-> data-> Dowling->folder with animal number->animalNumberPreTrainingPreCNOABR and click start and enter animals number and PreTraining PreCNO ABR
20. Check that the waveforms look reasonable and select channel 1 trace above threshold and drag it to workspace
21. Filter trace from 80 to 3000 Hz
22. Wait until there appears to be no signal and drag channel 1 from that dB over
23. Filter trace from 80 to 3000 Hz
24. Hold CTRL button to select both waveforms, double click on the above threshold waveform to thicken it then stop pressing control and click above the believed threshold waveform
25. Compare the two waveforms, if there are peaks even delayed peaks above the general noise of the signal then it is not threshold and check on below it.
26. Click open config file-> Windows 7->TDT-> TDT files->FFR350msINS4channel
27. Click stimulus and in the same folder find IRN_complex_startle_(threshold + 40)
28. Click begin ebartle-> data-> Dowling->folder with animal number->animalNumberPreTrainingPreCNOEFR and click start and enter animals number and PreTraining PreCNO EFR
29. Inject an IP injection of the CNO and wait 40 minutes
30. Repeat steps 17-27 with PostCNO instead of PreCNO naming
31. Remove electrodes, clean them with cotton swabs and ethanol, and place them into the box
32. Inject the reversal using an IM injection into the other back leg and move the animal back into the cage
33. Remove paper towels from heating pad and return electrodes to the box
34. Unplug the medusa from inside the chamber and charge it outside of the chamber
35. Turn off the heating pad, turn off the TDT equipment, and log out

4. Chronic Surgery Surgeon Instructions

PRIOR TO SURGERY DAY

1. Ensure that a PreSurgery EEG has been run
2. Day before surgery pack autoclaved surgical supplies and autoclave them
 - a. Large scissors
 - b. 4 towel clamps
 - c. 4 hemostats or a skin spreader
 - d. Glass plate
 - e. Metal utensil holder
 - f. Mountain of gauges
 - g. Straight scissors
 - h. Curved scissors
 - i. Periosteum remover
 - j. Different size tweezers
 - k. Scalpel holder
 - l. Needle drivers
 - m. 2 or 3 drapes inside kit
 - n. Wrap with 2 drapes
 - o. Connectors to stereotactic setup
3. Day before set aside nonsterile equipment
 - a. Scalpel blade
 - b. Large syringe and needle
 - c. Dental Spears
 - d. Sutures
 - e. Small needle
 - f. Drill holder
 - g. Drill
 - h. Drill bits
 - i. 2 Hamilton syringes (ensuring needles are straight)
 - j. Hamilton syringe pump
 - k. Ear bars
 - l. 3 cotton balls
 - m. Bowl for iodine
 - n. 70% ethanol
 - o. Saline
 - p. Eye ointment
 - q. Antibiotic ointment
 - r. Loupes
 - s. Electric razor
 - t. Tape
4. Day before check equipment
 - a. Amount of oxygen (>500)
 - b. Amount of iso (>1/2)
 - c. Pulse oximeter
 - d. Microscope light

- e. Heating pad
- f. Stereotatic control
- g. Syringe pump controller
- 5. Day before check sterile equipment
 - a. Sterile soap
 - b. Sterile gloves
 - c. Sterile gown
 - d. Hair net
 - e. Face mask

DAY OF SURGERY

1. Weigh rat and calculate amount of metacam needed
2. Pull Metacam in 1 mL syringe and fill the rest with saline
3. Ensure autoclaved and nonsterile supplies are at the surgical station
4. Use iso chamber in acute chamber to knock rat out with 4% iso for about 4 minutes
5. Place towel mat on heating pad and turn on oxygen, heating pad, pulse oximeter, and iso to 2-3% immediately before moving rat over
6. Move rat to surgical station, clean the iso chamber, and turn off oxygen in acute chamber
7. Place ear bars on rat
8. Set up pulse oximeter
9. Apply eye ointment
10. Shave rat using electric razor and tape to remove shaved fur on top of head where surgical field will be
11. Use bowl of iodine and rip the cotton balls in half
12. Dip one half in iodine and apply to shaved region
13. Dip other half in ethanol and apply to shaved region
14. Repeat 2 more times
15. Check toe pinch and drop iso to 2% and drop again soon after to 1.8%
16. Use sub-Q injection of metacam
17. Go to the bathroom/drink/eat
18. Place hair in hairnet and face mask on as well as loupes
19. Wash hands thoroughly with sterile soap
20. Have assistant turn off water and carefully open sterile surgical gown
21. Dry hands and put on surgical gown
22. Have assistant Velcro back and hold tag
23. Pull on string to release one side of the tag and rotate around and pull other string
24. Tie strings together
25. Assistant opens sterile gloves and dumps them into sterile gown field
26. Put on gloves and have the assistant throw the remains away.
27. Have assistant open outer drape of the autoclaved drapes
28. Place packed drape over animal and attach towel clamps
29. Place other packed drape to the right of the stereotaxic control
30. Cut hole in drape for surgical field
31. Get scalpel blade from assistant
32. Make initial incision using scalpel

33. Get large syringe and needle from assistant
34. Fill with Saline with assistant help
35. Use gauges to minimize bleeding
36. Raise skin with tweezers and use curved scissors to separate the skin from connective tissue
37. Use skin spreader/hemostats to pull skin apart
38. Use periosteum remover to clear skull along with saline and gauges
39. Continue until periosteum is removed and lambda, bregma, and midline are clear
40. Use scalpel and periosteum remover to reflect contralateral and ipsilateral muscle just past skull ridges
41. Have drill bit placed in the bead sterilizer and drill and drill holder ethanoled and handed over
42. Plug in drill in drill holder with smaller drill bit
43. Turn on drill controller and attach drill to stereotactic control with attachment
44. Move drill to intersection of bregma and midline and zero stereotax
45. Get smaller needle and use glass plate to ensure needle is blunt
46. Move to contralateral and ipsilateral IC drill locations and drill injection sites and check sites
47. Rezero stereotax and mark locations for auditory cortex injections sites
48. Remove drill from stereotax and switch to larger drill bit
49. Drill into the marked locations on the contralateral and ipsilateral injection sites and check sites
50. Get one Hamilton syringe and syringe pump
51. Rinse with saline while assistant gets DREADDs
52. Place syringe in pump and attach it to stereotax
53. Have assistant set control to MDN and withdraw 2000 nL of DREADDs into syringe
54. Have assistant return DREADDs to freezer
55. Zero stereotax and move to contralateral injection site
56. Use location in calculations to determine injection angle and depth
57. Move to injection angle and burst dura where the needle will go through
58. Insert needle to required depth and inject 1000 nL of DREADDs into brain at rate of 100 nL a minute
59. After injection is complete wait 5 minutes and pull syringe from brain
60. Repeat steps 53 through 58 for the ipsilateral injection site
61. Get second Hamilton syringe and pass first one to assistant to clean
62. Rinse second syringe with saline while assistant gets CRE
63. Rotate stereotax around to get desired rotation axis
64. Place syringe in pump and attach to stereotax
65. Withdraw 2000 nL of CRE into syringe
66. Have assistant return CRE to freezer
67. Repeat steps 53 through 58 for the contralateral IC CRE injection
68. Repeat steps 53 through 58 for the ipsilateral IC CRE injection
69. Remove skin spreader
70. Get sutures from assistant and perform individual sutures using needle drivers, tweezers, and scissors while assistant cleans Hamilton syringes, and other surgical supplies
71. Upon completion of sutures, apply antibiotic ointment to surgical area

72. Remove animal from iso and upon initial recovery from iso move to cage
73. Turn off oxygen and heating pad
74. Clean all remaining equipment
75. Give animal gel diet and rat treats
76. Bring animal downstairs with the biohazard tag
77. Ensure surgical log is saved and log out of the computer

5. Chronic Surgery Assistant Instructions

1. Weigh rat and calculate amount of metacam needed
2. Pull Metacam in 1 mL syringe and fill the rest with saline
3. Ensure autoclaved and nonsterile supplies are at the surgical station
4. Use iso chamber in acute chamber to knock rat out with 4% iso for about 4 minutes
5. Place towel mat on heating pad and turn on oxygen, heating pad, pulse oximeter, and iso to 2-3% immediately before moving rat over
6. Move rat to surgical station, clean the iso chamber, and turn off oxygen in acute chamber
7. Monitor rat and work with pulse oximeter
8. Turn off water after surgeon washes
9. Carefully open surgical gown
10. Velcro back of surgical gown and hold surgical gown tag for surgeon
11. Open gloves
12. Open autoclave supplies
13. Banana peel the scalpel when asked
14. Mark on surgical log when different times and stats occur
15. Banana peel the large syringe and needle when asked
16. Use ethanol and kim wipe to clean saline and hold bottle upside down for surgeon
17. Turn on stereotactic measurement
18. Stick tips of the drill bits into bead sterilizer
19. Ethanol the drill and drill holder and hand them to surgeon when asked
20. Zero stereotactic measurements when told to
21. Banana peel the small needle when asked
22. Banana peel the dental spears when asked
23. Ethanol Hamilton syringe and syringe pump
24. Get DREADDs (no coloring on lid) from -80 freezer on 3rd floor in red thor labs box
25. Pass to surgeon
26. Turn on syringe pump controller and plug syringe pump in
27. Ensure controller is set to MDN
28. Set it to withdraw 2000 nL at a rate of 2000 nL/min and click run when told and tell surgeon when at 500, 1000, 1500, and complete
29. Zero stereotax
30. Return DREADDs upstairs with tape on it
31. Enter M/L location into contralateral auditory injection site and tell surgeon the angle
32. Check the angle the stereotax is set to
33. DO NOT TOUCH THE TABLE ONCE THE SYRINGE IS IN THE BRAIN
34. Tell surgeon the depth and ensure they go to the right depth

35. Set timer for 15 minutes
36. Set syringe pump controller to infuse 1000 nL at a rate of 100 nL/min and click run and press go on the timer
37. Repeat steps 29 and 31 through 36 for other DREADDs injection into ipsilateral auditory cortex
38. Take Hamilton syringe and hand the other one that is ethanoled
39. Get CRE (black colored lid) from -80 freezer on the 3rd floor in red thor labs box
40. Pass to surgeon
41. Repeat steps 28 through 36 for contralateral IC injection site
42. Repeat steps 29 and 31 through 36 for ipsilateral IC injection site
43. Banana peel suture for surgeon
44. Take other Hamilton syringe
45. Rinse syringes with microside, pbs, water, and acetone
46. Clean all surgical supplies that the surgeon isn't using with alconox detergent.
47. Watch rat once removed from iso to monitor and move back into cage
48. Turn off oxygen and heating pad and ensure rat gets gel diet and rat treats
49. Bring rat downstairs with new tags
50. Ensure surgical log is saved and log out of the computer

REFERENCES

- [1] H. Okamoto and R. Kakigi, "Encoding of frequency-modulation (FM) rates in human auditory cortex," *Sci. Rep.*, vol. 5, no. 1, p. 18143, Nov. 2016.
- [2] B. H. Gaese, I. King, C. Felsheim, J. Ostwald, and W. von der Behrens, "Discrimination of Direction in Fast Frequency-Modulated Tones by Rats," *JARO J. Assoc. Res. Otolaryngol.*, vol. 7, no. 1, p. 48, Mar. 2006.
- [3] M. F. Joannis and D. D. DeSouza, "Sensitivity of human auditory cortex to rapid frequency modulation revealed by multivariate representational similarity analysis.," *Front. Neurosci.*, vol. 8, p. 306, 2014.
- [4] J. Mendelson, C. Schreiner, M. Sutter, and K. Grasse, "Functional topography of cat primary auditory cortex: responses to frequency-modulated sweeps," *Exp. Brain Res.*, vol. 94, no. 1, pp. 65–87, May 1993.
- [5] L. A. Screven and M. L. Dent, "Discrimination of frequency modulated sweeps by mice," *J. Acoust. Soc. Am.*, vol. 140, no. 3, pp. 1481–1487, Sep. 2016.
- [6] M. Trujillo, K. Measor, M. M. Carrasco, and K. A. Razak, "Selectivity for the rate of frequency-modulated sweeps in the mouse auditory cortex," *J. Neurophysiol.*, vol. 106, no. 6, pp. 2825–2837, Dec. 2011.
- [7] J. Ma, R. T. Naumann, and J. S. Kanwal, "Fear Conditioned Discrimination of Frequency Modulated Sweeps within Species-Specific Calls of Mustached Bats," *PLoS One*, vol. 5, no. 5, p. e10579, May 2010.
- [8] A. Krishnan and J. T. Gandour, "The role of the auditory brainstem in processing linguistically-relevant pitch patterns," *Brain Lang.*, vol. 110, pp. 135–148, 2009.
- [9] H. Luo, A. Boemio, M. Gordon, and D. Poeppel, "The perception of FM sweeps by Chinese and English listeners."
- [10] L. V. Heinemann, B. Rahm, J. Kaiser, B. H. Gaese, and C. F. Altmann, "Repetition Enhancement for Frequency-Modulated but Not Unmodulated Sounds: A Human MEG Study," *PLoS One*, vol. 5, no. 12, p. e15548, Dec. 2010.
- [11] A. Parthasarathy, J. Datta, J. A. L. Torres, C. Hopkins, and E. L. Bartlett, "Age-Related Changes in the Relationship Between Auditory Brainstem Responses and Envelope-Following Responses," *J. Assoc. Res. Otolaryngol.*, vol. 15, no. 4, pp. 649–661, Aug. 2014.

- [12] T. Schoof and S. Rosen, "The Role of Age-Related Declines in Subcortical Auditory Processing in Speech Perception in Noise.," *J. Assoc. Res. Otolaryngol.*, vol. 17, no. 5, pp. 441–60, Oct. 2016.
- [13] J. R. Mendelson and C. Ricketts, "Age-related temporal processing speed deterioration in auditory cortex," *Hear. Res.*, vol. 158, no. 1–2, pp. 84–94, Aug. 2001.
- [14] J. P. Walton, "Timing is everything: Temporal processing deficits in the aged auditory brainstem," *Hear. Res.*, vol. 264, no. 1–2, pp. 63–69, Jun. 2010.
- [15] Q. Huang and J. Tang, "Age-related hearing loss or presbycusis," *Eur. Arch. Oto-Rhino-Laryngology*, vol. 267, no. 8, pp. 1179–1191, Aug. 2010.
- [16] C. G. Clinard, K. L. Tremblay, and A. R. Krishnan, "Aging alters the perception and physiological representation of frequency: Evidence from human frequency-following response recordings," *Hear. Res.*, vol. 264, no. 1–2, pp. 48–55, Jun. 2010.
- [17] D. C. Peterson and R. N. Hamel, *Neuroanatomy, Auditory Pathway*. StatPearls Publishing, 2019.
- [18] J. O. Pickles, "Auditory pathways: anatomy and physiology," *Handb. Clin. Neurol.*, vol. 129, pp. 3–25, Jan. 2015.
- [19] J. P. Walton and R. Burkard, "Neurophysiological Manifestations of Aging in the Peripheral and Central Auditory Nervous System," *Funct. Neurobiol. Aging*, pp. 581–595, Jan. 2001.
- [20] R. J. Kulesza and B. Grothe, "Yes, there is a medial nucleus of the trapezoid body in humans," *Front. Neuroanat.*, vol. 9, p. 35, Mar. 2015.
- [21] B. Hu, V. Senatorov, and D. Mooney, "Lemniscal and non-lemniscal synaptic transmission in rat auditory thalamus.," *J. Physiol.*, vol. 479, no. 2, pp. 217–231, Sep. 1994.
- [22] A. Lumani and H. Zhang, "Responses of neurons in the rat's dorsal cortex of the inferior colliculus to monaural tone bursts," *Brain Res.*, vol. 1351, pp. 115–129, Sep. 2010.
- [23] R. F. Huffman and O. W. Henson, "The descending auditory pathway and acousticomotor systems: connections with the inferior colliculus.," *Brain Res. Brain Res. Rev.*, vol. 15, no. 3, pp. 295–323.
- [24] M. J. Tramo, G. D. Shah, and L. D. Braidă, "Functional Role of Auditory Cortex in Frequency Processing and Pitch Perception," *J. Neurophysiol.*, vol. 87, no. 1, pp. 122–139, Jan. 2002.

- [25] M. S. Malmierca, L. A. Anderson, and F. M. Antunes, “The cortical modulation of stimulus-specific adaptation in the auditory midbrain and thalamus: a potential neuronal correlate for predictive coding,” *Front. Syst. Neurosci.*, vol. 9, Mar. 2015.
- [26] M. S. Malmierca, L. A. Anderson, and F. M. Antunes, “The cortical modulation of stimulus-specific adaptation in the auditory midbrain and thalamus: a potential neuronal correlate for predictive coding,” *Front. Syst. Neurosci.*, vol. 9, p. 19, 2015.
- [27] N. Suga, “Processing of auditory information carried by species-specific complex sounds.” 1995.
- [28] J. I. Gold and E. I. Knudsen, “A site of auditory experience-dependent plasticity in the neural representation of auditory space in the barn owl’s inferior colliculus.,” *J. Neurosci.*, vol. 20, no. 9, pp. 3469–86, May 2000.
- [29] N. Suga, “Biosonar and Neural Computation in Bats,” *Scientific American*, vol. 262. Scientific American, a division of Nature America, Inc., pp. 60–71, 1990.
- [30] C. Ricketts, J. . Mendelson, B. Anand, and R. English, “Responses to time-varying stimuli in rat auditory cortex,” *Hear. Res.*, vol. 123, no. 1–2, pp. 27–30, Sep. 1998.
- [31] P. K. Pandya, D. L. Rathbun, R. Moucha, N. D. Engineer, and M. P. Kilgard, “Spectral and Temporal Processing in Rat Posterior Auditory Cortex,” *Cereb. Cortex*, vol. 18, no. 2, pp. 301–314, Feb. 2008.
- [32] J. Lai and E. L. Bartlett, “Age-related shifts in distortion product otoacoustic emissions peak-ratios and amplitude modulation spectra,” *Hear. Res.*, vol. 327, pp. 186–198, Sep. 2015.
- [33] I. Nelken, J. K. Bizley, F. R. Nodal, B. Ahmed, A. J. King, and J. W. H. Schnupp, “Responses of Auditory Cortex to Complex Stimuli: Functional Organization Revealed Using Intrinsic Optical Signals,” *J. Neurophysiol.*, vol. 99, no. 4, pp. 1928–1941, Apr. 2008.
- [34] I. J. Moon and S. H. Hong, “What is temporal fine structure and why is it important?,” *Korean J. Audiol.*, vol. 18, no. 1, pp. 1–7, Apr. 2014.
- [35] R. V Shannon, “Is Birdsong More Like Speech or Music?,” *Trends Cogn. Sci.*, vol. 20, no. 4, pp. 245–247, Apr. 2016.
- [36] W. P. Shofner, W. A. Yost, and W. M. Whitmer, “Pitch perception in chinchillas (*Chinchilla laniger*): Stimulus generalization using rippled noise.,” *J. Comp. Psychol.*, vol. 121, no. 4, pp. 428–439, Nov. 2007.

- [37] J. Swaminathan, A. Krishnan, J. T. Gandour, and Yisheng Xu, “Applications of Static and Dynamic Iterated Rippled Noise to Evaluate Pitch Encoding in the Human Auditory Brainstem,” *IEEE Trans. Biomed. Eng.*, vol. 55, no. 1, pp. 281–287, Jan. 2008.
- [38] B. Chandrasekaran, A. Krishnan, and J. T. Gandour, “Experience-dependent neural plasticity is sensitive to shape of pitch contours,” *Neuroreport*, vol. 18, no. 18, pp. 1963–1967, Dec. 2007.
- [39] J. B. Kelly and B. Masterton, “Auditory sensitivity of the albino rat.,” *J. Comp. Physiol. Psychol.*, vol. 91, no. 4, pp. 930–936, 1977.
- [40] F.-G. Zeng, K. Nie, G. S. Stickney, Y.-Y. Kong, M. Vongphoe, A. Bhargave, C. Wei, and K. Cao, “Speech recognition with amplitude and frequency modulations,” 2005.
- [41] Y. Nir, V. V Vyazovskiy, C. Cirelli, M. I. Banks, and G. Tononi, “Auditory responses and stimulus-specific adaptation in rat auditory cortex are preserved across NREM and REM sleep.,” *Cereb. Cortex*, vol. 25, no. 5, pp. 1362–78, May 2015.
- [42] M. Teplan, “FUNDAMENTALS OF EEG MEASUREMENT,” 2002.
- [43] S. Sur and V. K. Sinha, “Event-related potential: An overview.,” *Ind. Psychiatry J.*, vol. 18, no. 1, pp. 70–3, Jan. 2009.
- [44] M. P. Paulraj, K. Subramaniam, S. Bin Yaccob, A. H. Bin Adom, and C. R. Hema, “Auditory evoked potential response and hearing loss: a review.,” *Open Biomed. Eng. J.*, vol. 9, pp. 17–24, 2015.
- [45] N. Miyazaki, “CHEMOGENETIC INHIBITION OF THE INFERIOR COLLICULUS : EFFECTS ON ELECTROPHYSIOLOGY AND BEHAVIOR,” Purdue University, 2018.
- [46] A. Parthasarathy and E. Bartlett, “Two-channel recording of auditory-evoked potentials to detect age-related deficits in temporal processing,” *Hear. Res.*, vol. 289, no. 1–2, pp. 52–62, Jul. 2012.
- [47] A. Parthasarathy and E. Bartlett, “Two-channel recording of auditory-evoked potentials to detect age-related deficits in temporal processing.,” *Hear. Res.*, vol. 289, no. 1–2, pp. 52–62, Jul. 2012.
- [48] D. Möhrle, K. Ni, K. Varakina, D. Bing, S. C. Lee, U. Zimmermann, M. Knipper, and L. Rüttiger, “Loss of auditory sensitivity from inner hair cell synaptopathy can be centrally compensated in the young but not old brain,” *Neurobiol. Aging*, vol. 44, pp. 173–184, Aug. 2016.

- [49] M. C. Liberman and S. G. Kujawa, “Cochlear synaptopathy in acquired sensorineural hearing loss: Manifestations and mechanisms,” *Hear. Res.*, vol. 349, pp. 138–147, Jun. 2017.
- [50] S. G. Kujawa and M. C. Liberman, “Adding Insult to Injury: Cochlear Nerve Degeneration after ‘Temporary’ Noise-Induced Hearing Loss,” *J. Neurosci.*, vol. 29, no. 45, pp. 14077–14085, 2009.
- [51] J. Ping, N. Li, G. C. Galbraith, X. Wu, and L. Li, “Auditory frequency-following responses in rat ipsilateral inferior colliculus,” *Neuroreport*, vol. 19, no. 14, pp. 1377–1380, Sep. 2008.
- [52] A. Krishnan, Y. Xu, J. T. Gandour, and P. A. Cariani, “Human frequency-following response: representation of pitch contours in Chinese tones,” *Hear. Res.*, vol. 189, no. 1–2, pp. 1–12, Mar. 2004.
- [53] H. Guest, K. J. Munro, G. Prendergast, R. E. Millman, and C. J. Plack, “Impaired speech perception in noise with a normal audiogram: No evidence for cochlear synaptopathy and no relation to lifetime noise exposure,” *Hear. Res.*, vol. 364, pp. 142–151, Jul. 2018.
- [54] S. Ananthakrishnan and A. Krishnan, “Human frequency following responses to iterated rippled noise with positive and negative gain: Differential sensitivity to waveform envelope and temporal fine-structure,” *Elsevier*, 2018.
- [55] A. Parthasarathy, J. Datta, J. A. L. Torres, C. Hopkins, and E. L. Bartlett, “Age-related changes in the relationship between auditory brainstem responses and envelope-following responses,” *J. Assoc. Res. Otolaryngol.*, vol. 15, no. 4, pp. 649–661, Aug. 2014.
- [56] M. Koch and H.-U. Schnitzler, “The acoustic startle response in rats—circuits mediating evocation, inhibition and potentiation,” *Behav. Brain Res.*, vol. 89, no. 1–2, pp. 35–49, Dec. 1997.
- [57] N. R. SWERDLOW, D. L. BRAFF, and M. A. GEYER, “Cross-species Studies of Sensorimotor Gating of the Startle Reflex,” *Ann. N. Y. Acad. Sci.*, vol. 877, no. 1 ADVANCING FRO, pp. 202–216, Jun. 1999.
- [58] P. K. Pilz, H. U. Schnitzler, and D. Menne, “Acoustic startle threshold of the albino rat (*Rattus norvegicus*).,” *J. Comp. Psychol.*, vol. 101, no. 1, pp. 67–72, Mar. 1987.
- [59] M. Koch, “The neurobiology of startle,” *Prog. Neurobiol.*, vol. 59, no. 2, pp. 107–128, Oct. 1999.

- [60] R. GÃ³mez-Nieto, J. de A. C. Horta-JÃ³nior, O. Castellano, L. Millian-Morell, M. E. Rubio, and D. E. LÃ³pez, "Origin and function of short-latency inputs to the neural substrates underlying the acoustic startle reflex," *Front. Neurosci.*, vol. 8, Jul. 2014.
- [61] J. R. Ison and H. S. Hoffman, "Reflex modification in the domain of startle: II. The anomalous history of a robust and ubiquitous phenomenon.," *Psychol. Bull.*, vol. 94, no. 1, pp. 3–17, 1983.
- [62] M. Koch and H.-U. Schnitzler, "The acoustic startle response in rats—circuits mediating evocation, inhibition and potentiation," *Behav. Brain Res.*, vol. 89, no. 1–2, pp. 35–49, Dec. 1997.
- [63] J. T. Friedman, A. M. Peiffer, M. G. Clark, A. A. Benasich, and R. H. Fitch, "Age and experience-related improvements in gap detection in the rat," 2004.
- [64] O. R. Floody and M. P. Kilgard, "Differential reductions in acoustic startle document the discrimination of speech sounds in rats," *J. Acoust. Soc. Am.*, vol. 122, no. 4, pp. 1884–1887, Oct. 2007.
- [65] G. . Varty, R. . Hauger, and M. . Geyer, "Aging Effects on the Startle Response and Startle Plasticity in Fischer F344 Rats," *Neurobiol. Aging*, vol. 19, no. 3, pp. 243–251, May 1998.
- [66] N. Vogt, "Chemogenetic manipulation of neurons," *Nat. Methods*, vol. 12, no. 7, pp. 603–603, Jul. 2015.
- [67] S. Kaur, R. Lazar, and R. Metherate, "Intracortical Pathways Determine Breadth of Subthreshold Frequency Receptive Fields in Primary Auditory Cortex," *J. Neurophysiol.*, vol. 91, no. 6, pp. 2551–2567, Jun. 2004.
- [68] J. Zhang, Y. Zhang, and X. Zhang, "Auditory cortex electrical stimulation suppresses tinnitus in rats.," *J. Assoc. Res. Otolaryngol.*, vol. 12, no. 2, pp. 185–201, Apr. 2011.
- [69] G. Aston-Jones and K. Deisseroth, "Recent advances in optogenetics and pharmacogenetics," *Brain Res.*, vol. 1511, pp. 1–5, May 2013.
- [70] E. Vardy, J. E. Robinson, C. Li, R. H. J. Olsen, J. F. DiBerto, P. M. Giguere, F. M. Sassano, X.-P. Huang, H. Zhu, D. J. Urban, K. L. White, J. E. Rittiner, N. A. Crowley, K. E. Pleil, C. M. Mazzone, P. D. Mosier, J. Song, T. L. Kash, C. J. Malanga, M. J. Krashes, and B. L. Roth, "A New DREADD Facilitates the Multiplexed Chemogenetic Interrogation of Behavior," *Neuron*, vol. 86, no. 4, pp. 936–946, May 2015.

- [71] C. J. Burnett and M. J. Krashes, “Resolving Behavioral Output via Chemogenetic Designer Receptors Exclusively Activated by Designer Drugs,” 2016.
- [72] M. Michaelides and Y. L. Hurd, “Chemogenetics: DREADDs,” in *Neuroscience in the 21st Century*, New York, NY: Springer New York, 2016, pp. 2847–2856.
- [73] B. L. Roth, “DREADDs for Neuroscientists.,” *Neuron*, vol. 89, no. 4, pp. 683–94, Feb. 2016.
- [74] H. Zhu and B. L. Roth, “Silencing Synapses with DREADDs,” *Neuron*, vol. 82, no. 4, pp. 723–725, May 2014.
- [75] D. J. Urban and B. L. Roth, “DREADDs (Designer Receptors Exclusively Activated by Designer Drugs): Chemogenetic Tools with Therapeutic Utility,” *Annu. Rev. Pharmacol. Toxicol.*, vol. 55, no. 1, pp. 399–417, Jan. 2015.
- [76] P. D. Whissell, S. Tohyama, and L. J. Martin, “The Use of DREADDs to Deconstruct Behavior.,” *Front. Genet.*, vol. 7, p. 70, 2016.
- [77] C. Zincarelli, S. Soltys, G. Rengo, and J. E. Rabinowitz, “Analysis of AAV serotypes 1-9 mediated gene expression and tropism in mice after systemic injection.,” *Mol. Ther.*, vol. 16, no. 6, pp. 1073–80, Jun. 2008.
- [78] G. Aviello and G. D’Agostino, “Tools for Controlling Activity of Neural Circuits Can Boost Gastrointestinal Research.,” *Front. Pharmacol.*, vol. 7, p. 43, 2016.
- [79] S. Bogaerts, J. D. Clements, J. M. Sullivan, and S. Oleskevich, “Automated threshold detection for auditory brainstem responses: comparison with visual estimation in a stem cell transplantation study.,” *BMC Neurosci.*, vol. 10, p. 104, Aug. 2009.
- [80] C. F. Rabang, A. Parthasarathy, Y. Venkataraman, Z. L. Fisher, S. M. Gardner, and E. L. Bartlett, “A computational model of inferior colliculus responses to amplitude modulated sounds in young and aged rats.,” *Front. Neural Circuits*, vol. 6, p. 77, 2012.
- [81] C. Watson and G. Paxinos, *The Rat Brain in Stereotaxic Coordinates*, 6th ed. 2007.
- [82] J. Csicsvari, H. Hirase, A. Czurkó, A. Mamiya, and G. Buzsáki, “Oscillatory coupling of hippocampal pyramidal cells and interneurons in the behaving Rat.,” *J. Neurosci.*, vol. 19, no. 1, pp. 274–87, Jan. 1999.